YIL / YEAR | 2025

CİLT - SAYI / VOLUME - ISSUE | 11 / 2

e-ISSN | 2667-8209

KASTAMONU ÜNİVERSİTESİ MÜHENDİSLİK VE FEN BİLİMLERİ DERGİSİ

KASTAMONU UNIVERSITY JOURNAL OF ENGINEERING AND SCIENCE

KASTAMONU ÜNİVERSİTESİ
MÜHENDİSLİK VE
FEN BİLİMLERİ DERGİSİ

KASTAMONU UNIVERSITY
JOURNAL OF ENGINEERING
AND SCIENCES

İLETİŞİM | CONTACT

Kastamonu Üniversitesi Mühendislik ve Mimarlık Fakültesi, Kastamonu, TÜRKİYE
90 366 2802901 kujes@kastamonu.edu.tr https://dergipark.org.tr/en/pub/kastamonujes

KASTAMONU ÜNİVERSİTESİ
MÜHENDİSLİK VE
FEN BİLİMLERİ DERGİSİ

KASTAMONU UNIVERSITY
JOURNAL OF ENGINEERING
AND SCIENCES

EDİTÖR KURULU | EDITORIAL BOARD

Kastamonu University
Journal of Engineering and Science

Vol: 11 Issue: 2 December 2025 E-ISSN:2667-8209

Reviewers for This Issue

Prof. Dr. Şahlan ÖZTÜRK
Prof. Dr. Nesrin ŞENER
Prof. Dr. Erdinç DOĞANCI
Prof. Dr. İlhami HORUZ
Prof. Dr. Elif ŞEYKUYTU
Assoc. Prof. Dr. Salih GÖRGÜNOĞLU
Assoc. Prof. Dr. Mehmet GÜMÜŞTAŞ
Assoc. Prof. Dr. Derya DAVARCI
Asst. Prof. Dr. Haşim Fırat KARASU
Asst. Prof. Dr. Sait DEMİR
Asst. Prof. Dr. Özkan ASLAN
Asst. Prof. Dr. Ömer KARABEY

Compositors:

Res. Assist. Halil Oğuzhan KARA

Kastamonu University
Journal of Engineering and Science

Vol: 11 Issue: 2 December 2025 E-ISSN:2667-8209

CONTENTS

Kastamonu University
Journal of Engineering and Sciences
e-ISSN 2667-8209
http://dergipark.gov.tr/kastamonujes

Bibliometric Analysis of Studies on "Machine Learning in Geothermal Energy"

Orkun Teke*

Electric and Energy Department, Manisa Technical Sciences Vocational School, Manisa Celal Bayar University, Manisa, Türkiye
***Corresponding Author:** orkun.teke@cbu.edu.tr

Received: **September 13, 2025** ◆ Accepted: **December 8, 2025** ◆ Published Online: **December 25, 2025**

Abstract: This study examines the scientific literature developing at the intersection of geothermal energy and machine learning from a bibliometric perspective. 300 academic publications published between 2010 and 2025, obtained from the Web of Science database, were analyzed using the R-based Biblioshiny tool. The study revealed the distribution of publications by year, citation performance, author, institution and country collaborations, the most cited studies and keyword co-occurrence networks. The findings show that there has been a significant acceleration in the field after 2019 and especially from 2022, with production reaching a high level in 2024–2025. While Geothermics was the journal with the most publications, multidisciplinary journals such as Renewable Energy, Energies, and Applied Energy also attracted attention. In the keyword analysis, technical themes such as Organic Rankin Cycle, Enhanced Geothermal System, reservoir, and temperature optimization were central; By 2024, new trends such as hydrogen and advanced geothermal systems have emerged. China leads by far in the number of publications and citations and maintains strong collaborations with the United States and Germany. The study comprehensively summarizes the status of the geothermal energy-machine learning field and provides a guiding framework for future research trends and areas of collaboration.

Keywords: Machine Learning, Geothermal Energy, Bibliometric Analysis, Biblioshiny, Web of Science

"Jeotermal Enerjide Makine Öğrenmesi" Konulu Çalışmaların Bibliyometrik Analizi

Öz: Bu çalışma, jeotermal enerji ve makine öğrenmesi kesişiminde gelişen bilimsel literatürü bibliyometrik bir bakış açısıyla incelemektedir. Web of Science veri tabanından elde edilen 2010-2025 yılları arasında yayınlanmış 300 akademik yayın, R tabanlı Biblioshiny aracı kullanılarak analiz edilmiştir. Çalışmada yayınların yıllara göre dağılımı, atıf performansı, yazar, kurum ve ülke iş birlikleri, en çok atıf alan çalışmalar ve anahtar kelime eş-geçiş ağları ortaya konulmuştur. Bulgular, 2019'dan sonra ve özellikle 2022'den itibaren alanda önemli bir ivmelenme olduğunu, üretimin 2024-2025'te yüksek bir seviyeye ulaştığını göstermektedir. En çok yayını olan dergi Geothermics olmakla birlikte, Renewable Energy, Energies ve Applied Energy gibi multidisipliner dergiler de dikkat çekmiştir. Anahtar kelime analizinde Organik Rankin Döngüsü, Geliştirilmiş Jeotermal Sistem, rezervuar ve sıcaklık optimizasyonu gibi teknik temalar merkezi konumdadır; 2024 yılına gelindiğinde, hidrojen ve gelişmiş jeotermal sistemler gibi yeni trendler ortaya çıkmıştır. Çin, yayın ve atıf sayısında açık ara lider konumda olup, Amerika Birleşik Devletleri ve Almanya ile güçlü iş birliklerini sürdürmektedir. Çalışma, jeotermal enerji-makine öğrenmesi alanının durumunu kapsamlı bir şekilde özetlemekte ve gelecekteki araştırma trendleri ve iş birliği alanları için yol gösterici bir çerçeve sunmaktadır.

Anahtar Kelimeler: Makine Öğrenmesi, Jeotermal Enerji, Bibliyometrik Analiz, Biblioshiny, Web of Science

1. Introduction

As fossil fuels, a limited and exhaustible resource, are projected to be depleted soon, researching and implementing alternative energy sources to secure energy supplies and achieve sustainable development is increasingly urgent [1]. Furthermore, increasing global energy demand and intensifying efforts to combat climate change have made the shift towards sustainable and clean energy sources more crucial than ever. In this context, geothermal energy, which stands out among renewable energy sources with its potential to provide baseload power, is attracting attention as a stable and reliable alternative [2]. The exploration, development, and management of geothermal resources involve challenging processes requiring the understanding of complex geological structures and the analysis of large data sets. Traditional methods can be time-consuming and costly in these processes [3].

In recent years, as a reflection of the "Fourth Industrial Revolution," technologies such as artificial intelligence (AI), machine learning, and deep learning have led to a paradigm shift in the energy sector, as in many other areas of scientific research. Artificial intelligence applications, particularly in geothermal energy, have led to: It opens new horizons in critical areas such as reservoir modeling, identifying potential fields, optimizing drilling operations, and increasing production efficiency. The intersection of these two dynamic and innovative fields is attracting increasing interest in both academia and industry [4].

The aim of this study is to reveal the intellectual structure and research trends of scientific literature emerging at the intersection of geothermal energy and artificial intelligence using a bibliometric analysis method. For this purpose, 300 scientific documents published between 2010 and 2025 were examined using the Web of Science (WoS) database [5]. R-based Biblioshiny library is used for data analysis and visualization.

This analysis seeks to answer the following fundamental research questions:

- What is the distribution of publications on geothermal energy and artificial intelligence over the years, and how has scientific interest in this field evolved?
- Which authors, institutions, and countries have published the most and are the most influential in this field?
- What is the map of the main themes, key concepts, and intellectual accumulation of research?
- What are the potential future research trends and potential areas for collaboration?

This bibliometric analysis hopes to provide a comprehensive snapshot of the current state of knowledge in the field of geothermal energy and artificial intelligence, providing researchers, policy makers, and industry professionals with a roadmap for future work.

2. Material and Method

Bibliometrics [6], a widely used subdiscipline of science measurement, encompasses the study and measurement of scholarly communication. This field uses quantitative methods to analyze and evaluate scholarly literature, including journals, articles, and authors, allowing researchers to gain insight into the direction of the field [7]. Thus, it can provide valuable information about the productivity, impact, and growth of a particular research field. Bibliometric analysis can also reveal collaboration patterns, identify leading researchers, and track the evolution of research frontiers.

This study used scholarly mapping analysis to gain a comprehensive understanding of the evolving architecture of a particular field of study [8].

WoS database used in this study is an internationally recognized, comprehensive, and reliable information source. Owned by Thomson Reuters Corporation, the platform is considered the most comprehensive search resource of its kind, featuring journals from high-quality publishers and high-impact studies. Therefore, it has become the standard data source for bibliometric analysis [5].

Data collection was conducted in a general manner, and all articles resulting from the "Topic Sentences (TS)" search were included in the dataset. Therefore, a dataset consisting of 300 "Articles" was created, covering publications between 2010 and 2025. All bibliographic information (authors, institutions, countries, keywords, abstracts, citations, etc.) of relevant publications were exported in "Plain Text" format and prepared for analysis. The study methodology is presented in Figure 1, and TS was chosen as *("("geothermal energy" OR "geothermal power" OR "geothermal reservoir") AND ("artificial intelligence" OR "AI" OR "machine learning" OR "deep learning")".*

Biblioshiny, an interactive web interface supported by the R programming language-based Bibliometrix [9] package, was used for data analysis and visualization. The analysis process was conducted under two main headings, Performance Analysis and Scientific Mapping Analysis, as indicated in Figure 1. Performance analysis aims to measure the overall productivity and impact of the research field. The following metrics were examined in this context:

- *Publication and Citation Counts:* Annual publication counts and the total number of citations to these publications were analyzed to examine the temporal evolution of the field and the growth in scientific interest.

- *Publication Types and Research Areas:* Analyses were conducted to determine the publication types (articles, reviews, proceedings, etc.) the literature comprises and the research areas it focuses on according to WoS categories.
- *Highly Cited Publications:* The most cited articles were listed to identify the key publications that form the intellectual foundation of the field and have the greatest impact.

Scientific mapping is used to visualize the conceptual structure and social networks of a research field. These analyses reveal the intellectual dynamics of the field and the relationships between actors:

- *Burst Detection:* Kleinberg's burst detection algorithm was used to identify emerging and "hot" research topics by identifying sudden increases in the popularity of specific keywords.
- *Most Frequent Words:* Author keywords were analyzed to identify the key themes and concepts on which the research focused.
- *Author and Institution Co-authorship Analysis:* Co-authorship analyses were conducted to reveal collaboration networks between researchers and institutions. This analysis helps identify key research groups and centers in the field.
- *Collaboration Mapping*: A world collaboration map was created to visualize the level of scientific collaboration between countries.

This methodological framework provides a solid foundation for comprehensively assessing the current status of geothermal energy and artificial intelligence research and discussing future trends.

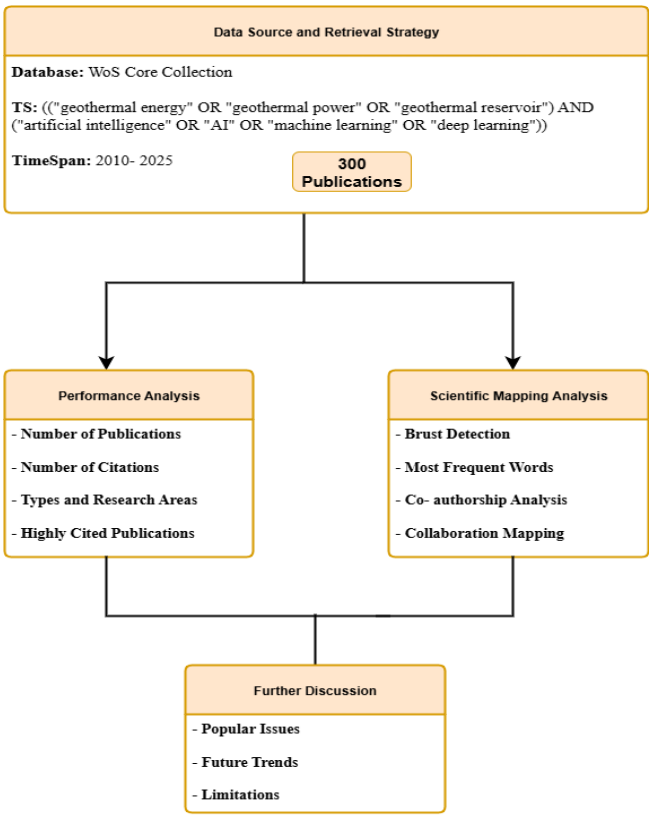

Figure 1. Framework of methodology

3. Result

3.1. Performance Analysis

Performance analysis in the examined period includes indicators such as the number of publications varying by year, the number of citations, the prevalence of the study and its role as a basis for different studies, research areas and the journals in which publications are concentrated, and the most highly cited studies.

The sixteen-year period examined in the study demonstrates two main phases in scientific production (Figure 2). The results, which appear as a stagnant initial period and a rapid acceleration period, indicate that the growth coefficient increased, particularly starting in 2022. A similar number of studies were published in 2024 and 2025. The process, which began with three publications in 2010, was interrupted by zero publications in 2011, 2014, and 2016. This suggests that the relevant research topic was either not yet discovered or had not attracted sufficient attention from the academic community during

these years. The four publications recorded in 2019 can be considered the first harbinger of an increasing trend in the following years.

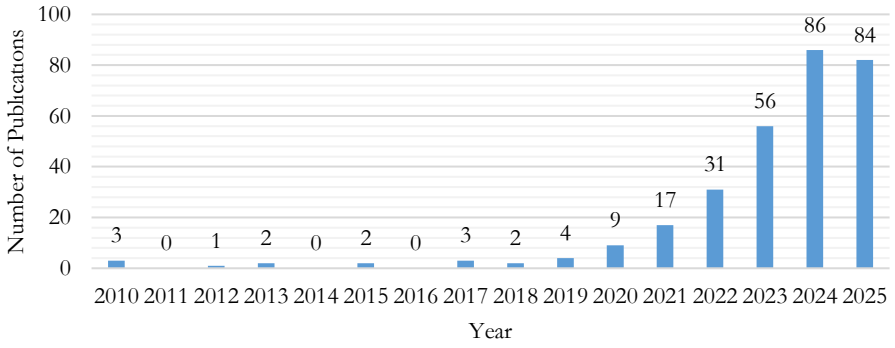

Figure 2. Annual scientific production

Examination of the dataset inferred (Table 1) "4" publications is single-authored. The collaboration index is a metric that measures the degree of collaboration among authors in a particular field or on a specific topic. It is calculated by dividing the number of co-authored publications by the total number of publications expressed as a percentage. A higher collaboration index indicates a higher degree of collaboration among authors in the field, while a lower collaboration index suggests that most of the publications are single-authored or have a small number of authors. The collaboration index is often used to study the collaboration patterns and trends within a field of research and to identify the most productive institutions and researchers. The collaboration index is calculated to be "3.17". This shows that collaboration is common in research in the field and that studies are generally conducted by multiple authors. Additionally, the average citations per document were computed to be "15.36".

Table 1. Spatial accessibility status of health service centers

Average citations per document	**15.36**
Authors	1350
Multi-authored documents	1346
Single-authored documents	4
Co-Authors per Documents	5.18
Collaboration Index	4.49

Table 2 shows that classification of publications in different categories. While the dataset contains mostly articles (265), it appears that there are very few scientific products in this field, such as papers and book chapters, scanned within WoS. This is a significant shortcoming.

Table 2. Document types

Document Type	**Numbers**
Article	265
Book Chapter	1
Proceeding Paper	7
Review	25
Early Access	2

Figure 3 indicated that the top 10 scientific sources where the publications were published most frequently and the number of publications in these sources. It is important for revealing which journals concentrate academic knowledge in the field and the interdisciplinary nature of the topic. The most striking finding is that the journal "Geothermics" is the clear leader, with 40 publications, compared to other sources. This clearly demonstrates that "Geothermics" is the primary, most fundamental, and specialized (core) publication outlet for this research topic. It appears that researchers in the field primarily choose this journal to publish their work. Journals such as "Renewable Energy" (21 publications), "Energies" (18 publications), and "Energy" (12 publications), which are at the top of the list, confirm that the topic is not limited to a specific niche area but also attracts broad and current interest within the renewable and general energy disciplines. This demonstrates that the research appeals to a broad academic audience and is relevant to general energy policy and studies. The presence of journals focused on applied science and engineering, such as "Applied Thermal Engineering" (9 publications), "Applied Energy" (7 publications), "Geoenergy Science and Engineering" (7 publications), "Energy Conversion and Management" (6 publications), and "Case Studies in Thermal Engineering" (5 publications), is noteworthy. This highlights that, in addition to the theoretical

basis of the research, it has a strong engineering, application, and thermal sciences dimension. The field has a clear central and specialized focus, centered around the journal "Geothermics". The subject is strongly related to broader fields such as general energy and renewable energy. A significant portion of the research focuses on practical engineering solutions and thermal applications.

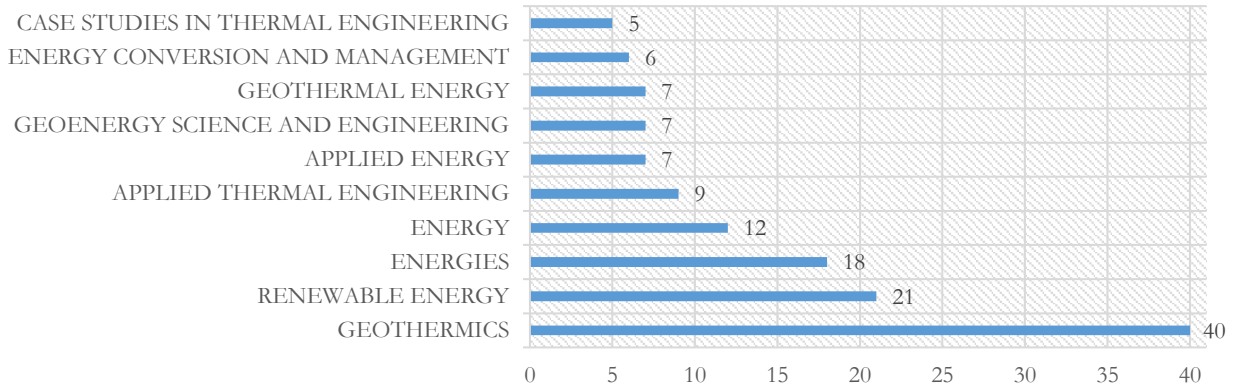

Figure 3. Top 10 most relevant sources

When examining the most cited journals (Figure 4), Geothermics reinforces its position as the leading field in the most cited fields. Despite its large number of publications, Energies appears to have received relatively few citations. In general, with the exception of Energies, the number of citations is high relative to the number of publications.

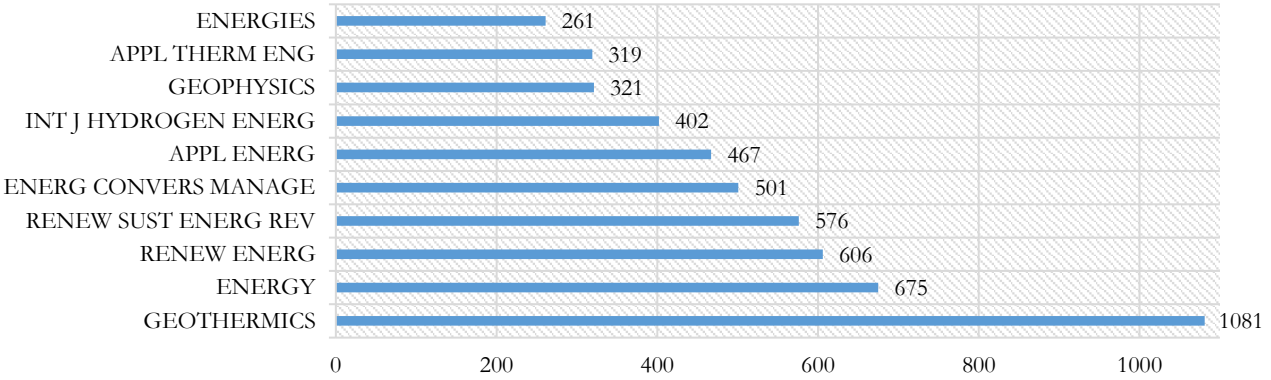

Figure 4. Top 10 most cited journals

Table 3 presents a comprehensive breakdown of information about the source, type, year of publication, citation count (NoC), average citations (ACit), number of authors (NoA), number of institutions (NoI), and number of countries/regions (NCount) for the publications under consideration. As expected, during the rising popularity of the concept, the oldest publications on this concept appear to be among the most cited. Furthermore, an examination of research types reveals that eight of the most cited publications are articles, while only two are reviews. It has been shown that method-based studies tend to receive more citations and attention than reviews. All studies have at least two authors, while some have more than five. Generally, there is not much institutional diversity. Studies have been conducted by a combination of at most three institutions.

Table 3. Highly cited publications

Paper	Sources	Type	Year	NoC	ACit	NoA	NoI	NCount
A review on renewable energy and electricity requirement forecasting models for smart grid and buildings [10]	Renewable Sustainable Energy Review	Review	2020	310	51.66	3	3	2
Contribution of the exploration of deep crystalline fractured reservoir of Soultz to the knowledge of Enhanced Geothermal Systems (EGS) [11]	Comptes Rendus Geoscience	Article	2010	224	14	5	4	2
Renewable energy: Present research and future scope of Artificial Intelligence [12]	Renewable Sustainable Energy Review	Article	2017	216	24	5	5	3

From Fluid Flow to Coupled Processes in Fractured Rock: Recent Advances and New Frontiers [13]	Geophysics	Article	2021	148	37	11	10	1
A review on machine learning forecasting growth trends and their real-time applications in different energy systems [14]	Renewable and Sustainable Energy Reviews	Review	2020	114	19	2	2	2
Machine learning optimization of a novel geothermal driven system with LNG heat sink for hydrogen production and liquefaction [15]	Energy Conversion and Management	Article	2022	105	26.25	4	1	1
Prediction of two-phase flow patterns in upward inclined pipes via deep learning [16]	Energy	Article	2020	98	16.33	4	3	3
Productivity prediction of a multilateral-well geothermal system based on a long short-term memory and multi-layer perceptron combinational neural network [17]	Applied Energy	Article	2021	87	17.40	2	2	1
A comparative performance analysis, working fluid selection, and machine learning optimization of ORC systems driven by geothermal energy [18]	Energy Conversion and Management	Article	2023	83	27.66	3	2	1
Machine learning in subsurface geothermal energy: Two decades in review [19]	Geothermics	Article	2022	75	18.75	7	3	1

3.2. Performance Analysis

Scientific mapping analysis is used to identify patterns, trends, and connections within a field of study. This technique involves visualizing data and information using various types of maps, diagrams, and graphs. The goal of scientific mapping analysis is to provide a comprehensive overview of the state of research in each field and identify areas that may be open to further research. In bibliometric analysis, "burst detection analysis" is a technique used to detect sudden and significant increases in the number of publications on a given topic, also known as "bursts" in literature. This method helps identify research focuses and emerging trends in a field by detecting sudden increases in the number of publications that cannot be explained by normal growth or background noise. The analysis is typically conducted by comparing the number of publications in a given period with the number of publications in previous periods and identifying significant increases in the data. It can help researchers understand new and growing research directions.

Keyword analysis can be seen as a critical component in identifying topics within a given field. A minimum occurrence threshold of 2 was set, and 128 keywords meeting this criterion were found. The resulting concurrency network, shown in Figure 5, shows the connections between keywords appearing in the same publication which calld as “Co-Occurrence Analysis of Keywords”. Node size indicates keyword frequency, while link width corresponds to the number of concurrences. The main cluster related to the organic ranking cycle which is one most important process in geothermal power plants, enhanced geothermal system for efficiency, reservoir and reservoir temperature. These words are critical for geothermal systems in underground and surface applications. It can be said that researchers are focusing on these issues and are turning to production efficiency by improving geothermal systems or controlling their temperatures. It is understood that concepts related to plant efficiency increase and reservoir improvement studies have intensified after 2020.

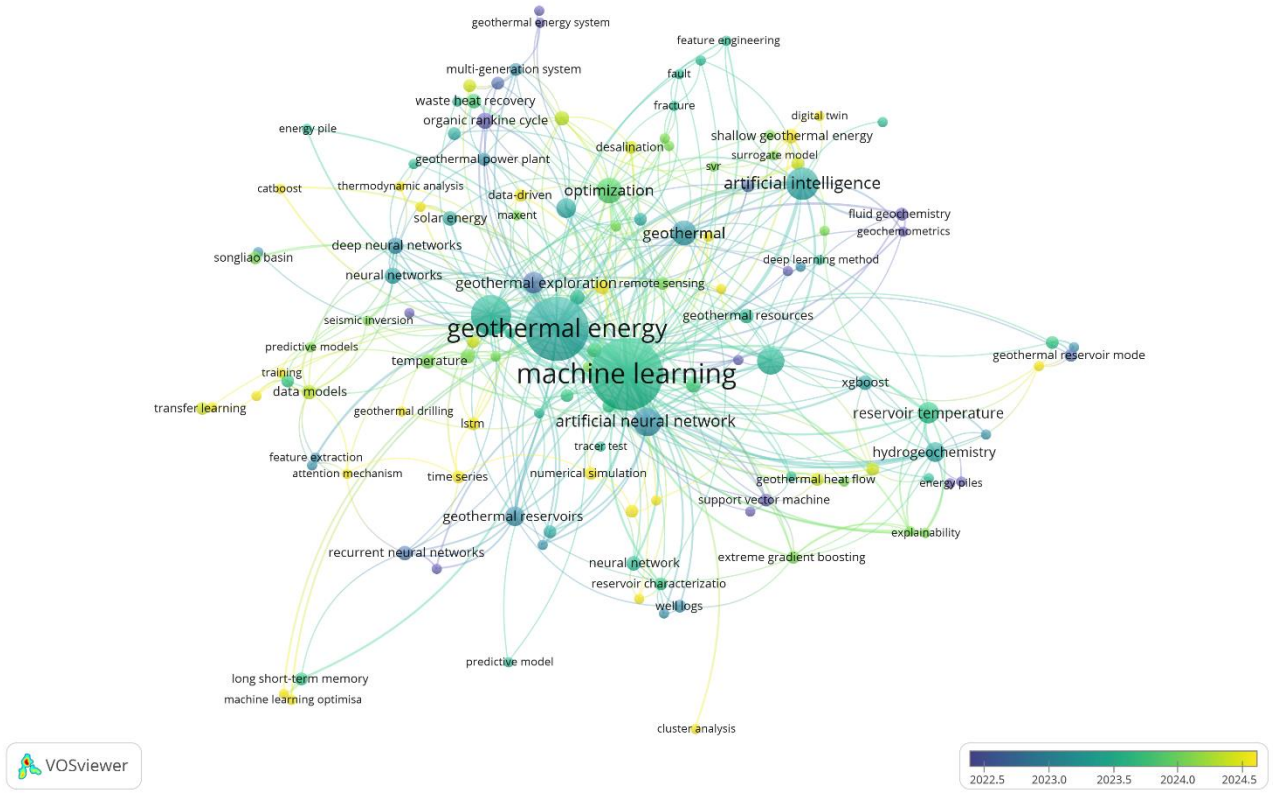

Figure 5. Network and time distribution visualization of keywords

Burst detection is a method utilized to identify sudden increases in the frequency of a specific keyword within a given period. This technique is employed to discern the emergence of new research trends or the sudden popularity of a particular topic. The burst score, which serves as a metric to measure the degree of burstiness, is calculated based on the relative increase in the frequency of the keyword in comparison to its historical trend. By visualizing burst scores over time, researchers can identify patterns in the emergence of new research topics and track the evolution of a field. Furthermore, burst analysis can also aid in identifying sudden changes in the discourse surrounding a particular keyword, providing valuable insights for researchers and practitioners.

According to Burst Analysis, research in geothermal energy and machine learning has been revealed to focus primarily on topics such as "performance" and "optimization" (Table 4). Also, word cloud is presented in Figure 6. This emphasis on predicting and identifying improvements for sustainable power plant operations, as well as predicting financial gains, aims to achieve greater competitiveness in the market. Furthermore, studies conducted after 2024, particularly in terms of "hydrogen" and "enhanced geothermal system," focus on both direct geothermal byproducts and holistic system improvement (Figure 7).

Table 4. Occurrences

Words	Occurrences
Machine Learning	94
Geothermal Energy	87
Performance	48
Optimization	42
Energy	38
System	36
Deep Learning	30
Prediction	28
Artificial Intelligence	27
Model	24

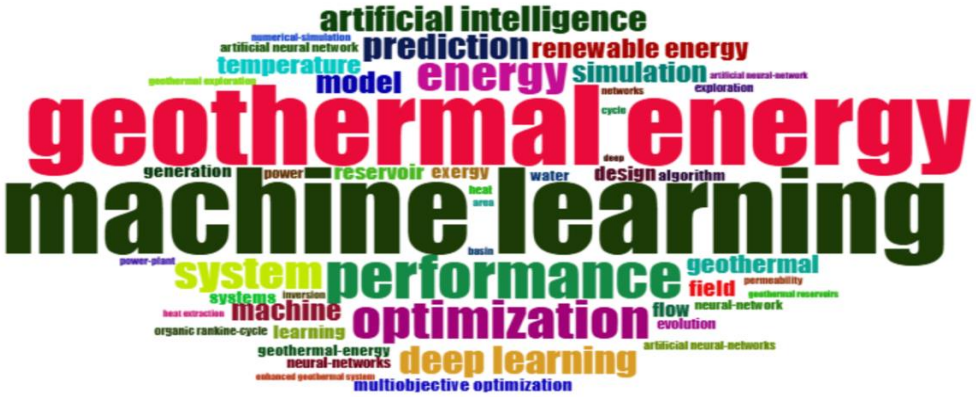

Figure 6. Word cloud

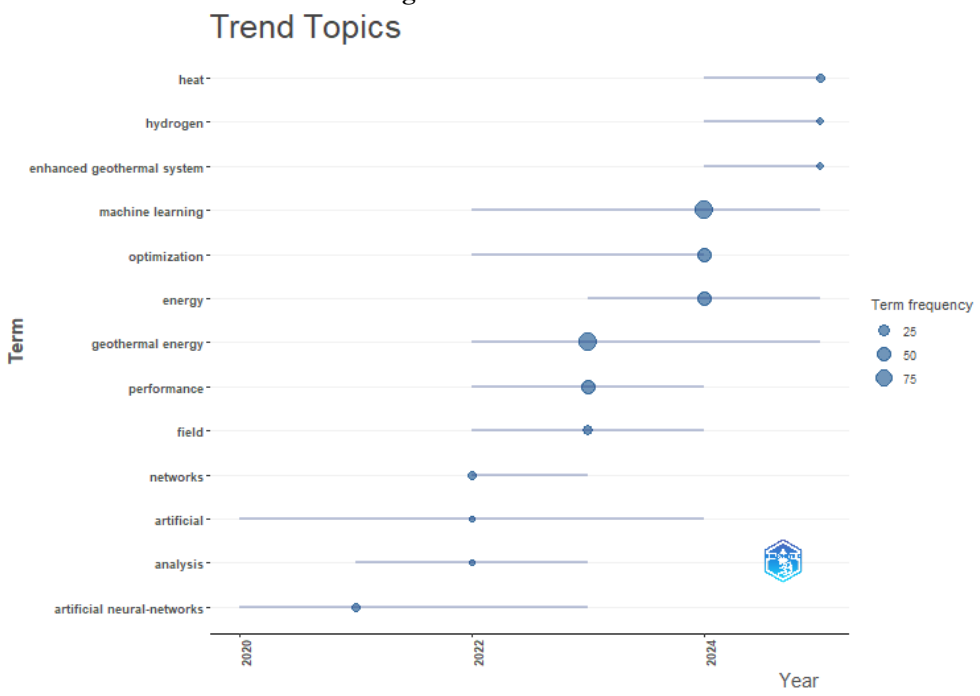

Figure 7. Trend topics

Co-authorship analysis is crucial for examining collaborations between researchers in a given field. The goal of this analysis is to understand the network of relationships between researchers and identify key players in the field. Country co-authorship analysis can be explained as a method for identifying collaboration patterns between researchers from different countries. This technique can provide valuable information about the global distribution of research activities and the nature of international collaborations. The goal of country co-authorship analysis is to identify the most active countries in each research field and the country's most likely to collaborate with each other.

According to the dataset, China has the highest number of documents with 95, significantly outpacing the United States, which has 40 documents, by approximately 2.5 times. Germany comes in third with 15 documents (Figure 8). In terms of citations, Chinese publications also have the highest number of publications with 1,319. This comparison reveals an approximately three-fold difference between the United States, which has 549 citations, and China (Table 5). The competition between the United States and China, the dominant powers in science, is also prominent here, with China leading the race. It produces twice as much scientific material as its closest rival and receives citations for these publications. This gives a positive impression of the quality of the published work. China is particularly active in joint projects with the United States and Germany, and countries such as Turkey and Saudi Arabia are also working to develop partnerships. Collaborations are also developing with countries such as Iran, India, South Korea, the United Kingdom, and Poland in a wide range of areas.

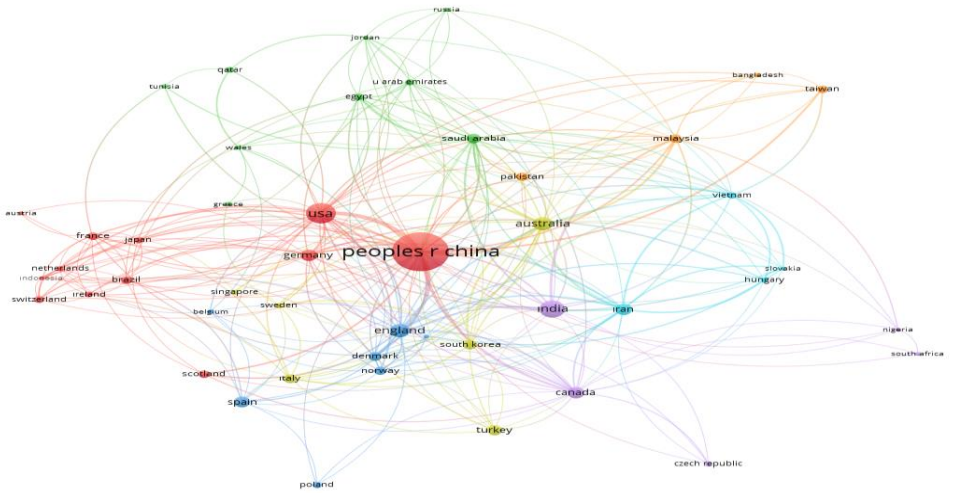

Figure 8. Network visualization of countries

Table 5. Most cited countries

Country	Total Cite
China	1319
United States	549
Iran	300
Canada	276
France	231
Germany	229
Poland	226
Mexico	193
Saudi Arabia	182
Italy	171

Collaboration network analysis uses bibliometric data such as co-authorship and citation networks to create a visual representation of collaboration patterns, enabling the identification of key actors and institutions, as well as potential areas for future collaboration.

The application of collaboration network analysis in the bibliometric field can provide a comprehensive understanding of the research landscape in a field. By identifying collaboration patterns, leading institutions and researchers in the field, as well as potential collaboration opportunities, can be identified. Furthermore, this approach can be used to evaluate the effectiveness of existing collaborations and identify potential new collaborations between researchers and institutions. By examining this map, a researcher can update the map of project and collaboration partnerships, identifying countries where they should focus their efforts.

The country collaboration map shown in Figure 9 provides a visual representation of collaborations between countries in each field of study. Examining the map reveals a significant number of collaborations established between countries. China and the United States appear to have a high level of collaboration with other countries. Additionally, partnerships with Canada, Middle Eastern countries, and, to a lesser extent, European countries demonstrate the potential for rich collaboration in this field. Despite significant geothermal resources in Africa (Kenya-Olkaria, etc.), the fact that research there is primarily conducted by East African researchers or researchers from other countries may be attributable to the region's socioeconomic underdevelopment.

This scientific alliance, which connects all continents, opens a window to more comprehensive and high-quality research that transcends national borders in the future. It can be concluded that this trend in international collaboration will foster innovation and lead to the production of value-added knowledge that can benefit society.

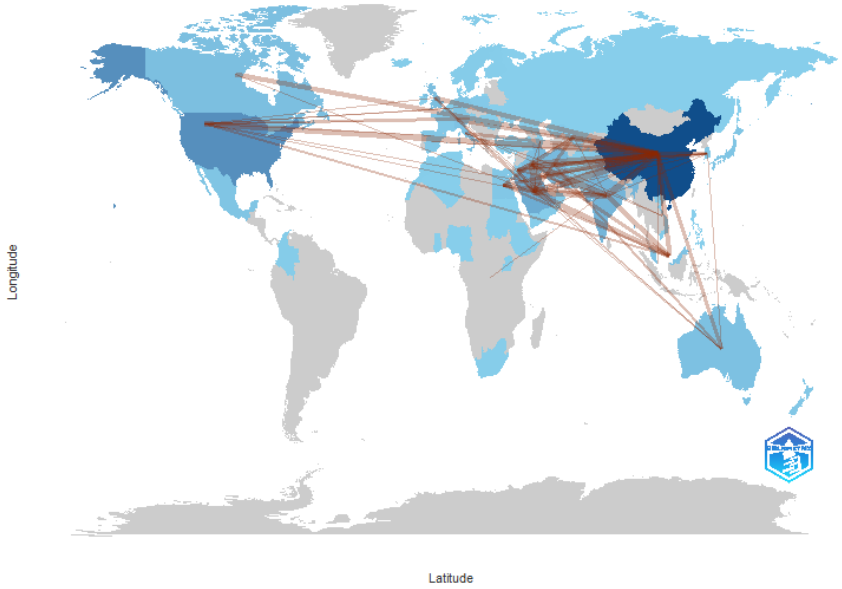

Figure 9. Collaboration map

4. Discussion

This bibliometric review reveals both the quantitative growth and intellectual structure of the literature accumulated at the intersection of geothermal energy and artificial intelligence/machine learning between 2010 and 2025. The findings indicate that the field has accelerated since 2019, with a particularly significant acceleration after 2022, and that production has plateaued in the 2024–2025 period. This pattern points to an application-oriented paradigm shift from exploration to optimization and operational efficiency, driven by both the global shift in renewable energy policies and the maturation of data-driven methods.

The predominance of articles (n=265) in the distribution of publication types confirms the experimental/applied nature of the field, while the relatively small number of reviews and presentations suggests that "status assessment" studies still offer opportunities in this rapidly developing field. The clear leadership of "Geothermics" in the source journals indicates the formation of a core subject-specific publication ecosystem. The concentration in journals such as "Renewable Energy," "Energies," "Energy," and "Applied Energy" demonstrates that this intersection is not merely a niche but is also being pursued by the general energy science and policy communities. The fact that a significant portion of the most cited studies are method/application-based articles suggests that innovative modeling contributions in this intersection resonate more quickly than in review articles. Author collaboration indicators (average co-authors per document ≈5.18; collaboration index ≈4.49; very low number of single-author publications) suggest that the network-oriented production model dominates and interdisciplinary clusters operate efficiently. The centrality of nodes such as ORC (Organic Rankine Cycle), EGS (Enhanced Geothermal Systems), reservoir, and temperature control in the keyword co-occurrence network suggests a strengthening of efficiency/optimization focuses after 2020, and the rise of holistic energy transformation themes such as "hydrogen" and advanced geothermal systems by 2024.

China's distinct superiority in document and citation production, coupled with its extensive partnerships with the US and Germany, highlight the importance of scale and R&D investments in data-intensive engineering problems. The growing multi-center networks between North America, the Middle East, and Europe provide a fertile ground for data sharing, comparable experimental setups, and the development of common software/benchmarking platforms. Conversely, despite Africa's rich geothermal potential, its relative limited representation in scientific production fuels calls for capacity building and equitable collaboration.

Trend-oriented topics center around "performance," "optimization," "prediction," and "deep learning." This aligns with the goal of generating real-time or near-real-time decision support using heterogeneous field data (drilling/circulation, two-phase flow, reservoir behavior). The following technical directions appear critical for the upcoming phase: (i) data-efficient learning with physics-informed models, (ii) uncertainty quantization and reliability (UQ) layers, (iii) multi-objective optimization (LCOE–emission–thermal depletion trade-off), (iv) portable/edge inference and autonomous control loops, and (v) online calibration of digital twins (especially drilling and surface facility) throughout their lifecycle.

From the perspective of implications for practitioners and policymakers, ML/AI integration across the geothermal value chain (exploration–drilling–reservoir management–surface facility–interconnection) has the potential to reduce investment risk and operating costs. This requires (a) open/anonymized data repositories and transparent benchmark sets at the institutional and

international levels, (b) multi-scale performance metrics and reporting standards, (c) a reproducible software ecosystem (code/shared notebooks), and (d) model traceability within the security/ethics/occupational health context.

5. Conclusion

This study was based on a sample limited to WoS based and specific subject heading queries. Indexing policies, language/access biases, and differences in "early access" timestamps may affect the absolute magnitude of trends. Furthermore, stylistic inconsistencies in some table titles and in-text numerical indicators (e.g., title tags) highlight the need for standardized literature reporting. Therefore, the findings are indicative but open to validation with other databases and broader queries.

Open benchmarks: Common data/code packages for organic rankine cycle configurations, enhanced geothermal system scenarios, and two-phase flow prediction.

- *Physically informed and hybrid models:* Increasing generalizability in data scarcity, adapting to the field with transfer learning.
- *Uncertainty and explainability:* Decision transparency with methods like SHAP (Shapley Additive Explanations); risk-based maintenance and operations planning.
- *Real-time integration:* Low-latency inference in edge devices; closed-loop control with SCADA (Supervisory control and data acquisition).
- *Equitable and inclusive collaborations:* Capacity building in Africa and Latin America; data sovereignty and fair-sharing principles.

The geothermal-AI intersection is entering a mature phase, evolving from exploration and modeling to holistic system optimization. While geothermal-specific journals are at the core of the field, interdisciplinary expansion is strong, and collaboration networks are increasingly dense. The next leap forward will be made possible by physics-informed methods, standardized benchmarking environments, and transparent data/sharing protocols. Such a foundation will increase both scientific productivity and the speed and quality of energy transformation in the field, broadening the path to sustainable, reliable, and competitive geothermal systems.

Competing Interest / Conflict of Interest

The authors declare that they have no competing interests.

Author Contribution

This manuscript is written by single author.

Acknowledgements

Not applicable.

5. References

[1] Chen, Y., Yu, S., Islam, S., Lim, C. P., & Muyeen, S. M. (2022). Decomposition-based wind power forecasting models and their boundary issue: An in-depth review and comprehensive discussion on potential solutions. Energy Reports, 8, 8805-8820.

[2] Zhu, Y. (2024). Leveraging machine learning for subsurface geothermal energy development. Highlights in Science, Engineering and Technology, 121, 440-449.

[3] Teke, O. (2024). unlocking the power of artificial intelligence: building digital twins with classification algorithms for optimized geothermal drilling. International Journal of Advanced Natural Sciences and Engineering Research, 8(5), 52–59.

[4] Al-Fakih, A., Abdulraheem, A., & Kaka, S. (2024). Application of machine learning and deep learning in geothermal resource development: Trends and perspectives. Deep Underground Science and Engineering, 3(3), 286-301.

[5] Clarivate. Web Of Science Core Collection. Available: https://clarivate.com (Accessed: 20/08/2025)

[6] Donthu, N., Kumar, S., Mukherjee, D., Pandey, N., & Lim, W. M. (2021). How to conduct a bibliometric analysis: An overview and guidelines. Journal of business research, 133, 285-296.

[7] Ji, B., Zhao, Y., Vymazal, J., Mander, Ü., Lust, R., & Tang, C. (2021). Mapping the field of constructed wetland-microbial fuel cell: A review and bibliometric analysis. Chemosphere, 262, 128366.

[8] Yu, D., Xu, Z., Kao, Y., & Lin, C. T. (2017). The structure and citation landscape of IEEE Transactions on Fuzzy Systems (1994–2015). IEEE Transactions on Fuzzy Systems, 26(2), 430-442.

[9] Aria, M., & Cuccurullo, C. (2017). bibliometrix: An R-tool for comprehensive science mapping analysis. Journal of informetrics, 11(4), 959-975.

[10] Ahmad, T., Zhang, H., & Yan, B. (2020). A review on renewable energy and electricity requirement forecasting models for smart grid and buildings. Sustainable Cities and Society, 55, 102052.

[11] Genter, A., Evans, K., Cuenot, N., Fritsch, D., & Sanjuan, B. (2010). Contribution of the exploration of deep crystalline fractured reservoir of Soultz to the knowledge of enhanced geothermal systems (EGS). Comptes Rendus Geoscience, 342(7-8), 502-516.

[12] Jha, S. K., Bilalovic, J., Jha, A., Patel, N., & Zhang, H. (2017). Renewable energy: Present research and future scope of Artificial Intelligence. Renewable and Sustainable Energy Reviews, 77, 297-317.

[13] Viswanathan, H. S., Ajo-Franklin, J., Birkholzer, J. T., Carey, J. W., Guglielmi, Y., Hyman, J. D., ... & Tartakovsky, D. M. (2022). From fluid flow to coupled processes in fractured rock: Recent advances and new frontiers. Reviews of Geophysics, 60(1), e2021RG000744.

[14] Ahmad, T., & Chen, H. (2020). A review on machine learning forecasting growth trends and their real-time applications in different energy systems. Sustainable Cities and Society, 54, 102010.

[15] Mehrenjani, J. R., Gharehghani, A., & Sangesaraki, A. G. (2022). Machine learning optimization of a novel geothermal driven system with LNG heat sink for hydrogen production and liquefaction. Energy Conversion and Management, 254, 115266.

[16] Lin, Z., Liu, X., Lao, L., & Liu, H. (2020). Prediction of two-phase flow patterns in upward inclined pipes via deep learning. Energy, 210, 118541.

[17] Shi, Y., Song, X., & Song, G. (2021). Productivity prediction of a multilateral-well geothermal system based on a long short-term memory and multi-layer perceptron combinational neural network. Applied Energy, 282, 116046.

[18] Chitgar, N., Hemmati, A., & Sadrzadeh, M. (2023). A comparative performance analysis, working fluid selection, and machine learning optimization of ORC systems driven by geothermal energy. Energy Conversion and Management, 286, 117072.

[19] Okoroafor, E. R., Smith, C. M., Ochie, K. I., Nwosu, C. J., Gudmundsdottir, H., & Aljubran, M. J. (2022). Machine learning in subsurface geothermal energy: Two decades in review. Geothermics, 102, 102401.

Kastamonu University
Journal of Engineering and Sciences
e-ISSN 2667-8209
http://dergipark.gov.tr/kastamonujes

Visibility of Programming Languages in Turkish Universities: An Analysis of Bologna Information Packages

Hüseyin Demirel*

Department of Managament Information Systems, Ankara Yıldırım Beyazıt University, Ankara, Türkiye
***Corresponding Author:** huseyindemirel@aybu.edu.tr

Received**: October 4, 2025** ◆ Accepted**: December 10, 2025** ◆ Published Online**: December 25, 2025**

Abstract: As of June 2025, the course contents published in the YÖK (Council of Higher Education) Bologna Information Packages of 1,128 information technology–related departments in Türkiye were systematically examined to identify programming language references within the curricula. A total of 3,990 individual course records were analyzed, revealing that the most frequently represented languages are C (574; 14.4%) and Python (543; 13.6%), followed by SQL (363; 9.1%), MATLAB (345; 8.6%), Java (342; 8.6%), and C++ (338; 8.5%). In course contents related to web technologies, HTML (256; 6.4%), CSS (230; 5.8%), and JavaScript (207; 5.2%) appear at moderate levels, while contemporary languages such as Kotlin (7), Swift (5), Go (3), and Rust (2) collectively account for only 0.4% of all references. These findings indicate that curricula in Türkiye remain predominantly focused on traditional languages, with data- and computation-oriented languages maintaining a strong presence, whereas modern and emerging languages are still marginally represented. Comparative European-level studies, including ESSA–CEDEFOP and GitHub Octoverse reports, similarly show that Python, Java, JavaScript, SQL, C++, and C# are among the most demanded technologies in the industry. These results underline the need to strengthen the alignment between academia and industry by allocating greater curricular space to contemporary languages and ensuring a more balanced integration of modern web and application development components.

Keywords: Bologna Information Package; Programming Languages; Curriculum Analysis; Universities in Türkiye

Türk Üniversitelerinde Programlama Dillerinin Görünürlüğü: Bologna Bilgi Paketlerinin Analizi

Öz: Haziran 2025 itibarıyla, Türkiye'deki 1.128 bilgi teknolojisiyle ilişkili bölümün YÖK (Yükseköğretim Kurulu) Bologna Bilgi Paketlerinde yayımlanan ders içerikleri incelenmiş ve müfredatlar içinde yer alan programlama dili atıfları sistematik olarak analiz edilmiştir. Toplam 3.990 ders kaydı değerlendirilmiş olup, en sık temsil edilen dillerin C (574; %14,4) ve Python (543; %13,6) olduğu belirlenmiştir. Bunları sırasıyla SQL (363; %9,1), MATLAB (345; %8,6), Java (342; %8,6) ve C++ (338; %8,5) izlemiştir. Web teknolojileriyle ilgili ders içeriklerinde HTML (256; %6,4), CSS (230; %5,8) ve JavaScript (207; %5,2) orta düzeyde temsil edilirken, Kotlin (7), Swift (5), Go (3) ve Rust (2) gibi çağdaş programlama dilleri toplamda yalnızca %0,4 oranında yer almıştır. Bulgular, Türkiye'deki müfredatların hâlâ ağırlıklı olarak geleneksel dillere dayandığını, veri ve hesaplama odaklı dillerin güçlü konumunu koruduğunu, buna karşın modern ve yeni nesil dillerin oldukça sınırlı biçimde temsil edildiğini göstermektedir. ESSA–CEDEFOP ve GitHub Octoverse gibi Avrupa düzeyindeki çalışmalar da benzer şekilde Python, Java, JavaScript, SQL, C++ ve C# dillerinin sektörde en fazla talep gören teknolojiler arasında olduğunu ortaya koymaktadır. Bu sonuçlar, akademi ile sanayi arasındaki uyumun güçlendirilmesi, çağdaş dillere müfredatta daha fazla yer verilmesi ve modern web/uygulama geliştirme bileşenlerinin daha dengeli biçimde bütünleştirilmesi gerekliliğini vurgulamaktadır.

Anahtar Kelimeler: Bologna Bilgi Paketi; Programlama Dilleri; Müfredat Analizi; Türkiye Üniversiteleri

1. Introduction

The rapid advancement of information and communication technologies has positioned software development at the core of global strategies, both economically and technologically. In this context, programming languages play a decisive role not only in academic curricula but also in practical applications. However, the existing "mismatch in language preferences" between academia and industry constitutes a significant barrier in terms of digital skills and employability.

In the case of Türkiye, this study examined 1,128 information technology-related departments as of June 2025, analyzing a total of 3,990 course contents. The findings indicate that the most frequently represented programming languages in curricula are C (574; 14.4%) and Python (543; 13.6%), followed by SQL, MATLAB, Java, and C++, all of which are primarily data- and computation-oriented. Conversely, modern languages such as Kotlin, Swift, Go, and Rust account for only 0.4% of the total representation, clearly revealing the limited integration of contemporary programming languages in Türkiye's computing education.

Similar tendencies are evident in the European context. The ESSA–CEDEFOP (2020–2025) project, supported by the European Commission, highlights Java, JavaScript, SQL, HTML, PHP, C++, C#, and Python as the most demanded languages by industry and public institutions [1]. Likewise, the DevStyler (2024) report demonstrates that Python dominates in data science, machine learning, and automation; JavaScript leads in web development; Java is widely adopted in enterprise and Android applications; while C# maintains dominance in gaming and Microsoft ecosystems [2]. In addition, SQL, PHP, and Ruby continue to receive considerable demand in certain sectors. GitMax [3] also lists Python, JavaScript, Java, C#, C++, and PHP as the six most popular languages across Europe, emphasizing their continued strength in both traditional and modern systems.

From a global perspective, the GitHub Octoverse [4] report reveals that Python has surpassed JavaScript to become the most widely used programming language, primarily due to its central role in artificial intelligence, data science, and the Jupyter Notebook ecosystem. The report also indicates ongoing usage of TypeScript, Java, C#, C++, PHP, Shell, C, and Go, while Rust has shown a noteworthy increase in adoption within system programming. Similarly, the TIOBE Index (August 2025) places Python (26.14%) at the top, followed by C (9.03%), C++ (9.18%), Java (8.59%), C# (5.52%), JavaScript (3.15%), and Go (2.11%), reaffirming the global persistence of traditional language preferences [5].

The DevJobsScanner [6] analysis of job postings between January 2023 and September 2024 further supports these findings: JavaScript/TypeScript accounted for approximately 31% of all postings in Europe, followed by Python at 20%. Other prominent languages in development environments included Java (18%), C# (12%), PHP (~10%), along with C/C++ and Ruby. Additionally, the GitHub Octoverse [4] report highlights Rust as a rapidly rising system language, particularly in new technology domains.

Taken together, these results reveal a similar pattern across both Türkiye and Europe: traditional languages remain dominant, while modern languages are still marginal. Therefore, updating curricula, enriching them with programming languages relevant to emerging technological domains, and fostering stronger university–industry collaboration appear essential to address this gap. Similar studies conducted in Türkiye have also highlighted the need for curriculum modernization in engineering education [7-8].

2. Material and Method

This research was conducted to identify the distribution of programming languages included in the course contents of undergraduate programs related to information technologies in Turkish universities. The study was designed within the framework of a descriptive research method and employed the document analysis technique [9].

2.1. Data Source

The dataset was obtained from the Bologna Information Packages of the Council of Higher Education (YÖK) as of June 2025, based on updated course plans and syllabi. Across Türkiye, programs related to information technologies were reviewed, and a total of 1,128 departments were included within the scope of the study. These departments comprised Computer Engineering, Software Engineering, Management Information Systems, Information Technologies, and similar fields [10].

2.2. Data Collection Process

As illustrated in Figure 1, references to programming languages contained in the Bologna Information Packages were systematically examined and recorded. In cases where a course syllabus included more than one programming language, each language was treated as a separate entry. The data obtained from all departments were compiled into an Excel file, as shown in Figure 2, and a total of 3,990 records were included in the analysis [11].

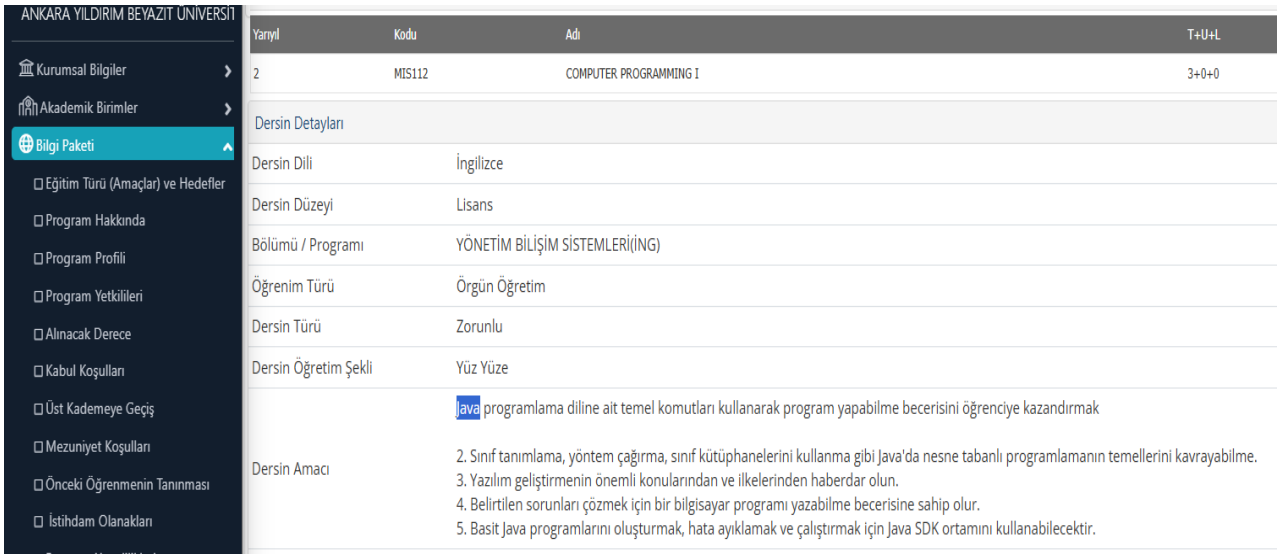

Figure 1. Identification of programming languages in Bologna Information Packages

Üniversite Adı	BÖLÜM ADI	AÇILIŞ TARİHİ	ÜNİVERSİTE TÜ	BÖLÜM İLİ	BÖLÜM D	Müfredattaki Programlama Dilleri													
						C	C++	C#	Java	Pyhton	HTML	ava Scrip	CSS	PHP	R	SQL	MATLAB	Swift	Kotlin
MUDANYA ÜNİVERSİTESİ	BİLGİSAYAR MÜHENDİSLİĞİ BÖLÜMÜ	14.06.2023	VAKIF	BURSA	AKTİF	1	1	1	1							1			
MUDANYA ÜNİVERSİTESİ	ELEKTRİK-ELEKTRONİK MÜHENDİSLİĞİ BÖLÜMÜ	14.06.2023	VAKIF	BURSA	AKTİF	1			1	1									
MUDANYA ÜNİVERSİTESİ	ENDÜSTRİ MÜHENDİSLİĞİ BÖLÜMÜ	02.06.2022	VAKIF	BURSA	AKTİF	1			1	1						1			
MUĞLA SITKI KOÇMAN ÜNİVERSİTESİ	BİLGİSAYAR MÜHENDİSLİĞİ BÖLÜMÜ		DEVLET	MUĞLA	AKTİF	1			1	1	1	1	1			1			
MUĞLA SITKI KOÇMAN ÜNİVERSİTESİ	ELEKTRİK-ELEKTRONİK MÜHENDİSLİĞİ BÖLÜMÜ		DEVLET	MUĞLA	AKTİF	1					1						1		
MUĞLA SITKI KOÇMAN ÜNİVERSİTESİ	ENDÜSTRİ MÜHENDİSLİĞİ BÖLÜMÜ		DEVLET	MUĞLA	AKTİF														
MUĞLA SITKI KOÇMAN ÜNİVERSİTESİ	İNŞAAT MÜHENDİSLİĞİ BÖLÜMÜ		DEVLET	MUĞLA	AKTİF	1													
MUĞLA SITKI KOÇMAN ÜNİVERSİTESİ	MAKİNE MÜHENDİSLİĞİ BÖLÜMÜ		DEVLET	MUĞLA	AKTİF														
MUĞLA SITKI KOÇMAN ÜNİVERSİTESİ	YAPAY ZEKA VE VERİ MÜHENDİSLİĞİ BÖLÜMÜ	22.03.2022	DEVLET	MUĞLA	AKTİF														
MUĞLA SITKI KOÇMAN ÜNİVERSİTESİ	YAZILIM MÜHENDİSLİĞİ BÖLÜMÜ	16.12.2020	DEVLET	MUĞLA	AKTİF	1			1	1	1	1	1			1			
MUĞLA SITKI KOÇMAN ÜNİVERSİTESİ	BİLİŞİM SİSTEMLERİ MÜHENDİSLİĞİ BÖLÜMÜ	13.11.2009	DEVLET	MUĞLA	AKTİF	1		1		1	1	1	1	1		1			
MUĞLA SITKI KOÇMAN ÜNİVERSİTESİ	ENERJİ SİSTEMLERİ MÜHENDİSLİĞİ BÖLÜMÜ	13.11.2009	DEVLET	MUĞLA	AKTİF	1													
MUĞLA SITKI KOÇMAN ÜNİVERSİTESİ	YÖNETİM BİLİŞİM SİSTEMLERİ BÖLÜMÜ	17.10.2012	DEVLET	MUĞLA	AKTİF	1		1	1							1			
MUĞLA SITKI KOÇMAN ÜNİVERSİTESİ	BİLİŞİM SİSTEMLERİ MÜHENDİSLİĞİ BÖLÜMÜ	13.11.2009	DEVLET	MUĞLA	AKTİF	1		1		1	1	1	1	1		1			
MUNZUR ÜNİVERSİTESİ	BİLGİSAYAR MÜHENDİSLİĞİ BÖLÜMÜ		DEVLET	TUNCELİ	AKTİF		1		1		1	1		1		1	1		
MUNZUR ÜNİVERSİTESİ	ELEKTRİK-ELEKTRONİK MÜHENDİSLİĞİ BÖLÜMÜ		DEVLET	TUNCELİ	AKTİF	1	1										1		
MUNZUR ÜNİVERSİTESİ	ENDÜSTRİ MÜHENDİSLİĞİ BÖLÜMÜ		DEVLET	TUNCELİ	AKTİF			1											
MUNZUR ÜNİVERSİTESİ	İNŞAAT MÜHENDİSLİĞİ BÖLÜMÜ		DEVLET	TUNCELİ	AKTİF												1		
MUNZUR ÜNİVERSİTESİ	MAKİNE MÜHENDİSLİĞİ BÖLÜMÜ		DEVLET	TUNCELİ	AKTİF												1		
MUŞ ALPARSLAN ÜNİVERSİTESİ	BİLGİSAYAR MÜHENDİSLİĞİ BÖLÜMÜ	01.12.2010	DEVLET	MUŞ	AKTİF	1		1	1		1	1	1				1		
MUŞ ALPARSLAN ÜNİVERSİTESİ	MAKİNE MÜHENDİSLİĞİ BÖLÜMÜ	01.12.2010	DEVLET	MUŞ	AKTİF														
MUŞ ALPARSLAN ÜNİVERSİTESİ	YAZILIM MÜHENDİSLİĞİ BÖLÜMÜ	31.03.2021	DEVLET	MUŞ	AKTİF	1		1	1		1	1	1				1		
MUŞ ALPARSLAN ÜNİVERSİTESİ	BİLİŞİM SİSTEMLERİ VE TEKNOLOJİLERİ BÖLÜMÜ	31.03.2021	DEVLET	MUŞ	AKTİF	1		1	1		1	1	1				1		

Figure 2. Recording the identified programming languages by department into a Microsoft Excel table

2.3. Data Analysis

The collected data were preprocessed in Microsoft Excel, and typographical errors (e.g., *Python* → *Python*, *Javascript* → *JavaScript*) were corrected. Subsequently, the total frequencies for each programming language were calculated, and percentage distributions were obtained. The findings were then categorized under four groups: traditional languages (C, C++, Java, C#, etc.), data- and computation-oriented languages (SQL, MATLAB, etc.), web technologies (HTML, CSS, JavaScript, PHP, etc.), and contemporary languages (Rust, Go, Kotlin, Swift, etc.) [12].

2.4. Validity and Reliability

In order to minimize errors during the data collection process, all records were subjected to a two-stage verification procedure, and incomplete or ambiguous codings were corrected. Furthermore, recent reports published at the European and global levels [4, 14] were evaluated in a comparative context to support the external validity of the study [13].

3. Result

Within the scope of the study, 3,990 records obtained from the Bologna Information Packages of 1,128 departments in Türkiye were analyzed. The results indicate that the programming languages with the highest representation are C (574; 14.4%) and Python (543; 13.6%). Together, these two languages account for approximately one-third of the total records. They are followed by SQL (363; 9.1%), MATLAB (345; 8.6%), Java (342; 8.6%), and C++ (338; 8.5%). This distribution demonstrates that curricula continue to maintain a strong emphasis on both fundamental software development and data-/computation-oriented languages.

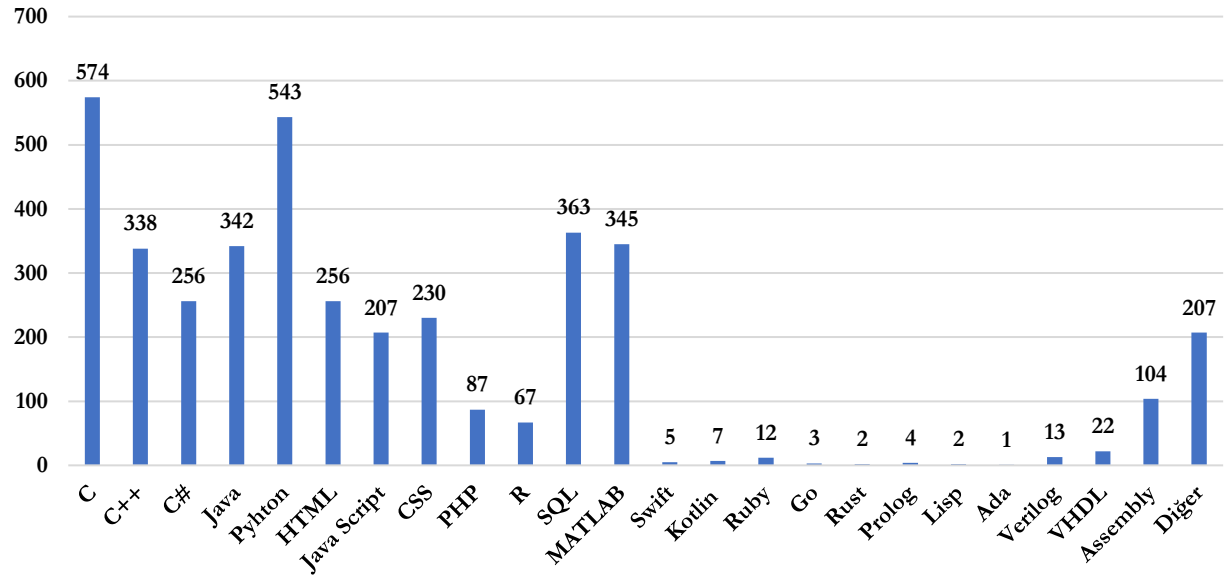

Figure 3. Programming languages offered in related departments of universities in Türkiye

The study also reveals a noticeable representation of web-based programming languages. In particular, HTML (256; 6.4%), CSS (230; 5.8%), and JavaScript (207; 5.2%) stand out as essential components of web technologies courses in information technology departments. On the other hand, PHP (87; 2.2%), another key language in the web ecosystem, is represented at a relatively lower level. This overall pattern suggests that while web development courses remain present in the curricula, they are comparatively less emphasized than core programming languages.

In recent years, contemporary programming languages such as Kotlin (7), Swift (5), Go (3), and Rust (2) have begun to gain wider adoption globally; however, their presence in computing curricula in Türkiye remains extremely limited. The combined representation of these four languages accounts for only 0.4% of the total. This finding indicates a significant deficiency in the integration of modern software development paradigms into university curricula.

The study also identified a low level of representation for other languages, including Assembly (104; 2.6%), R (67; 1.7%), VHDL (22; 0.6%), Verilog (13; 0.3%), Ruby (12; 0.3%), Prolog (4; 0.1%), Lisp (2; 0.05%), and Ada (1; 0.02%). Most of these languages are used in specific domains such as embedded systems, academic research, or logical programming, and therefore appear only in a limited number of courses.

Overall, the findings reveal that course contents in information technology departments in Türkiye are still predominantly based on traditional languages. In particular, C, Java, and C++ continue to serve as the primary tools for teaching fundamental programming skills in engineering-oriented departments, while Python has been widely adopted across diverse disciplines, including both engineering and management information systems. In contrast, the limited representation of contemporary languages stands out as a noteworthy gap when compared with recent reports at the European and global levels [4, 6, 14]. These reports highlight the growing adoption of modern languages such as Rust, Go, and Kotlin, especially in areas such as artificial intelligence, data science, mobile development, and cloud-based applications. Consequently, the minimal integration of these languages into Turkish curricula may be considered a substantial shortcoming in terms of alignment with international technological trends.

4. Discussion

This research, based on the analysis of course contents from 1,128 information technology-related departments in Türkiye, has revealed the distribution of programming languages within university curricula. The findings demonstrate that traditional programming languages (C, Java, C++, C#) continue to be predominantly utilized, while Python has achieved a strong interdisciplinary position, being widely adopted in both engineering and management information systems. In contrast, the representation of contemporary languages (Kotlin, Swift, Go, Rust) remains notably limited.

Comparable trends have been reported at the European level. The ESSA–CEDEFOP project and other recent reports emphasize that Java, JavaScript, SQL, C++, C#, and Python remain at the forefront in terms of industry demand [14]. The GitHub Octoverse [4] report further supports these results, highlighting that Python has surpassed JavaScript globally to become the most popular language][15]. Nevertheless, the increasing demand for modern languages such as Rust, Go, and Kotlin in Europe contrasts with their near absence in Turkish curricula. Although the level of awareness regarding these languages within the Turkish industry may still be limited, global reports underline the importance of updating curricula not only to address existing sectoral requirements but also to reflect emerging technological trends [16].

In this regard, it is essential to revise the course contents of computing programs in Türkiye in alignment with global technological developments. In particular, the inclusion of contemporary languages associated with artificial intelligence, big data, blockchain, mobile applications, and cloud computing would enhance students' adaptability to the future software ecosystem. Moreover, while web technologies continue to maintain their presence at a basic level, there is a growing need for curricular content that incorporates modern frameworks and languages (e.g., TypeScript).

5. Conclusion

In conclusion, this study has comprehensively revealed the programming language preferences of information technology-related departments in Türkiye through an examination of Bologna Information Packages. The results confirm that traditional languages (C, Java, C++) remain dominant, Python holds a strong interdisciplinary position, and modern languages (Kotlin, Swift, Go, Rust) are represented at a minimal level. These findings highlight the necessity of restructuring curricula to achieve a more balanced distribution of programming languages. Expanding the presence of contemporary languages and modern web/application development tools would enable students to better follow evolving trends in the software ecosystem and improve their preparedness for future professional demands.

Conflict of Interest

The authors declare that they have no competing interests.

Ethics Committee Approval

Ethics committee approval is not required.

Author Contribution

This manuscript is written by single author.

Acknowledgements

I would like to express my gratitude to all individuals and institutions that contributed to the realization of this study. Special thanks are due to my graduate students enrolled in the course Basic Principles of Programming, whose efforts in data collection and preliminary analysis made a significant contribution to the development of this research. Their dedication and collaboration enhanced the reliability of the findings. I also extend my appreciation to the Council of Higher Education (YÖK) for facilitating access to the necessary data during the course of the study.

6. References

[1] ESSA – CEDEFOP. (2021). European software skills alliance report. European Commission.

[2] DevStyler. (2024, March). What Are the Most Demanded Programming Languages in Europe? https://devstyler.io/blog/2024/03/28/what-are-the-most-demanded-programming-languages-in-europe

[3] GitMax. (2023). Top programming languages in Europe. https://www.crossover.com/resources/top-10-in-demand-programming-languages-for-2025-updated and https://www.reddit.com/r/learnprogramming

[4] GitHub. (2024). Octoverse 2024: Python Leads over JavaScript; Rise of Rust. The GitHub Blog. https://github.blog/news-insights/octoverse/octoverse-2024

[5] TIOBE Software. (2025, August). TIOBE index: Programming Language Popularity Rankings. https://www.tiobe.com/tiobe-index

[6] DevJobsScanner. (2024). Top demanded programming languages in Europe (2023–2024). https://www.devjobsscanner.com/blog/top-8-most-demanded-programming-languages-in-europe

[7] Kavuncu, O. (2018). Considerations to be taken into account in statistical applications. Kastamonu University Journal of Engineering and Science, 4(2): 22–26.

[8] Tarman, B. (2011). Development of social studies curriculum in Turkey and John Dewey's effect on the modernization of Turkish education. International Journal of Progressive Education, 7(1), 45-61.

[9] Yıldırım, A., & Şimşek, H. (2016). Sosyal bilimlerde nitel araştırma yöntemleri (10th ed.). Ankara: Seçkin Yayıncılık.

[10] Aydın, A. (2017). Türkiye'de bologna süreci ve yükseköğretimde program geliştirme. Ankara: Pegem Akademi.

[11] Miles, M. B., & Huberman, A. M. (1994). Qualitative data analysis: an expanded sourcebook. Thousand Oaks, CA: Sage.

[12] Creswell, J. W. (2012). Educational research: planning, conducting, and evaluating quantitative and qualitative research. Boston, MA: Pearson.

[13] European Software Skills Alliance (ESSA) – CEDEFOP. (2020–2025). Most Needed Programming Languages. European Commission. Retrieved from: https://www.cedefop.europa.eu/en/project-fiches/european-software-skills-alliance-essa

[14] CEDEFOP. (2024). European software skills alliance (ESSA) final report – Aligning ICT Education with Labour Market Needs. Publications Office of the European Union, Luxembourg.

[15] GitHub. (2024). The state of the Octoverse 2024: The world's most popular programming languages. https://octoverse.github.com/

[16] Stack Overflow. (2024). Developer survey 2024 results – programming, scripting, and markup languages. Stack Overflow Insights. https://survey.stackoverflow.co/2024

Kastamonu University
Journal of Engineering and Sciences
e-ISSN 2667-8209
http://dergipark.gov.tr/kastamonujes

A Prominent Candidate in Natural Product Discovery for Multi-Target Cancer Therapy: Structure-Based Assessment of Hyperforin

Gulsah Aydin*

Department of Chemistry and Chemical Processing Technologies, Ulubey Vocational School, Ordu University, Ordu, Türkiye
***Corresponding Author:** gulsahaydinn@gmail.com

Received: **November 16, 2025** ◆ Accepted: **December 13, 2025** ◆ Published Online: **December 25, 2025**

Abstract: In this study, the binding affinities of nine key phytochemical compounds found in the flora of Turkey on the targets Kirsten rat sarcoma viral oncogene homolog (KRAS), Mouse double minute 2 homolog (MDM2), WEE1 G2 checkpoint kinase (WEE1), fibroblast growth factor receptor 4 (FGFR4), and Poly(ADP-ribose) polymerase 1 (PARP1**)** were comparatively investigated using a structure-based approach. This aimed to uncover natural molecular scaffolds that could simultaneously affect critical axes of tumor progression such as cell proliferation, DNA damage response, and mitotic control. GA-based docking studies were performed on the target structures obtained from the PDB using AutoDock. Binding modes were selected using RMSD clustering, and interaction profiles were examined in detail in 2D and 3D. The results showed that hyperforin stood out by exhibiting the strongest multiple binding performance on the targets KRAS (–8.04 kcal/mol), MDM2 (–9.15 kcal/mol), and WEE1 (–8.29 kcal/mol). Significant affinity for FGFR4 was observed only for hyperforin. Docking results for PARP1 revealed that the investigated compounds did not significantly overlap with the catalytic site. Acetylchiconine, tiliroside, and berberine were considered rational seed cells for derivative development because they offered moderate-to-high binding potential on KRAS and WEE1. Overall, the consistent and strong binding profile of hyperforin along the KRAS–MDM2–WEE1 axis suggests a multilayered suppression strategy that allows simultaneous targeting of three key oncobiological mechanisms: suppression of proliferative signaling, reactivation of the p53-mediated DNA damage response, and control of the G2/M transition. This suggests that the molecule may be a high-potential candidate for preclinical validation.

Keywords: KRAS, MDM2, WEE1, Cancer, Hyperforin

Çok Hedefli Kanser Tedavisi için Doğal Ürün Keşfinde Öne Çıkan Bir Aday: Hiperforinin Yapıya Dayalı Değerlendirmesi

Öz: Bu çalışmada, Türkiye florasında yaygın bulunan dokuz temel fitokimyasal bileşiğin KRAS (Kirsten rat sarcoma viral oncogene homolog), MDM2 (Mouse double minute 2 homolog), WEE1 (WEE1 G2 checkpoint kinase), FGFR4 (fibroblast growth factor receptor 4) ve PARP1 (Poly(ADP-ribose) polymerase 1) hedefleri üzerindeki bağlanma eğilimleri yapı-temelli yaklaşımla karşılaştırmalı olarak incelendi. Böylece hücre proliferasyonu, DNA hasar yanıtı ve mitotik kontrol gibi tümör progresyonunun kritik eksenlerini aynı anda etkileyebilecek doğal moleküler iskeletlerin ortaya çıkarılması amaçlandı. PDB'den elde edilen hedef yapılar üzerinde AutoDock ile GA-tabanlı yerleştirme çalışmaları gerçekleştirildi ve bağlanma modları RMSD-kümeleme ile seçilerek etkileşim profilleri 2-boyutlu ve 3-boyutlu olarak ayrıntılı incelendi. Elde edilen sonuçlar hiperforinin; KRAS (–8.04 kcal/mol), MDM2 (–9.15 kcal/mol) ve WEE1 (–8.29 kcal/mol) hedeflerinde en güçlü çoklu bağlanma performansını sergileyerek açık ara öne çıktığını gösterdi. FGFR4 için anlamlı afinite yalnızca hiperforinde gözlendi. PARP1 için elde edilen yerleştirme sonuçları, incelenen bileşiklerin katalitik bölgeyle anlamlı bir şekilde örtüşmediğini ortaya koydu. Asetilşikonin, tilirosid ve berberin; KRAS ve WEE1 üzerinde orta-yüksek düzeyde bağlanma potansiyeli sunduğu için türev geliştirme açısından rasyonel çekirdekler olarak değerlendirildi. Genel olarak, hiperforinin KRAS–MDM2–WEE1 ekseni boyunca tutarlı ve güçlü bağlanma profili, proliferatif sinyallemenin baskılanması, p53 aracılı DNA hasar yanıtının yeniden etkinleştirilmesi ve G2/M geçişinin kontrol altına alınması gibi üç temel onkobiyolojik mekanizmanın eşzamanlı olarak hedeflenmesine olanak tanıyan çok katmanlı bir baskılama stratejisine işaret etmekte olup, molekülün klinik öncesi doğrulamalar için yüksek potansiyele sahip bir aday olabileceğini gösterdi.

Anahtar Kelimeler: KRAS, MDM2, WEE1, Kanser, Hiperforin

1. Introduction

The flora of Turkey is a geography where different ecological zones intersect. This makes Turkey a biogeographic bridge between Europe and Western Asia, not only in terms of taxonomy but also in terms of secondary metabolite diversity. This rich ecological diversity allows the cultivation of a large number of medicinal and aromatic plants that have long been used in folk medicine in Turkey [1]. Although major secondary metabolites have been identified in most of these plants, modern pharmacological evaluations of these metabolites are largely lacking [3]. Evaluation of the major active compounds of plant species commonly used in folk medicine from a molecular oncology perspective is of great importance for the development of targeted therapy strategies in cancer biology. Cancer is a complex disease characterized by the disruption of multilayered signal transduction pathways, DNA repair mechanisms, apoptosis regulation, and cell cycle control [2, 3] . Specific protein targets involved in these processes are key molecular nodes that determine the proliferation, metastasis, and drug resistance capacities of tumor cells . Evaluating not only the general pharmacological activities of naturally occurring phytochemical compounds but also their inhibitory potential on specific molecular targets is of critical importance in revealing the potential of these compounds and their possible derivatives as therapeutic candidates in certain types of cancer [4, 5]. Thus, not only whether these compounds are alternatives to classical chemotherapeutics, but also their target-specific activities, binding mechanisms and molecular interaction profiles can be scientifically clarified. This assessment requires demonstrating the relationship of natural products to specific targets meaningful in cancer biology, beyond mere phenotypic observations. Structure-based drug discovery (SBDD) approaches offer an important methodological framework in this regard.

SBDD exploits the high-resolution structure of the target protein to map covalent and non-covalent binding pockets and rationally narrows the chemical space using virtual screening and fragment-based approaches, significantly reducing wet-lab workload, cost, and iteration time. In the structure-based optimization process, predictions of the absorption, distribution, metabolism, excretion, and toxicity profiles (ADME/T) of compounds are evaluated early, allowing for optimization of selectivity and adaptability parameters [4]. Two striking examples of this in clinical oncology are the poly(ADP-ribose) polymerase 1 (PARP1) inhibitor olaparib and the Kirsten rat sarcoma viral oncogene homolog (KRAS) inhibitor sotorasib. Olaparib, developed based on the nicotinamide adenine dinucleotide (NAD^+) binding pocket of the PARP catalytic domain, has validated the principle of synthetic lethality in human studies and has become a standard of care in BRCA1/2-defective tumors [6, 7]. Similarly, the structural discovery of the covalent targetability of the Switch-II pocket (SII-P) in KRAS-G12C led first to the identification of lead covalent binders, followed by the rational design of the clinical candidate sotorasib and the demonstration of antitumor activity in early-phase studies [8-10].

Prospective studies have reported experimental validation of a significant portion of computationally prioritized candidate molecules in in vitro biological tests [4, 11]. There are also examples where studies of top-ranked compounds provide significant validation [12]. Thanks to the computational filter, only candidates with chemical advantage, target pocket compatibility, and rational binding energy are considered for laboratory evaluation; This significantly reduces experimental workload, synthesis costs, and time. In vitro validation rates are improved thanks to SBDD-specific outputs, such as atomic-level prediction of target protein-ligand interactions, identification of hydrophobic/electrostatic contacts, and optimization of binding modes. In this context, SBDD not only enables early identification of effective compounds but also enables more informed chemical scaffold optimization, early detection of selectivity issues, and more rational management of off-target risks. This significantly contributes to faster understanding of structure-activity relationships in highly chemically diverse groups such as natural products—especially compounds containing multiple pharmacophores—and to the prioritization of promising scaffolds.

Therefore, studying the major active compounds of traditional medicinal plants in the Turkish flora using such target-oriented approaches makes significant contributions both to the identification of new molecular candidates for cancer treatment and to the integration of ethnobotanical knowledge with modern pharmacology [1, 2, 4, 5]. In this context, the main criteria for selecting the plants to be studied were their widespread natural distribution in Turkey, the isolation and reliable structural characterization of their major active compounds, and the extremely limited target-level mechanistic data in the context of cancer biology [1, 2]. Thus, it was aimed to scientifically evaluate the phytochemical diversity of the indigenous flora, to elucidate target-based interactions that are missing in the literature, and to establish a scientific basis that will guide research on introducing new derivatives based on the phytochemicals found to be effective with further studies to the pharmaceutical industry[4, 5]. In this direction, Berberis crataegina, Arnebia densiflora, Anatolian-endemic Hypericum, Verbascum, Lamium, and Sideritis species representing the pharmacological potential of the Anatolian flora; as well as Centaurea urvillei subsp. stepposa, Astragalus species endemic to Turkey, Quercus species, and Punica granatum were selected as the main plants evaluated in this study [1, 13-17].

Berberis crataegina DC. is a species that grows naturally in the semiarid, rocky steppe ecosystems of Turkey, primarily in Central Anatolia. In traditional uses, the fruit and root bark are used for hypertension, hyperlipidemia, diabetes, gastrointestinal disorders, and commonly for "blood purification" [18-20]. The root and bark tissues of the plant are rich in isoquinoline alkaloids, especially berberine. Berberine has been isolated in pure form, its structural properties have been confirmed, and it has been intensively investigated for its broad pharmacological activities. The antioxidant, antimicrobial, antidiabetic, and cardioprotective effects of berberine have been reported in detail in the literature [20-22]. In the context of oncology, berberine has been shown to suppress cellular proliferation, induce apoptosis, reduce metastatic properties, and target various signaling pathways that contribute to treatment resistance [22, 23]. It has been reported that berberine can overcome resistance to

epidermal growth factor receptor (EGFR) tyrosine kinase inhibitors (e.g., osimertinib) in resistant lung adenocarcinoma models, particularly through MET tyrosine kinase signaling. These findings suggest that berberine can suppress pathways associated with tumor progression and therapeutic refractoriness, such as MET, signal transducer and activator of transcription 3 (STAT3), and NF-κB [23].

Arnebia densiflora (Nordm.) Ledeb is a medicinal plant belonging to the Boraginaceae family, distributed in the steppe and semi-arid regions of Eastern and Southeastern Anatolia. Extracts obtained from the roots of the plant are used in folk medicine, especially for wound healing, burn treatment, and the removal of various skin lesions. Traditional preparations prepared for this purpose are mostly in the characteristic "red oil" form, prepared by maceration in oil [24]. The root pigments contain biologically active naphthoquinone compounds, mainly shikonin and acetylated shikonin derivatives. These compounds have been isolated in pure form, their chemical structures have been characterized, and their pronounced cytotoxic effects have been confirmed in various in vitro models [25, 26]. In the cancer literature, acetylshikonin, one of the shikonin derivatives, has been shown to inhibit the serine-threonine kinase TOPK/PBK, particularly in colon cancer cells. This inhibition causes cell cycle arrest and, consequently, suppresses tumor growth. It has also been reported that acetylshikonin interferes with microtubule polymerization in hepatocellular carcinoma (HCC) models, leading to G2/M phase blockade, thus creating a phenotype similar to antimitotic agents [26].

Hypericum species (especially taxa endemic to Anatolia) are medicinal plants widely found in rural and mountainous areas of Turkey. These species possess a rich secondary metabolite profile, primarily consisting of essential oils, prenylated phloroglucinols (e.g., hyperforin), and naphthodianthrone class compounds (e.g., hypericin). Traditional uses include wound healing, anti-inflammatory activity, mild sedative/antidepressant, and antiseptic applications [27, 28]. Hypericum perforatum, in particular, is the best-studied species due to these pharmacological activities. Among the prenylated phloroglucinols, hyperforin has attracted attention in the modern literature for its anticancer potential. Hyperforin and structurally related derivatives have been shown to reduce cell viability, limit invasion and migration capacity, and promote apoptosis in melanoma, triple-negative breast cancer (TNBC), and other aggressive tumor models [29, 30]. It has been reported that the mechanism of these effects is mainly through the suppression of transcription factors involved in tumor progression and metastasis, such as nuclear factor kappa B (NF-κB), signal transducer and activator of transcription 3 (STAT3), and activator protein-1 (AP-1), thus inhibiting proliferative and inflammatory signaling axes [29].

Verbascum (mullet) species naturally occur in a wide geographical area in Turkey, extending from the semiarid areas of Central Anatolia to the high altitudes of Eastern Anatolia [31, 32]. These species are used in folk medicine as an emollient and expectorant, especially against respiratory tract infections, cough, and throat irritation, and also for anti-inflammatory and antimicrobial purposes [31, 33]. In terms of chemical composition, verbascoside (acteoside), a phenylethyloid glycoside, has been identified as the major compound in Verbascum species. Verbascoside is notable for its potent antioxidant, antimicrobial, and anti-inflammatory properties [34-36]. It has also been associated with the suppression of proliferation, reduction of cell migration, and induction of apoptosis in various cancer cell models [36, 37]. The mechanism of these anticancer effects has been reported to be related to the suppression of NF-κB and mitogen-activated protein kinase (MAPK) pathways. However, based on current knowledge, there is no confirmed evidence that verbascoside exhibits direct binding or enzymatic inhibition of oncogenic driver targets such as KRAS, Mouse double minute 2 homolog (MDM2), WEE1 G2 checkpoint kinase (WEE1), PARP1, or fibroblast growth factor receptor 4 (FGFR4).

Lamium (Ballibaba) species have been applied in Turkish folk medicine in the form of infusions or poultices to stop bleeding, accelerate wound healing, and reduce inflammation. Furthermore, young shoots of some species have been reported to be consumed for food purposes [38]. Phytochemically, Lamium extracts contain a rich class of compounds, primarily phenylethyloid glycosides (e.g., verbascoside) and acylated flavonoid glycosides (e.g., tiliroside, the p-coumaroyl-glucoside form of the kaempferol nucleus) [39]. These molecules have been characterized for their potent antioxidant and anti-inflammatory activities [39, 40]. Furthermore, Lamium-derived phenylethyloids and flavonoids have been reported to exhibit anticancer biological effects such as suppression of proliferation (antiproliferative/cytotoxic activity), inhibition of phosphatidylinositol 3-kinase/protein kinase B (PI3K/Akt) and nuclear factor kappa B (NF-κB) pathways, reduction in matrix metalloproteinase-2 and -9 (MMP-2 and MMP-9) levels and suppression of cell migration in various tumor cell models [40, 41]

Sideritis species, commonly known as "mountain tea" or "yayla tea" among the public in Turkey, are medicinal plants that grow naturally on high-altitude, rocky, calcareous or arid to semi-arid slopes. They are particularly widespread in Southeastern Anatolia, the mountainous regions of Central Anatolia, and the arid lower zones of the Mediterranean; their flowering aerial parts are traditionally consumed as a tea [42, 43]. In folk medicine, they have been reported to be used for colds, gastrointestinal complaints, wound healing, rheumatic pain, blood pressure regulation, and immune-boosting purposes [43, 44]. Phytochemical studies have shown that the flowering aerial parts of Sideritis species contain mainly acyl-flavonoid glycosides, diterpene derivatives (especially ent-kaurene-type diterpenoids), and essential oils [44-46]. The anti-inflammatory, antimicrobial, and antioxidant effects of these components have been supported by numerous studies [45, 46]. In the context of cancer, Sideritis extracts have been reported to be associated with decreased cell viability, suppressed migration, and decreased MMP-2/-9 levels in some breast and colon cancer cell models. These effects are thought to occur through inhibition of the PI3K/Akt and NF-κB axes, important signaling pathways associated with cell proliferation and metastasis [46].

Centaurea urvillei subsp. stepposa is one of the characteristic species of the Anatolian steppe flora, and its dried young shoots are consumed as "wild food" in some regions [47]. Phytochemical analyses on Turkish populations show that this subspecies is rich in chlorogenic acid (5-O-caffeoylquinic acid), di-caffeoylquinic and tri-caffeoylquinic acid derivatives, and apigenin glycosides [48]. Polyunsaturated fatty acids such as linoleic acid have also been reported to be among the dominant components in the fatty acid fraction. Methanolic extracts have been shown to exhibit significant antioxidant capacity and high free radical scavenging activity [48, 49]. In initial anticancer screening studies, extracts of Centaurea urvillei subsp. stepposa were reported to exhibit effects related to proliferation suppression and cell cycle arrest in colon and liver cancer cell lines. However, the specific molecular targets or signaling pathways through which these antitumor effects occur have not yet been elucidated; therefore, further investigation at the mechanistic level is needed.

Astragalus species (trachea) are widely distributed in Turkey, especially in the semiarid plateau and steppe ecosystems of Central and Eastern Anatolia, and are notable for their high taxon diversity in the country's flora; the genus is also known for its high endemism rate [50]. Pharmacognostically, the major quality indicator of Radix Astragali, used as the root drug, is Astragaloside IV (AS-IV). AS-IV content is especially high in Astragalus membranaceus and the related taxon A. mongholicus; for this reason, these two species are defined as the main source plants in pharmacopoeias and standardization in commercial preparations is mostly made based on the AS-IV amount [51-53]. Indeed, comparative phytochemical analyses performed on the roots of A. membranaceus and A. mongholicus have shown that AS-IV is present at high levels, and this compound is a distinct "marker" saponin that is central to pharmacological research [52, 53]. AS-IV; It has been intensively studied for its versatile biological functions, such as immunomodulation, anti-inflammation, cardioprotection, and antitumor activity. In contrast, AS-IV has either not been detected at all or has only been reported at trace levels in many native Astragalus species naturally distributed in Turkey [54]. This makes the selection of A. membranaceus as the representative ligand of AS-IV rational from both pharmacognostical and pharmacological perspectives.

Quercus species have a wide geographical distribution in Anatolia, and leaf, bark, and gall fractions have historically been valued both as sources of tannins and as medicinal drugs. In folk medicine, these preparations have been used primarily for their antidiarrheal, astringent, antiseptic, and wound-healing properties [55]. Phytochemically, Quercus species are rich in polyphenolic tannins, particularly those with a high degree of galloyl esterification; pentagalloyl glucose (PGG) is one of the best-characterized examples of this class [56]. PGG and related gallotannins have been shown to exhibit multiple antitumor activities in various cancer cell lines. These compounds have been reported to suppress transcription factors involved in cell survival, inflammation, and metastasis, particularly STAT3 and NF-κB, and to limit proliferation and induce apoptosis in prostate, breast, colon, and glioblastoma cells [16, 57]. PGG has also been reported to reduce the levels of MMP-2 and MMP-9, which are associated with metastasis [16, 57]. These findings indicate that gallotannins derived from Quercus species have significant biological potential in the context of molecular oncology.

Punica granatum L. (pomegranate) is a species widely cultivated in Turkey, particularly in the Aegean and Mediterranean regions, and its fruit and peel have medicinal uses. The pomegranate fruit is consumed directly, while extracts obtained from the peel and periseed tissue are used in folk medicine for anti-inflammatory, wound healing, gastrointestinal regulatory, and immune-boosting purposes [58]. Phytochemically, pomegranate peel contains high amounts of ellagitannins, among which punicalagin (A/B isomers) has been identified as the most prominent compound [59]. Punicalagin and its derivatives are notable for their potent antioxidant and anti-inflammatory biological profiles. Preclinical studies have shown that punicalagin suppresses proliferation, induces apoptosis, and reduces levels of invasion and metastasis markers MMP-2, MMP-9, and vascular endothelial growth factor (VEGF) in prostate, colon, breast, and lung cancer cell lines [60-62]. Punicalagin has also been reported to suppress angiogenesis [62]. These findings suggest that punicalagin can produce antitumor effects by targeting multiple signaling pathways and that pomegranate peel fractions offer remarkable potential in terms of molecular oncology.

Consistent with phenotypic results, suppression of critical oncogenic pathways such as PI3K/Akt, NF-κB, MAPK, and STAT3 has been observed in certain plants [63-66]. However, there is no reliable literature confirming these effects through direct interaction or inhibition of proteins such as KRAS, MDM2, WEE1, PARP1, and FGFR4, which are among the priority clinical targets in cancer biology. This situation therefore demonstrates a significant gap in expanding existing findings at a mechanistic level. In this context, the use of structure-based computerized screening (SBDD) approaches will reveal potential interactions of natural compounds with clinical priority targets, thus clarifying existing phenotypic observations at the molecular level and providing a rational basis for the development of new therapeutic candidates.

When the structural properties of the major active ingredients of the ten plant species evaluated in the study were examined, it was seen that berberine, acetylshikonin, hyperforin, verbascoside, tiliroside, 3,5-di-O-caffeoylquinic acid, astragaloside IV, pentagalloyl glucose (PGG) and punicalagin components were prominent. Among the isoquinoline alkaloids abundantly found in the root and bark tissue of Berberis crataegina, berberine was identified as the most dominant compound from the chemical and biological perspectives [67, 68]. Among the naphthoquinone pigments found in the roots of Arnebia densiflora, acetylshikonin is one of the best characterized compounds in terms of both its chemical identity and anticancer effects[68]. Among the prenylated phloroglucinols in Anatolian Hypericum species, hyperforin stands out with its anti-inflammatory and antitumor effects. In Verbascum species, verbascoside, a phenylethyloid glycoside class, is found in high amounts and is the best-characterized compound within this group [69]. In Lamium species, verbascoside and tiliroside are the major components of the phenolic fraction, and these two compounds are notable for their strong antioxidant and antiproliferative profiles [70]. In Centaurea urvillei subsp. stepposa, caffeoylquinates are the main compounds determining the phenolic profile; in particular, 3,5-di-O-caffeoylquinic acid has been reported in the highest amounts [71]. Astragaloside IV, one of the triterpenic saponins

found in Astragalus roots, is widely cited as the "main active compound" in the literature due to its immunomodulatory and antitumor activities[52]. Among the galloyl derivatives in the tannin fraction of Quercus species, pentagalloyl glucose (PGG) is notable for its biological activity as the major phenolic tannin [57]. In Punica granatum, among the ellagitannins, punicalagin was identified as the most dominant component in terms of both quantity and pharmacological activity [59]. In this context, the nine major phytochemical compounds—berberine, acetylshikonin, hyperforin, verbascoside, tiliroside, 3,5-di-O-caffeoylquinic acid, astragaloside IV, pentagalloyl glucose, and punicalagin—were computationally evaluated on five molecular targets that regulate fundamental processes in cancer biology, such as proliferation, DNA damage response, genomic stability, and tumor suppression.

As a member of the small GTPase family, KRAS continuously activates the RAF/MAPK and PI3K/Akt signaling pathways, which drive tumor cell-specific features such as cell proliferation, metabolic reprogramming, and invasion. In particular, high rates of G12D, G12V, and G12R mutations are observed in pancreatic ductal adenocarcinoma [72]. These mutations are also known to be common in lung adenocarcinoma and colorectal carcinoma [73]. For many years, the KRAS protein was considered "undruggable," primarily due to its lack of classical small molecule binding pockets and the presence of a smooth surface structure [72, 74]. However, this view has been challenged in recent years; the clinical efficacy of inhibitors targeting the KRAS (G12C) variant has revealed its potential to be classified as "druggable" [75].

MDM2 is the main negative regulator of the tumor suppressor p53 protein; it ubiquitinates p53 and degrades it, thereby suppressing the p53-mediated DNA damage response in the cell. MDM2 is overexpressed or amplified in many solid tumors; This condition is associated with poor prognosis and treatment resistance in liposarcoma, osteosarcoma, glioblastoma, and some breast cancer subtypes [76]. Importantly, although the TP53 gene remains unmutated in some of these tumors, the functional capacity of p53 is silenced due to MDM2 overactivity. Therefore, disrupting the MDM2–p53 interaction and reactivating p53 appears to be an attractive therapeutic strategy. It is theoretically possible that polyphenols and tannin structures selected from the Turkish flora (e.g., pentagalloyl glucose, punicalagin) could bind with high affinity to the hydrophobic pocket where MDM2 interacts with p53; however, high-resolution biophysical binding data or functional inhibition data have not yet been reported [76].

WEE1 tyrosine kinase, which functions in the G2/M checkpoint of the cell cycle, is a critical regulator that prevents cells from entering mitosis before DNA damage is repaired. WEE1 dependence is particularly pronounced in tumor cells with high replication stress (e.g., cells with high KRAS or MYC activity). Therefore, WEE1 is a prominent checkpoint in aggressive tumors such as pancreatic adenocarcinoma, high-grade ovarian carcinoma, non-small cell lung cancer, and triple-negative breast cancer [77]. WEE1 inhibitors (e.g., adavosertib) are available and are being investigated in combination with DNA-damaging approaches such as platinum chemotherapy or radiotherapy. However, there is no systematic literature demonstrating that selected natural compounds from the Turkish flora (e.g., naphthoquinone derivatives or acyl-flavonoid structures) directly bind to the WEE1 kinase domain or inhibit CDK1 phosphorylation; This makes WEE1 an as yet untested target for these compounds.

PARP1, which plays a central role in the DNA repair network, acts as a sensor and catalyst in the repair of single-stranded DNA breaks. PARP1 dependence is particularly pronounced in cells with homologous recombination defects; in this context, PARP1 inhibitors (e.g., olaparib) have entered clinical use in breast and ovarian cancers. Furthermore, PARP1 activity has been shown to be increased in prostate cancer, glioblastoma, and other tumors with high DNA damage stress; therefore, the need for next-generation PARP1 modulators continues [78]. Mechanistic data regarding the direct binding of compounds selected from the Turkish flora to the PARP1 catalytic pocket and inhibition are quite limited. Finally, FGFR4, a member of the receptor tyrosine kinase family, has been identified as an oncogenic axis promoting proliferation, invasion, and metastasis, particularly in hepatocellular carcinoma and cholangiocarcinoma, through overactivation of the FGF19–FGFR4 pathway. Therefore, selective FGFR4 inhibitors (e.g., BLU-9931, FGF-401) are among the strategies being developed for liver cancer treatment [79]. However, mechanistic data regarding the high-affinity binding of natural products to the FGFR4 kinase domain are still limited.

The common feature of these five molecular targets is their central role in many tumor types that are resistant to treatment and have high mortality rates. KRAS, MDM2, WEE1, PARP1, and FGFR4 are involved in fundamental biological axes at the intersection of cell proliferation, DNA damage repair, apoptosis regulation, and signal transduction. Therefore, these proteins represent the nodes of the molecular resistance mechanisms underlying oncological failure in the clinic. However, the direct molecular interactions of the nine natural compounds isolated from the Turkish flora evaluated in this study with these targets have not been systematically evaluated. This deficiency has led to the study examining natural compounds only for their phenotypic effects (e.g., proliferation suppression, apoptosis induction, or migration reduction), while the protein targets through which these effects occur have often remained unclear. Therefore, the in silico study of the nine selected compounds on five critical targets fills an important scientific gap by revealing the potential binding sites, inhibitory motifs, and possible mechanisms of action of the natural products. This approach enables the rich chemical diversity of the Turkish flora to be considered not only as a pharmacological resource but also as a molecular interaction platform targeted at clinically prioritized oncological targets. The results obtained will not only illuminate the targeted roles of these natural products in cancer biology but also guide the design of new derivatives based on structural data.

2. Materials and Methods

2.1. Docking Simulations

Docking simulations were performed using the AutoDock Vina software, known for its hybrid search strategies that include genetic algorithms, particle stacking optimization, and simulated annealing approaches [80-82]. AutoDock Vina's scoring function uses knowledge-based potentials combined with parametric components derived from experimental data to evaluate ligand–receptor interactions. This brings the method closer to realistically mimicking biological binding modes[83]. The key inputs of the scoring function are built on relational information obtained from the conformational sequences of receptor–ligand complexes, experimental binding energies, and extensive affinity datasets.

Before docking simulations, all protein structures obtained from the Protein Data Bank (PDB) were edited in the UCSF ChimeraX environment to remove unnecessary components and maintain three-dimensional integrity[84]. In this step, nonstandard residues, heteroatoms, and bonds were systematically removed. The cleaned protein models were then opened in AutoDock Tools 1.5.7, where the structures were completed with water molecules and missing hydrogen atoms and charges were removed to make the system more energetically stable. Subsequently, the docking space was constrained by defining a grid box to encompass the target active site using AutoDock Tools 1.5.7 [85]. The grid boxes defined for each target protein were created by referencing the centroid coordinates of the co-crystal ligands defining the active site in the corresponding PDB structures. The grid box was positioned to cover the entire native binding niche, verified by repositioning analysis during the validation phase, and a root-mean-square deviation (RMSD) tolerance threshold of 2.0 Å was adopted to ensure an acceptable reproducibility range. Allowing rotational groups in the active site to rotate allowed for more realistic modeling of binding conformations through side chain flexibility.

During ligand preparation, both standard ligands and phytochemical compounds were optimized using Avogadro software and then imported into AutoDock Tools 1.5.7 for docking [86]. Thus, all ligands were conformationally optimized, their atomic integrity ensured, and the necessary loading processes were completed.

A genetic algorithm-based (GA-based) search strategy was applied for each protein during the docking simulations. The genetic algorithm was chosen because of its ability to overcome local minima pitfalls in large and complex search spaces, its ability to provide a broader conformational sampling through population-based evolutionary optimization, and its more efficient search for global optima compared to similar alignment methods. This method allows for the exploration of binding potentials at different topological sites on the receptor surface by varying the conformations of ligands using random mutation, crossover, and selection principles [87, 88]. The maximum number of evaluations in the simulations was set to "medium," and the number of GA runs for each simulation was configured to be 100. Unlike Darwinian GAs, the Lamarckian GA approach was chosen as the output type, as it allows conformational improvements gained during the local search process to be transferred back to the genetic pool, allowing subsequent generations to proceed from a more refined starting population [82, 89]. This process increases computational efficiency by integrating global search and local refinement stages, thus enhancing the chance of reaching conformations with high binding probability, particularly in systems where receptor-ligand interactions can be multimodal.

After the simulations were completed, tools such as AutoDock Tools, UCSF ChimeraX [84], and Discovery Studio Visualizer [90] were used to evaluate binding modes [91]. These tools allowed for three-dimensional analysis of hydrophobic and polar contact points, hydrogen bonds, electrostatic clustering, and amino acid-level orientations; the results were presented in a visually and analytically reportable form.

2.2. Selection of Crystal Structures of Proteins

Because the reliable representation of the three-dimensional atomic coordinates of target proteins is critical in molecular docking studies, the structures of the proteins to be evaluated were obtained from the Protein Data Bank (PDB) database[92-94]. In structure selection, the target proteins were considered to be of human origin, presented at crystal or cryo-EM resolution that experimentally verifies the geometry of the active site, include substrate or inhibitor-bound conformations whenever possible, and define the boundaries of the binding pocket with high spatial accuracy[95-97]. Therefore, PDB structures, widely accepted as references in the literature and suitable for evaluating inhibitor binding models, were selected.

For KRAS, the crystal structure PDB ID: 6OIM was chosen because it defines the boundaries of the Switch-II allosteric pocket with high spatial accuracy while presenting the G12C mutation in the GDP-bound conformation, contains the binding mode solved by sotorasib, and is considered a standard reference in modern G12C-focused structure-based design studies with a resolution of ~2.3 Å [9, 10, 98]. For MDM2, the structure PDB ID: 5ZXF was chosen because it clearly reflects the atomic details of the binding niche governing the hydrophobic localization of the p53 transactivation motif, is co-crystallized with a nutlin-like inhibitor, and allows for the evaluation of hydrophobic contact regions and aromatic stacking at ~1.9 Å resolution [99, 100]. For WEE1, the PDB ID: 5V5Y structure was chosen because it realistically conveys the docking of the catalytic kinase domain with an ATP-competitive ligand and preserves the inhibitor-compatible conformation of the activation loop, allowing for reliable modeling of binding configurations. This structure has been reported in the literature as one of the widely used templates for structure-based development of WEE1 inhibitors [101, 102]. For FGFR4, the PDB ID: 6NVK structure was chosen, in which the tyrosine kinase domain is resolved in complex with a selective inhibitor. This structure is

suitable for structure-based inhibitor design because it clearly demonstrates the hinge-gatekeeper subassemblies and represents the hydrogen bonding/hydrophobic subcompartments of the active pocket at a resolution of ~2.8 Å [103-105]. For PARP1, the crystal structure PDB ID: 7KK3, which co-crystallizes the catalytic ADP-ribose transferase domain with an NAD+ mimetic inhibitor, was chosen. This structure was chosen because it conveys the architecture of the catalytic niche with high spatial accuracy and allows for reliable assessment of the ionic and hydrophobic subcompartments involved in the ribosylation mechanism at a resolution of ~2.4 Å [78, 106].

3. Results and Discussion

In this study, the binding profiles of nine major phytochemical compounds selected from the flora of Turkey on five molecular targets representing fundamental nodes of cancer biology—KRAS (PDB ID: 6OIM), MDM2 (PDB ID: 5ZXF), WEE1 (PDB ID: 5V5Y), FGFR4 (PDB ID: 6NVK), and PARP1 (PDB ID: 7KK3)—were evaluated using a molecular docking approach. During the molecular docking process, a genetic algorithm (GA) run was set at 100, and the resulting poses for each ligand were evaluated according to their clustering (RMSD-based cluster) distribution (Supplementary Figures 1-4). When generating tables reporting binding scores, the pose in the cluster with the highest population frequency for the relevant ligand was selected as the representative conformation (Table 1). Particularly prominent binding affinities were observed for KRAS, MDM2, WEE1, and FGFR4, while generally low interaction energies were observed for PARP1. Among the evaluated ligands, hyperforin from Hypericum perforatum stood out as the most remarkable molecule, exhibiting both versatility and high affinity.

3.1. Comparative Binding Affinity and Interaction Profile of Ligands Targeting KRAS-G12C (PDB ID: 6OIM)

Among phytochemical compounds, hyperforin (–8.04 kcal/mol) stood out as the ligand with the highest binding affinity to the Switch-II pocket (SII-P) region of KRAS (Table 1). Based on the binding pose of sotorasib in the 6OIM crystal structure, the –8.2 to –9.5 kcal/mol band is frequently referenced in redocking experiments, which represent an operational lower threshold for strong inhibitor binding [107]. Therefore, hyperforin's energetic positioning at –8 kcal/mol suggests that it can interact significantly with KRAS at the small-molecule level, indicating a binding strength rarely seen in natural product chemistry.

Table 1. Docking score results of selected phytochemical ligands against cancer-related target proteins (kcal/mol)

Botanical Source	Phytochemical Ligand	Target Proteins (PDB ID)				
		KRAS (6OIM)	MDM2 (5ZXF)	WEE1 (5V5Y)	FGFR4 (6NVK)	PARP1 (7KK3)
Berberis crataegina	Berberine	-7.00	-5.50	-6.80	-5.30	-3.99
Arnebia densiflora	Acetylshikonin	-6.99	-5.37	-7.29	-5.89	-3.73
Hypericum perforatum	Hyperforin	-8.04	-9.15	-8.29	-7.15	-3.39
Verbascum spp.	Verbascoside	-6.24	-4.16	-4.48	-3.11	-0.64
Sideritis spp.	Tiliroside	-6.91	-4.82	-7.08	-3.76	-1.95
Centaurea urvillei	Isochlorogenic acid A	-3.79	-5.35	-5.67	-4.88	-2.48
Astragalus membranaceus	Astragaloside IV	-5.66	-7.94	-6.09	-5.22	-0.12
Quercus spp.	Pentagalloylglucose	+0.58	+0.95	+0.96	-3.20	+4.56
Punica granatum	Punicalagin	-3.82	-4.78	-2.71	-1.93	+2.56

Hyperforin's positioning in the –8 kcal/mol band demonstrates a significant advantage compared to other natural KRAS binders reported in the literature. For example, plant metabolites such as limonene and β-sitosterol have reported KRAS SII-P binding scores ranging from –6.0 to –6.8 kcal/mol, while pentacyclic triterpenoids such as oleanolic acid and ursolic acid are reported to be around –6.5 [108]. The binding affinities of polymethoxyflavones such as nobiletin and tangeretin generally remain at –6.2 to –7.1 kcal/mol [109].

Sotorasib (AMG 510) and adagrasib (MRTX849) are the two most potent KRAS G12C inhibitors with clinical validation. In silico studies have reported values ranging from -8.2 to -9.6 kcal/mol for sotorasib and -8.5 to -10.1 kcal/mol for adagrasib [107, 110, 111]. Hyperforin's -8.04 value is positioned near the lower band of sotorasib. Although this compound lacks specific covalent binding potential to the G12C variant, its noncovalent allosteric capacity is thought to create a potential interaction window for more common and clinically aggressive variants such as KRAS-G12D/G12V [10]. Among the other phytochemicals evaluated in the study, berberine (–7.00 kcal/mol), acetylshikonin (–6.99 kcal/mol), and tiliroside (–6.91 kcal/mol) exhibited significant, but more limited, affinities than hyperforin. These values are similar to the previously reported

KRAS binding of common phytochemicals such as quercetin (–6.4 to –7.1), catechin (–6.0 to –6.6), and curcumin (–6.5 to –7.3)[112-114]. Therefore, berberine, acetylshikonin, and tiliroside may offer a suitable starting platform for combination or derivative generation strategies rather than for KRAS-directed "single agent" inhibitory effects. Berberine has reported KRAS-network-like phenotypic effects, particularly through modulation of STAT3, AMPK, and ERK; the present binding score provides an in silico anchor consistent with these reduced proliferative effects [115]. Acetylshikonin has been shown to induce G2/M suppression, particularly through microtubule dynamics and topological stress, and may offer potential functional complementarity in KRAS-altered pancreatic models [116, 117]. Recent studies reporting that tiliroside can attenuate KRAS-signaling-related cellular stress responses are consistent with the binding affinity observed here [118].

The binding mode of hyperforin in the KRAS G12C structure revealed the presence of a dense network of hydrophobic and polar contacts prominently located within the Switch-II pocket (SII-P) (Figures 1–2). In the 3D binding view (Figure 1), the molecule's oxygen-containing carbonyl groups were assessed to stabilize its position in the binding cavity by forming directed carbon-hydrogen contacts with Gln61 and Gln99. These interactions were thought to enhance electrostatic complementarity with polar residues on the inner surface of SII-P and support the axis of ligand entry into the pocket. Hyperforin's conjugated aliphatic backbone establishes numerous van der Waals/alkyl contacts with Ala11, Val9, Ala59, Ile100, Gly10, and Gly60 along the hydrophobic core of the pocket, thus contributing to binding stability (Figure 1). The intense alkyl/π-alkyl interactions observed, particularly with Ile100 and Tyr96, indicated that KRAS localizes toward the back wall of SII-P and receives support from the solvent-enclosed region of the pocket. His95, located at the center of the binding motif, exhibited a characteristic π-sigma orbital-surface interaction with hyperforin, significantly strengthening the ligand's orientation within SII-P (Figure 1). Since His95 has been identified as a critical steric-electronic node in the binding models of KRAS SII-P inhibitors, this contact with hyperforin suggested that it supports the correct orientation of the ligand within SII-P [10].

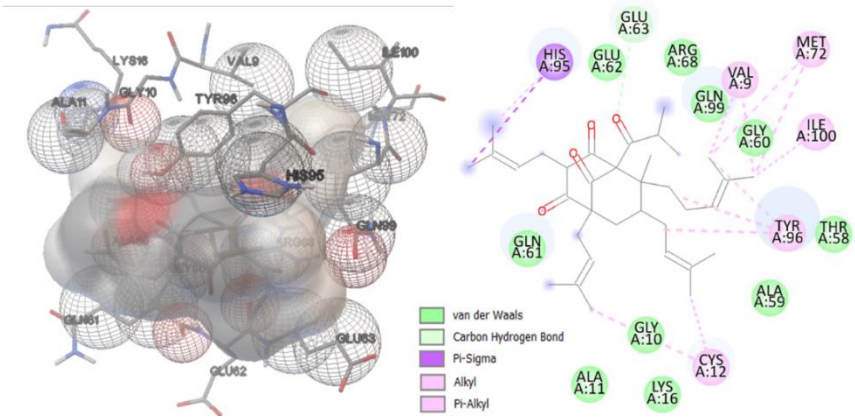

Figure 1. KRAS G12C (PDB: 6OIM) - Hyperforin 3D and 2D binding interaction maps.

Hyperforin is deeply buried in the KRAS SII pocket, where carbon–hydrogen contacts with Gln61/Gln99 and π–σ/π–alkyl interactions with His95 and Tyr96 anchor the ligand in a fixed orientation. The surrounding hydrophobic cluster formed by Ala11, Val9, Ala59, Ile100, Cys12 and neighboring residues creates a compact binding core that explains the high binding affinity observed for KRAS.

2D interaction maps (Figure 1) revealed that aliphatic segments at the terminal ends of hyperforin form additional hydrophobic contacts with Cys12, Met72, Arg68, and Thr58. Alkyl interactions, particularly observed near Arg68, optimized the binding volume by filling the lipophilic corridor along the pocket. These contacts were thought to create a "mechanical locking" effect that limits the molecule's sliding along the wall. 3D surface analysis (Figure 2) visually confirmed hyperforin's deep insertion into the pocket.

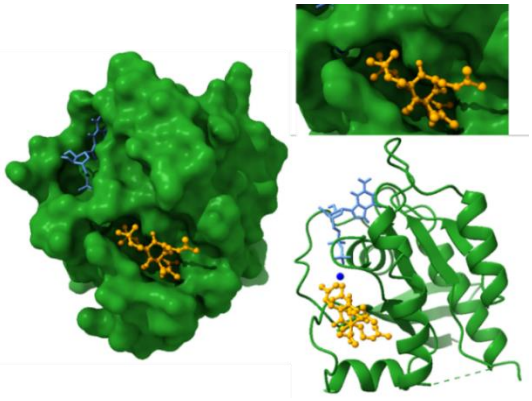

Figure 2. Surface and schematic representation of binding mode of hyperforin to KRAS G12C SII Pocket.

Hyperforin is shown to occupy the deepest region of the SII pocket, adopting a compact orientation that closely follows the curvature of the binding cavity. The ligand's burial beneath the Switch-II loop and its extensive hydrophobic contacts along the pocket floor generate a sterically stable pose that supports the high-affinity binding observed for KRAS.

The compact orientation of the ligand, which did not protrude from the pocket, indicated minimal steric clashes during binding and aligned well with the pocket geometry. When this binding pattern was evaluated as a whole, it was understood that hyperforin strengthened its binding pose within SII-P through polar/π interactions along the Gln61–Gln99–His95 pathway, hydrophobic burial observed in the Ala11–Ala59–Val9–Ile100 loop at the base of the pocket, and flanking alkyl contacts with peripheral residues such as Arg68 and Cys12. This contact cluster was considered important because it demonstrated that hyperforin exhibited a sterically and electronically favorable burial profile in SII-P and established good complementarity with both the central and peripheral regions of the pocket. Indeed, this arrangement provided a contact architecture that strengthened the binding mode by limiting the ligand's intrapocket rotamer maneuvers.

When these binding profiles were evaluated together, it was concluded that hyperforin provides a strong natural scaffold for KRAS, while berberine, acetylshikonin, and tiliroside, due to their moderate binding, are suitable candidates for structural modification studies (Table 1). Hyperforin's energy profile, which is close to the entry window of clinical inhibitors of the sotorasib/adagrasib class, makes this compound a particularly suitable natural template for targeting non-G12C variants. Its potential for effective allosteric modulation without the requirement for covalent binding suggests that it could offer significant clinical benefits, particularly in PDAC and LUAD subtypes where G12D/G12V mutations predominate[10].

They also demonstrate that the currently limited druggability of KRAS can be overcome through a natural product chemistry perspective.

3.2. Comparative Binding Affinity and Interaction Profile of Ligands Targeting MDM2 (PDB ID: 5ZXF)

The binding energies calculated for MDM2 clearly showed that hyperforin (–9.15 kcal/mol) and astragaloside IV (–7.94 kcal/mol) stood out among the ligands. Other phytochemicals were observed to fall below the significance threshold or to fail to adequately mimic the p53 transactivation motif in terms of their binding geometry.

The binding energy of –9.15 kcal/mol for hyperforin suggests that nutlin-3a offers a better score than the typical benchmark range of approximately –8.0 to –8.5 kcal/mol for redocking studies [119]. In a comparative context, computational data suggest that docking scores reported for idasanutlin (RG7388), among clinical candidates, may lie in the range of approximately –7.3 to –7.8 kcal/mol; these values indicate a range similar to or slightly lower than nutlin-3a [120, 121]. In the present study, hyperforin was positioned above this band at –9.15 kcal/mol, indicating that hyperforin could be a promising candidate for a hit inhibitor for MDM2. Furthermore, studies have reported that candidates exceeding the reference co-crystal nutlin-3a in docking scores were identified in extensive natural product screens. These findings are consistent with the general observation that the superiority of hyperforin in our dataset is not a methodological anomaly but rather the energetically advantageous occupancy of natural scaffolds with high hydrophobic complementarity into MDM2 cavities [122]. Astragaloside IV (–7.94 kcal/mol) was the second highest-affinity ligand, with an affinity just around the lower end of the nutlin-benchmark range. In docked poses, multiple hydroxyl groups were observed to extend into side pockets via water-mediated H-bond networks, stabilizing the cavities with a "soft" polar cage. This interaction pattern, while distinct from the hydrophobic stem-centered tight packing similar to spirooxindole, may represent an alternative localization strategy based on the complementarity of the hydrophobic core + polar edge at the p53-MDM2 interface. Therefore, astragaloside IV offers a suitable starting point for the design of derivatives that increase the hydrophobic core density by pharmacophore reduction and glycosidic tail modifications [119, 120]. In contrast, compounds containing bulky, high polarity, or multiple binding groups from the polyphenolic tannin class, such as pentagalloylglucose and punicalagin, remained in the negative/positive region or below significance. This suggests that this class of compounds should be considered in conjunction with upstream/downstream signaling modulation or carrier systems rather than a strategy based on direct pocket occupancy for MDM2 [122].

The binding mode of hyperforin in the MDM2 (PDB: 5ZXF) structure revealed that the molecule is deeply embedded in the hydrophobic pocket that defines the p53 transactivation domain and exhibits a dense hydrophobic-aromatic contact pattern that enhances binding (Figures 3–4). In the 3D binding view (Figure 3), the ligand's intrapocket positioning was observed to be particularly concentrated around Val72, Leu54, Ile61, Ile82, Phe86, and His75. These residues represent the hydrophobic layer that forms the main pharmacophore domain of MDM2. The overlap of hyperforin's extensive aliphatic backbone with this region offered high surface complementarity with the pocket, supporting the binding mode. 2D interaction maps (Figure 3) revealed weak carbon-hydrogen bonds formed between the carbonyl oxygens of hyperforin and His75. This polar contact was thought to stabilize the ligand's orientation within the pocket. Since His75 has also been identified as a contact-making node in the p53 binding motif, the hyperforin–His75 interaction supported that the binding mode may have p53-mimetic properties. Multiple π–alkyl and π–σ interactions observed with Phe86, Phe65, Phe70, Tyr79, and Tyr46 located in the hydrophobic heart of the pocket indicated that hyperforin exhibited tight burial with the aromatic platform; π-stacking, in particular, with Phe86 and Tyr79 enhanced deep pocket localization and contributed significantly to the binding mode (Figure 3). These interactions were considered to be compatible with the binding photophysical motifs of nutlin and its derivatives, classical MDM2 inhibitors. In the peripheral positioning of the ligand, van der Waals contacts observed with Leu33, Ile40, Ile78, Leu82, Met41, Val54, and Gly37 created a broad hydrophobic environment at the pocket rim; This suggests a burial structure that could limit hyperforin's displacement from the pocket and increase binding duration. The compact contact

distribution, particularly observed along the Ile78–Leu82 line, indicated that hyperforin fits into the lower region of the pocket, with the molecule's flexible arms framed by edge residues.

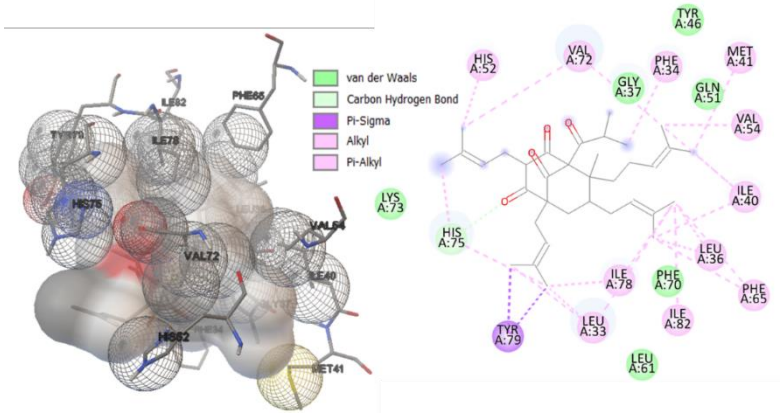

Figure 3. MDM2 (PDB: 5ZXF) - Hyperforin 3D and 2D binding interaction maps.

Hyperforin forms a dense hydrophobic and aromatic contact network within the MDM2 pocket, engaging key residues such as Phe86, Phe65, Tyr79, and His75 that define the p53 transactivation interface. This tight burial across the pocket floor stabilizes the ligand in a p53-mimetic orientation, consistent with its high binding affinity.

The ligand's upper surface was observed to partially cover the pocket entrance, with its aromatic backbone positioned parallel to the broad hydrophobic platform at the pocket base (Figure 4). This compact orientation was evaluated to provide intense contact with the pocket without creating steric clashes and to be compatible with inhibitor binding models that block the p53 binding surface of MDM2. When this binding pattern is evaluated as a whole, hyperforin is stabilized in the MDM2 pocket by weak polar contacts via His75 and forms pronounced π-stacking via aromatic residues such as Phe86, Phe65, Phe70, Tyr79, and Tyr46. It appeared to fill the pocket base with hydrophobic burial along Leu33, Ile40, Ile78, and Leu82.

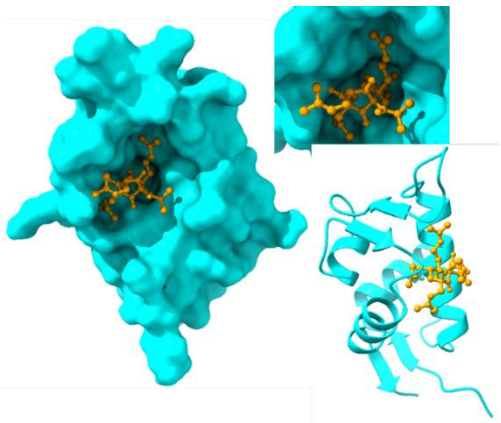

Figure 4. Surface and schematic representation of binding mode of hyperforin to MDM2.

Hyperforin is tightly embedded within the hydrophobic core of the MDM2 pocket, occupying the same sterically recessed region that accommodates the p53 transactivation motif. The ligand's deep burial and extensive aromatic/hydrophobic contacts stabilize a binding pose that is characteristic of high-affinity MDM2 inhibitors.

Hyperforin's -9.15 kcal/mol value suggested that it could mimic the hydrophobic triplet anchor of the spirooxindole architecture with a natural chemical scaffold. This finding provided a strong starting point for non-nutlin-based natural precursor scaffolds in functional p53 reactivation strategies [119, 122]. Astragaloside IV's -7.94 kcal/mol limiting region was noted as a significant result, indicating an open field for derivatization studies where the polar network could be rebalanced in favor of rational hydrophobic cores. Compared to clinical-grade idasanutlin and milademetan, the two natural candidates in our dataset could achieve an energetically competitive level [123-125]. This rational supports translational prioritization in MDM2-amplified and TP53-WT tumors (e.g., dedifferentiated liposarcoma); however, co-crystal-based re-dock/ΔΔG normalization, biophysical binding measurements such as ITC/SPR and cellular functional validations via p53 target gene transactivation are mandatory for progress [119, 123, 124].

3.3. Comparative Binding Affinity and Interaction Profile of Ligands Targeting WEE1 (PDB ID: 5V5Y)

Molecular docking analyses of the WEE1 tyrosine kinase revealed a similarly high binding affinity for hyperforin (–8.29 kcal/mol). It was observed that it formed two-way hydrogen bonds around the hinge region and effectively filled the hydrophobic subspaces in the ATP-binding pocket. This binding pattern was found to be quite similar to the redocking score range of approximately –8.0 to –9.1 kcal/mol reported for adavosertib (AZD1775), a clinical-grade WEE1 inhibitor [126-128]. Furthermore, hyperforin was found to partially stabilize the orientations of Lys328, Glu309, and Asp463 in the phosphotransfer node; Thus, it was assessed that the CDK1-Tyr15 phosphorylation cycle is located in a way that could disrupt the energy landscape.

In binding analyses for WEE1, acetylshikonin (–7.29 kcal/mol), tiliroside (–7.08 kcal/mol), and berberine (–6.80 kcal/mol) showed moderate to high affinity, respectively. These three compounds were found to position themselves around the hinge via single-duplex hydrogen bonds and π-hydrophobic stacking, but they did not achieve the degree of extensive pocket occupancy and side-space complementarity seen in hyperforin. These scores are consistent with the –6.5 to –7.4 kcal/mol range reported in the literature for flavonoid and naphthoquinone class WEE1 binders [128-130]. The placement of acetylshikonin and tiliroside in the upper part of this band indicated that the ATP binding pocket partially meets the pharmacophore requirements (specifically, the hydrophobic core and polar anchor). The binding energy in the ~−6 to −8 kcal/mol band obtained for berberine is consistent with the molecule activating the ataxia-telangiectasia mutated (ATM)–checkpoint kinase 1 (Chk1) axis by triggering the DNA damage response (DDR) and cell cycle arrest at the G2/M checkpoint; this effect was also supported by Wee1/Cdc25C/cyclin-B1–cyclin-dependent kinase 1 (CDK1) modulation [131-134].

The binding window of acetylshikonin at -7.29 kcal/mol was consistent with previously observed G2/M blockade and apoptotic phenotypes due to increased topological stress [117]. It was considered that this molecule's inhibition of the WEE1-associated phosphorylation cycle could be functionally conjugated to the blockade of microtubule stability-dependent circulatory activity. Similarly, the binding window of tiliroside at -7.08 kcal/mol was noted to be in a range compatible with the pharmacodynamics of mitotic entry repression via the CDK1 phosphorylation axis. Tiliroside has been reported in the literature to have cyclazymanipulatory effects through the regulation of p21 and p27, strengthening its binding relationship with WEE1 [118]. Berberine's calculated binding energy, which was in the moderate to good range, was weaker compared to WEE1 inhibitors, suggesting that it may contribute to secondary signaling modulation by enhancing mitotic delay in microenvironments with intense DNA damage stress. This positioning, docked with the replication burden associated with hyperactivity of the MAPK/ERK–MYC axis in KRAS-mutated tumors, raises the possibility of exploiting the selective toxicity profile of WEE1 blockade.

The binding mode of hyperforin in the WEE1 structure (PDB: 5V5Y) revealed that the ligand binds by utilizing both hydrophobic and polar contacts, burying it strongly around the catalytic site (Figure 5–6).

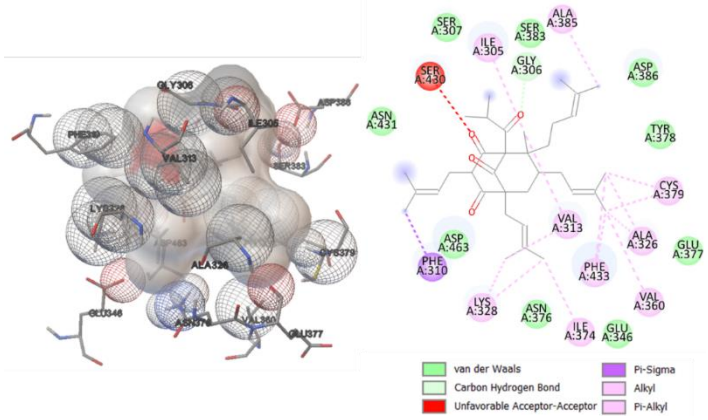

Figure 5. WEE1 (PDB: 5V5Y) - Hyperforin 3D and 2D binding interaction maps.

Hyperforin occupies the hydrophobic floor of the WEE1 catalytic pocket, forming extensive van der Waals and π-alkyl interactions with residues such as Val313, Ala326, Phe310 and Phe433 that anchor the ligand in a stable orientation. The weak polar contacts around Ser430 and Asp463 further constrain the ligand's alignment, supporting a binding pose consistent with ATP-competitive WEE1 inhibitors.

3D binding maps (Figure 5) showed that the molecule forms strong van der Waals and alkyl contacts, particularly with Val313, Ala326, Ile305, Phe310, Phe433, Val360, Asp463, and Glu377; this contact distribution provides hyperforin with extensive surface complementarity with the pocket and enhances the steric stability of the binding. The 2D interaction map (Figure 5) showed that the conjugated aliphatic skeleton of the ligand develops prominent π–alkyl/π–σ contacts with Phe310, Phe433, and Phe368. These aromatic-centered interactions indicated that the molecule oriented parallel to the hydrophobic platform

in the WEE1 binding pocket and filled the base of the pocket, supporting the binding mode. The π-stacking observed with Phe433, in particular, was considered one of the key interactions stabilizing the aromatic backbone of hyperforin.

The ligand's carbonyl groups formed a weak but directed acceptor-acceptor contact with Ser430 in 2D analysis; although this interaction was classified as "unfavorable acceptor-acceptor," it was considered noteworthy for contributing to conformational alignment by partially constraining the local orientation of the molecule (Figure 5). The carbon-hydrogen bonds observed around residues Asn376 and Gly306 strengthened the ligand's association with the pocket and supported the binding mode. Van der Waals contacts between hyperforin and Ala385, Cys379, Tyr378, Ala326, Glu346, and Glu377 at the pocket edge formed a hydrophobic shield surrounding the pocket. The Val313–Ala326 line, in particular, was observed to provide a compact hydrophobic surface facing the hyperforin skeleton and contribute to a burial motif that may limit ligand dissociation from the pocket (Figure 5).

The molecule was observed to be buried in the WEE1 pocket, partially obscuring the entrance orifice and creating a significant volumetric occupation of the binding surface (Figure 6).

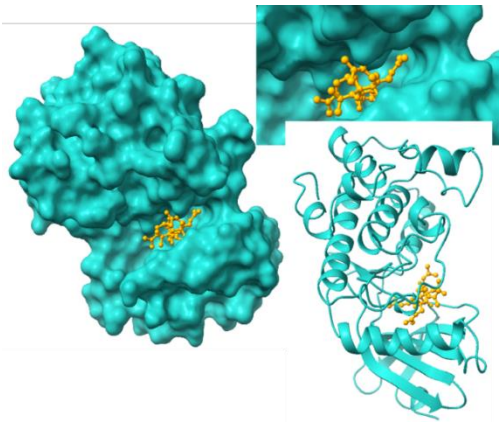

Figure 6. Surface and schematic representation of binding mode of hyperforin to WEE1.

Hyperforin is deeply positioned within the ATP-binding cleft of WEE1, adopting a compact orientation that mirrors the burial pattern of ATP-competitive inhibitors. Its extensive hydrophobic contacts along the pocket floor stabilize the ligand and help anchor it in a conformation consistent with high-affinity binding.

When this binding pattern was evaluated as a whole, it was understood that hyperforin made a limiting polar contact via Ser430 in the WEE1 binding pocket; occupied the aromatic platform with extensive π-stacking around Phe310–Phe433; exhibited strong hydrophobic burial in the Val313–Ala326–Val360 loop; and formed surrounding van der Waals contacts with surrounding residues such as Ala385, Cys379, and Glu377. This contact architecture supported the sterically and electronically favorable seating of hyperforin on WEE1 and suggested that the ligand's conformation with the pocket provided binding stability.

The current study demonstrated that hyperforin offers a natural scaffold approaching adavosertib in terms of WEE1 binding conformation, while acetylshikonin and tiliroside, with their mid- to high-end pharmacophore conformations, could be considered suitable ligand templates for derivation. Berberine, despite its more limited binding to WEE1, exhibited a profile suitable for combination design, contributing to secondary signaling in stress adaptation and the proliferation cycle. These four ligands, which target the WEE1–CDK1 axis, were among the primary candidates for validation in contexts where WEE1 dependence is evident, such as KRAS-mut PDAC, LUAD, cyclin E1 (CCNE1)-amplified ovarian cancer, and TNBC.

3.4. Comparative Binding Affinity and Interaction Profile of Ligands Targeting FGFR4 (PDB ID: 6NVK)

In the localization analyses performed for FGFR4, significant binding was detected only with hyperforin (–7.15 kcal/mol), while the other ligands were below this threshold and failed to create sufficient hydrophobic complementarity around the hinge and in the back pocket.

The binding mode of hyperforin with FGFR4 (PDB: 6NVK) revealed that the molecule occupies a hydrophobic depth similar to the ATP-binding pocket and achieves a stable binding position through multiple van der Waals contacts spread over a wide area (Figures 7–8). 3D interaction maps (Figure 7) showed that hyperforin forms tight contacts with small hydrophobic residues that define the base of the pocket, particularly Val481, Ala501, Val550, Leu810, Leu473, Ala620, and Ala553. The extensive distribution of these contacts along the aliphatic stem enhances the steric compatibility of the ligand and favors its binding mode. The 2D interaction map (Figure 7) revealed that one of the carbonyl oxygens at the center of the binding conformation forms a conventional hydrogen bond with Ala553. This polar contact stabilizes hyperforin's orientation with the pocket, facilitating burial of the molecule within the pocket. This hydrogen bond was observed to act as a guiding hook

between the molecule and the aliphatic domain located in the hydrogen-bonding core of the pocket. This supported hyperforin's localization at a depth similar to the ATP-binding site.

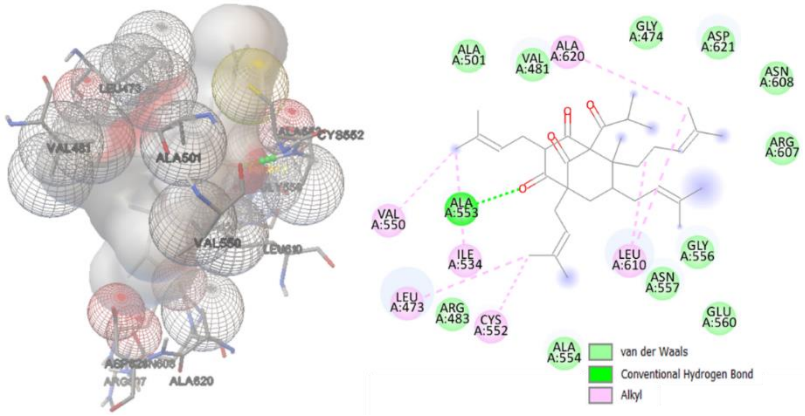

Figure 7. FGFR4 (PDB: 6NVK) - Hyperforin 3D and 2D binding interaction maps**.**

Hyperforin binds deeply within the FGFR4 hinge and back-pocket region, forming a stabilizing hydrogen bond with Ala553 and extensive hydrophobic contacts along the Val481–Ala501–Val550 axis.

Hyperforin's peripheral branches formed alkyl contacts with Ile534, Leu610, Cys552, Arg483, and Gly556 in 2D analysis; these hydrophobic interactions were observed to allow the branches extending around the pocket to overlap with the edge residues, creating a wall that strengthens binding. In particular, the Ile534–Leu610 line was thought to provide a hydrophobic corridor surrounding hyperforin, ensuring the molecule's stable locking within the pocket.

The schematic representation showed that the ligand aligns parallel to the folded structure of the FGFR4 protein, occupying the base of the pocket and filling the binding surface (Figure 8). When this binding pattern is evaluated as a whole, it is understood that hyperforin forms conventional hydrogen bonds with Ala553 in the FGFR4 binding pocket; exhibits intense hydrophobic burial along the Val481–Ala501–Val550–Leu810 axis; and promotes attachment to the pocket wall by forming alkyl contacts with peripheral residues such as Ile534, Leu610, and Cys552. This contact architecture supports the steric and electrostatic conformation of hyperforin to the pocket geometry, demonstrating a stable binding mode on FGFR4 (Figures 7–8).

Comparison with the most clinically mature FGFR4 inhibitors also revealed the difference in binding modes. While covalent and FGFR4-selective inhibitors such as BLU-9931 are effective by covalent adduction targeting the single Cys552 residue of FGFR4 (high selectivity among 456 targets in the kinase panel; equilibrium dissociation constant (Kd) ≈ 6 nM for FGFR4), the covalent chemistry of this class of molecules does not lend itself to direct comparison by pure docking scores; however, the basic pharmacophore (pyrimidine/naphthyridine-type core + suitable electrophilic warhead) located in the hinge region appeared to overlap with the non-covalent anchoring geometry exhibited by hyperforin. Structural-design data reported for selective H3B-6527 also highlighted the key role of a specific covalent interaction (Cys552) in addition to hinge anchoring in FGFR4, while demonstrating that the initial non-covalent occupancy (pre-reaction complex) determines positioning; hyperforin's ability to capture the hinge in a non-covalent "pre-complex"-like pose provided a promising gateway for non-covalent natural scaffolds [103].

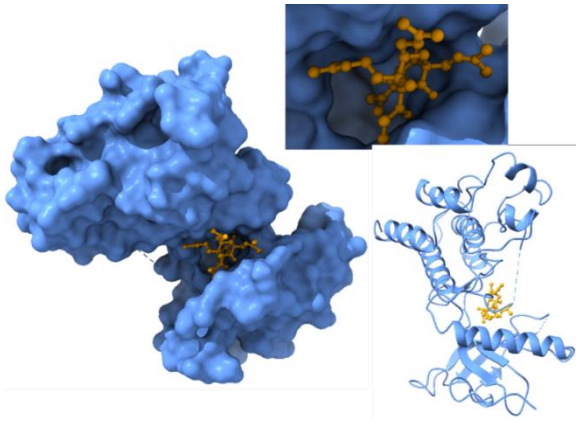

Figure 8. Surface and schematic representation of binding mode of hyperforin to FGFR4.

Hyperforin is positioned deeply within the FGFR4 binding cleft, adopting a compact pose that follows the contour of the hinge and back-pocket region. Its extensive hydrophobic contacts anchor the ligand firmly inside the cavity, supporting a stable non-covalent binding mode consistent with selective FGFR4 engagement.

Early-phase results of FGF401 (roblitinib) and other selective FGFR4 inhibitors advancing to the clinical stage demonstrate biological validation of FGFR4 blockade in FGF19-high HCC subtypes; in such a clinical setting, hyperforin, which exhibits a hinge-focused non-covalent occupancy of –7.15 kcal/mol, emerged as a natural chemical template for further validation of FGF19-high models [135]. Furthermore, the clustering of the best score bands in the ~–7 band in recent FGFR4-focused structure-based screening studies (reporting new candidates) supported that hyperforin achieved an energy window equivalent to this literature bar [136]. On the other hand, the positive/very weak scores calculated for pentagalloylglucose and punicalagin, from the polyphenolic tannin class, indicated that high polarity and volumetric hindrance led to diffuse and energetically unfavorable contact within the FGFR4 ATP pocket. These compounds failed to meet the hinge-centered pharmacophore requirements and failed to form stable hydrophobic packing in the back pockets. The low/moderate energies detected for berberine, acetylshikonin, tiliroside, verbascoside, 3,5-di-O-caffeoylquinic acid, and astragaloside IV specifically pointed to a lack of donor/acceptor orientation and hydrophobic core density at the hinge junction. This suggested that the chemical architecture that confers selectivity and potency in FGFR4 (e.g., as seen in BLU-9931, H3B-6527) requires either covalent fixation with an electrophilic warhead or a denser hydrophobic core and appropriate ring geometry [103]. Fine-tuning the length/position of the prenyl chains and the planarity of the aromatic core generated rational modification heads that could increase the selective binding energy in FGFR4 without mimicking the chemical mechanics of the BLU-9931/H3B-6527 class [103, 137]. Consequently, the hyperforin–FGFR4 localization in the –7.15 kcal/mol band provided an energy window compatible with the "upper quantile" threshold of current FGFR4 virtual screens and was identified as a natural, non-covalent scaffold that could be carried forward into functional testing in FGFR4-activated contexts, particularly in FGF19-high HCC [103, 135, 136].

3.5. Comparative Binding Affinity and Interaction Profile of PARP1 (PDB ID: 7KK3) Targeting Ligands

Computational docking assessments for PARP1 revealed that none of the studied natural ligands were able to bind significantly to the catalytic site. Effective binding to the PARP1 catalytic pocket requires a heteroaromatic plane, multiple hydrogen bonds in the hinge region, π–π stacking, and a compact core structure filling the Tyr-rich hydrophobic microdomains. In this context, considering the co-crystal structure of 7KK3 with talazoparib, it was observed that the pharmacophore components required for direct binding were not present in the studied natural pool [138]. In particular, it was determined that tannins with high polarity and volume, such as pentagalloylglucose and punicalagin, were unable to fit easily into the narrow and deep nicotinamide pocket, and desolvation costs and steric hindrance made binding energetically disadvantageous. These data indicated that the examined phytochemical compounds could not strongly modulate PARP1 directly via the catalytic pocket, thus they were not appropriate to be prioritized for this target.

4. Conclusion

This study evaluated the binding affinities of selected natural compounds on multiple cancer targets. Specifically, it was demonstrated that therapeutically significant vulnerabilities in cellular proliferation, DNA damage response, and mitotic control can be simultaneously targeted. The findings suggest that specific chemical scaffolds can guide candidate selection by simultaneously affecting critical oncobiological nodes. Among the nine natural compounds evaluated, hyperforin was the only molecule that stood out with its high binding affinities on multiple targets. Its strong binding to both KRAS (–8.04 kcal/mol), MDM2 (–9.15 kcal/mol), and WEE1 (–8.29 kcal/mol) suggests that hyperforin offers a chemical scaffold that can simultaneously influence interdependent oncobiological axes such as proliferation signaling, DNA damage response, and cell cycle control. The binding score calculated for KRAS was notable for its similarity to the lower band reported in the sotorasib/adagrasib redocking studies. This proximity provided a meaningful starting point for new allosteric blocking windows, particularly for non-G12C variants. The -9.15 kcal/mol level detected for MDM2 was above the typical score range reported for nutlin-3a in the literature, suggesting a potential hit for restoring p53 activation. The -8.29 kcal/mol level for WEE1 was comparable to the redocking scores of adavosertib class inhibitors, suggesting pharmacological support, particularly in replication stress-dependent tumor subtypes (KRAS-mut pancreatic ductal adenocarcinoma (PDAC)/lung adenocarcinoma (LUAD), MYC proto-oncogene (MYC)-high phenotypes). Hyperforin's high binding affinity for these three targets suggested that it may have a synergistic profile that suppresses tumor cells through multilayered vulnerabilities. The possibility of attenuating proliferative flux via the KRAS–MAPK axis while reactivating p53-mediated cell death pathways through MDM2 suppression and increasing mitotic entry repression at the G2/M transition through WEE1 inhibition provided a biological framework consistent with the available in silico data.

On the other hand, significant binding to FGFR4 was observed only with hyperforin (–7.15 kcal/mol). This score corresponded to the upper quantile range identified in structure-based virtual screens for FGFR4, suggesting that hyperforin could be a non-covalent starting scaffold for FGFR4-activated tumors (especially FGF19-high HCC). However, compared to the BLU-9931/H3B-6527 class inhibitors, where covalent selectivity is achieved via Cys552, hyperforin's more hinge-centered, non-covalent orientation indicated a pharmacophore space requiring optimization. Critical structural requirements such as hinge bonds, aromatic stacking, and compact filling of the Tyr-rich catalytic pocket were not met. This result indicated that

the studied natural products are unlikely to effectively inhibit PARP1 via direct catalytic pocket occupation. Therefore, PARP1 was not considered a prioritized target within the existing natural compound pool.

Taking this general profile together, hyperforin was noted to be the dominant hit molecule among the five targets for inhibiting the KRAS–MDM2–WEE1 triad. Accordingly, the binding parameters exhibited by hyperforin on these targets offered a profile rarely seen in natural product chemistry in terms of multi-targeting capability. Furthermore, the positioning of compounds such as acetylshikonin, tiliroside, and berberine, particularly in the mid- to upper-band regions of KRAS and WEE1, identified these molecules as plausible starting points for structural derivative development. This integrated approach demonstrated that natural compounds found in the Turkish flora hold significant potential not only at the phenotypic level but also in the context of targeted molecular interactions. In particular, the enhancement of selectivity for the KRAS–MDM2–WEE1 axis through hyperforin-centered chemical refinements was noted as a parameter that will provide a structural roadmap for further validation and preclinical evaluation.

Despite the comprehensive nature of the docking-based assessment, this study has several limitations. Docking analyses are based solely on static crystal structures that do not fully capture the conformational flexibility and dynamic rearrangements that occur in solution or upon ligand binding. Similarly, docking scores provide an approximate estimate of affinity and cannot replace quantitative measurements such as ΔG binding derived from molecular dynamics-based free energy calculations. Future studies should include molecular dynamics simulations, molecular mechanics/Poisson–Boltzmann surface area (MM/PBSA)- or free energy perturbation (FEP)-based affinity predictions, and ensemble docking to better account for protein flexibility. Experimental validations, including biophysical analyses (isothermal titration calorimetry [ITC], surface plasmon resonance [SPR]), enzymatic inhibition studies, and cellular phenotyping in KRAS-mut, MDM2-amplified, and WEE1-dependent models, will be vital to confirm the translational significance of hyperforin and its derivatives.

Conflict of Interest

The authors declare that they have no competing interests.

Ethics Committee Approval

Ethics committee approval is not required.

Author Contribution

This manuscript is written by single author.

Acknowledgements

Not applicable.

5. References

[1] Emre, G., Dogan, A., Haznedaroglu, M. Z., Senkardes, I., Ulger, M., Satiroglu, A., Can Emmez, B., & Tugay, O. (2021). An ethnobotanical study of medicinal plants in Mersin (Turkey). Frontiers in pharmacology, 12, 664500.

[2] Newman, D. J., & Cragg, G. M. (2020). Natural products as sources of new drugs over the nearly four decades from 01/1981 to 09/2019. Journal of Natural Products, 83(3), 770-803.

[3] Yip, H. Y. K., & Papa, A. (2021). Signaling pathways in cancer: therapeutic targets, combinatorial treatments, and new developments. Cells, 10(3), 659.

[4] Wei, H., & McCammon, J. A. (2024). Structure and dynamics in drug discovery. npj Drug Discovery, 1(1), 1.

[5] Batool, M., Ahmad, B., & Choi, S. (2019). A structure-based drug discovery paradigm. International journal of molecular sciences, 20(11), 2783.

[6] Curtin, N. J., & Szabo, C. (2013). Therapeutic applications of PARP inhibitors: anticancer therapy and beyond. Molecular aspects of medicine, 34(6), 1217-1256.

[7] Fong, P. C., Boss, D. S., Yap, T. A., Tutt, A., Wu, P., Mergui-Roelvink, M., Mortimer, P., Swaisland, H., Lau, A., & O'Connor, M. J. (2009). Inhibition of poly (ADP-ribose) polymerase in tumors from BRCA mutation carriers. New England Journal of Medicine, 361(2), 123-134.

[8] Ostrem, J. M., Peters, U., Sos, M. L., Wells, J. A., & Shokat, K. M. (2013). K-Ras (G12C) inhibitors allosterically control GTP affinity and effector interactions. Nature, 503(7477), 548-551.

[9] Lanman, B. A., Allen, J. R., Allen, J. G., Amegadzie, A. K., Ashton, K. S., Booker, S. K., Chen, J. J., Chen, N., Frohn, M. J., & Goodman, G. (2019). Discovery of a Covalent Inhibitor of KRASG12C (AMG 510) for the Treatment of Solid Tumors. In: ACS Publications.

[10] Canon, J., Rex, K., Saiki, A. Y., Mohr, C., Cooke, K., Bagal, D., Gaida, K., Holt, T., Knutson, C. G., & Koppada, N. (2019). The clinical KRAS (G12C) inhibitor AMG 510 drives anti-tumour immunity. Nature, 575(7781), 217-223.

[11] Aydin, G., Paksoy, M. N., Orhan, M. D., Avsar, T., Yurtsever, M., & Durdagi, S. (2020). Proposing novel MDM2 inhibitors: Combined physics-driven high-throughput virtual screening and in vitro studies. Chemical Biology & Drug Design, 96(1), 684-700.
[12] Vass, M., Schmidt, É., Horti, F., & Keserű, G. M. (2014). Virtual fragment screening on GPCRs: a case study on dopamine D3 and histamine H4 receptors. European journal of medicinal chemistry, 77, 38-46.
[13] Erdoğan, Ü., Onem, E., Muhammed Tilahun, M., Soyocak, A., Ak, A., Arın, U. E., & Erzurumlu, Y. (2025). Investigation of Antioxidant, Antibacterial, and Anticancer Activities, and Molecular Modeling Studies of Berberis crataegina Fruit Extract. Chemistry & Biodiversity, e202402591.
[14] Zhao, Q. (2015). Molecular mechanisms of shikonin and its derivatives in cancer therapy Mainz, Univ., Diss., 2015].
[15] Menegazzi, M., Masiello, P., & Novelli, M. (2020). Anti-tumor activity of Hypericum perforatum L. and hyperforin through modulation of inflammatory signaling, ROS generation and proton dynamics. Antioxidants, 10(1), 18.
[16] Wen, C., Dechsupa, N., Yu, Z., Zhang, X., Liang, S., Lei, X., Xu, T., Gao, X., Hu, Q., & Innuan, P. (2023). Pentagalloyl glucose: a review of anticancer properties, molecular targets, mechanisms of action, pharmacokinetics, and safety profile. Molecules, 28(12), 4856.
[17] Rauf, A., Olatunde, A., Akram, Z., Hemeg, H. A., Aljohani, A. S., Al Abdulmonem, W., Khalid, A., Khalil, A. A., Islam, M. R., & Thiruvengadam, R. (2025). The role of pomegranate (Punica granatum) in cancer prevention and treatment: Modulating signaling pathways from inflammation to metastasis. Food Science & Nutrition, 13(2), e4674.
[18] Vyas, S., Kothari, S., & Kachhwaha, S. (2019). Nootropic medicinal plants: Therapeutic alternatives for Alzheimer's disease. Journal of Herbal Medicine, 17, 100291.
[19] Yeşil, Y., & Akalın, E. (2009). Folk medicinal plants in Kürecik area (Akçadağ/Malatya Turkey). Turkish Journal of Pharmaceutical Sciences, 6(3), 207-220.
[20] Rahimi-Madiseh, M., Lorigoini, Z., Zamani-Gharaghoshi, H., & Rafieian-Kopaei, M. (2017). Berberis vulgaris: specifications and traditional uses. Iranian journal of basic medical sciences, 20(5), 569.
[21] Imenshahidi, M., & Hosseinzadeh, H. (2016). Berberis vulgaris and berberine: an update review. Phytotherapy research, 30(11), 1745-1764.
[22] Tillhon, M., Ortiz, L. M. G., Lombardi, P., & Scovassi, A. I. (2012). Berberine: new perspectives for old remedies. Biochemical Pharmacology, 84(10), 1260-1267.
[23] Damare, R., Engle, K., & Kumar, G. (2024). Targeting epidermal growth factor receptor and its downstream signaling pathways by natural products: A mechanistic insight. Phytotherapy research, 38(5), 2406-2447.
[24] Polat, R., Cakilcioglu, U., & Satıl, F. (2013). Traditional uses of medicinal plants in Solhan (Bingöl—Turkey). Journal of ethnopharmacology, 148(3), 951-963.
[25] Papageorgiou, V. P., Assimopoulou, A. N., Samanidou, V., & Papadoyannis, I. (2006). Recent advances in chemistry, biology and biotechnology of alkannins and shikonins. Current Organic Chemistry, 10(16), 2123-2142.
[26] Zhao, R., Choi, B. Y., Wei, L., Fredimoses, M., Yin, F., Fu, X., Chen, H., Liu, K., Kundu, J. K., & Dong, Z. (2020). Acetylshikonin suppressed growth of colorectal tumour tissue and cells by inhibiting the intracellular kinase, T-lymphokine-activated killer cell-originated protein kinase. British journal of pharmacology, 177(10), 2303-2319.
[27] Uslusoy, F., Nazıroğlu, M., Övey, İ. S., & Sönmez, T. T. (2019). Hypericum perforatum L. supplementation protects sciatic nerve injury-induced apoptotic, inflammatory and oxidative damage to muscle, blood and brain in rats. Journal of pharmacy and pharmacology, 71(1), 83-92.
[28] Özkan, E. E., & Mat, A. (2013). An overview on Hypericum species of Turkey. Journal of Pharmacognosy and Phytotherapy, 5(3), 38-46.
[29] Cardile, A., Zanrè, V., Campagnari, R., Asson, F., Addo, S. S., Orlandi, E., & Menegazzi, M. (2023). Hyperforin elicits cytostatic/cytotoxic activity in human melanoma cell lines, inhibiting pro-survival NF-κB, STAT3, AP1 transcription factors and the expression of functional proteins involved in mitochondrial and cytosolic metabolism. International journal of molecular sciences, 24(2), 1263.
[30] Barathan, M., Zulpa, A. K., Vellasamy, K. M., Ibrahim, Z. A., Hoong, S. M., Mariappan, V., Venkatraman, G., & Vadivelu, J. (2023). Hyperforin-mediated anticancer mechanisms in MDA-MB-231 cell line: insights into apoptotic mediator modulation and caspase activation. Journal of Taibah University for Science, 17(1), 2237712.
[31] Tatli, I. I., & Akdemir, Z. F. (2006). Traditional uses and biological activities of Verbascum species. Fabad Journal of Pharmaceutical Sciences, 31(2), 85.
[32] Kahraman, C., Ekizoglu, M., Kart, D., Akdemir, Z., & Tatli, I. I. (2011). Antimicrobial activity of some Verbascum species growing in Turkey. Fabad Journal of Pharmaceutical Sciences, 36(1), 11-16.
[33] Ozcan, B., Yilmaz, M., & Caliskan, M. (2010). Antimicrobial and antioxidant activities of various extracts of Verbascum antiochium Boiss.(Scrophulariaceae). Journal of medicinal food, 13(5), 1147-1152.
[34] Alipieva, K., Korkina, L., Orhan, I. E., & Georgiev, M. I. (2014). Verbascoside—A review of its occurrence,(bio) synthesis and pharmacological significance. Biotechnology advances, 32(6), 1065-1076.
[35] Vertuani, S., Beghelli, E., Scalambra, E., Malisardi, G., Copetti, S., Toso, R. D., Baldisserotto, A., & Manfredini, S. (2011). Activity and stability studies of verbascoside, a novel antioxidant, in dermo-cosmetic and pharmaceutical topical formulations. Molecules, 16(8), 7068-7080. vyas
[36] Khullar, M., Sharma, A., Wani, A., Sharma, N., Sharma, N., Chandan, B., Kumar, A., & Ahmed, Z. (2019). Acteoside ameliorates inflammatory responses through NFkB pathway in alcohol induced hepatic damage. International immunopharmacology, 69, 109-117.

[37] Daneshforouz, A., Nazemi, S., Gholami, O., Kafami, M., & Amin, B. (2021). The cytotoxicity and apoptotic effects of verbascoside on breast cancer 4T1 cell line. BMC Pharmacology and Toxicology, 22(1), 72.
[38] Bilecenoğlu, D. K., & Yalçın, F. N. (2023). Lamium sp. In Medicinal Plants of Turkey (pp. 118-127). CRC Press.
[39] Yalçin, F. N., & Kaya, D. (2006). Ethnobotany, pharmacology and phytochemistry of the genus Lamium (Lamiaceae). Fabad Journal of Pharmaceutical Sciences, 31(1), 43.
[40] Ren, Y., He, J., Zhao, W., & Ma, Y. (2022). The anti-tumor efficacy of verbascoside on ovarian cancer via facilitating CCN1-AKT/NF-κB pathway-mediated M1 macrophage polarization. Frontiers in oncology, 12, 901922.
[41] Jia, W.-Q., Wang, Z.-T., Zou, M.-M., Lin, J.-H., Li, Y.-H., Zhang, L., & Xu, R.-X. (2018). Verbascoside inhibits glioblastoma cell proliferation, migration and invasion while promoting apoptosis through upregulation of protein tyrosine phosphatase SHP-1 and inhibition of STAT3 phosphorylation. Cellular Physiology and Biochemistry, 47(5), 1871-1882.
[42] Güner, A., Özhatay, N., Ekim, T., Başer, K. H. C., Hedge, I. C., & Hedge, I. C. (2000). Flora of Turkey and the East Aegean Islands: Volume 11, Supplement 2. Edinburgh University Press.
[43] Öztürk, M., Altay, V., & Keskin, M. (2023). Folkloric Knowledge of Endemic Plants: Their Traditional Uses as Spices, Food and Herbal Teas by the Local Communities in Turkiye. In Ethnic Knowledge and Perspectives of Medicinal Plants (pp. 137-152). Apple Academic Press.
[44] Bardakci, H., Cevik, D., Barak, T. H., Gozet, T., Kan, Y., & Kirmizibekmez, H. (2020). Secondary metabolites, phytochemical characterization and antioxidant activities of different extracts of Sideritis congesta PH Davis et Hub.-Mor. Biochemical Systematics and Ecology, 92, 104120.
[45] Öztürk Sarıkaya, S. B., & Zehiroğlu, C. (2025). Chemical Composition and Bioactivities of Sideritis libanotica Labill subsp. Libanotica: LC–HRMS Phytochemical Profiling, Mineral Content, Antioxidant, Antibacterial, and Neuroprotective–Antidiabetic Enzyme Inhibitory Potentials. Chemistry & Biodiversity, e01314.
[46] González-Burgos, E., Carretero, M., & Gómez-Serranillos, M. (2011). Sideritis spp.: Uses, chemical composition and pharmacological activities—A review. Journal of ethnopharmacology, 135(2), 209-225.
[47] Karamenderes, C., Konyalioglu, S., Khan, S., & Khan, I. A. (2007). Total phenolic contents, free radical scavenging activities and inhibitory effects on the activation of NF-kappa B of eight Centaurea L. species. Phytotherapy Research: An International Journal Devoted to Pharmacological and Toxicological Evaluation of Natural Product Derivatives, 21(5), 488-491.
[48] Sharonova, N., Nikitin, E., Terenzhev, D., Lyubina, A., Amerhanova, S., Bushmeleva, K., Rakhmaeva, A., Fitsev, I., & Sinyashin, K. (2021). Comparative assessment of the phytochemical composition and biological activity of extracts of flowering plants of Centaurea cyanus L., Centaurea jacea L. and Centaurea scabiosa L. Plants, 10(7), 1279.
[49] Milošević, T., Argyropoulou, C., Solujić, S., Murat-Spahić, D., & Skaltsa, H. (2010). Chemical composition and antimicrobial activity of essential oils from Centaurea pannonica and C. jacea. Natural product communications, 5(10), 1934578X1000501030.
[50] Uzun, A., Uzun, S. P., & Durmaz, A. (2019). Spatial analyses of Astragalus species distribution and richness in Kahramanmaraş (Turkey) by geographical information systems (GIS). Turkish Journal of Forest Science, 3(1), 37-59.
[51] Dai, Y., Wang, D., Zhao, M., Yan, L., Zhu, C., Li, P., Qin, X., Verpoorte, R., & Chen, S. (2020). Quality markers for Astragali radix and its products based on process analysis. Frontiers in pharmacology, 11, 554777.
[52] Liang, Y., Chen, B., Liang, D., Quan, X., Gu, R., Meng, Z., Gan, H., Wu, Z., Sun, Y., & Liu, S. (2023). Pharmacological effects of astragaloside IV: a review. Molecules, 28(16), 6118.
[53] Yang, Y., Hong, M., Lian, W.-W., & Chen, Z. (2022). Review of the pharmacological effects of astragaloside IV and its autophagic mechanism in association with inflammation. World journal of clinical cases, 10(28), 10004.
[54] Dinçman, G. E., Aytaç, Z., & Çalış, İ. (2024). Turkish Astragalus Species: Botanical Aspects, Secondary Metabolites, and Biotransformation. Planta medica.
[55] Sezik, E., Tabata, M., Yesilada, E., Honda, G., Goto, K., & Ikeshiro, Y. (1991). Traditional medicine in Turkey I. Folk medicine in northeast Anatolia. Journal of ethnopharmacology, 35(2), 191-196.
[56] Niemetz, R., & Gross, G. G. (2005). Enzymology of gallotannin and ellagitannin biosynthesis. Phytochemistry, 66(17), 2001-2011.
[57] Lee, H.-J., Seo, N.-J., Jeong, S.-J., Park, Y., Jung, D.-B., Koh, W., Lee, H.-J., Lee, E.-O., Ahn, K. S., & Ahn, K. S. (2011). Oral administration of penta-O-galloyl-β-D-glucose suppresses triple-negative breast cancer xenograft growth and metastasis in strong association with JAK1-STAT3 inhibition. Carcinogenesis, 32(6), 804-811.
[58] Başer, D. F., Akkol, E. K., Bozkurt, M., Süntar, İ., & Civelek, T. (2021). Hepatoprotective Effect of Pomegranate (Punica Granatum L.) in A Rabbit Model of Steatohepatitis. Kocatepe Veterinary Journal, 14(4), 507-519.
[59] Cai, D., Li, X., Chen, J., Jiang, X., Ma, X., Sun, J., Tian, L., Vidyarthi, S. K., Xu, J., & Pan, Z. (2022). A comprehensive review on innovative and advanced stabilization approaches of anthocyanin by modifying structure and controlling environmental factors. Food Chemistry, 366, 130611.
[60] Albrecht, M., Jiang, W., Kumi-Diaka, J., Lansky, E. P., Gommersall, L. M., Patel, A., Mansel, R. E., Neeman, I., Geldof, A. A., & Campbell, M. J. (2004). Pomegranate extracts potently suppress proliferation, xenograft growth, and invasion of human prostate cancer cells. Journal of medicinal food, 7(3), 274-283.
[61] Adhami, V. M., Khan, N., & Mukhtar, H. (2009). Cancer chemoprevention by pomegranate: laboratory and clinical evidence. Nutrition and cancer, 61(6), 811-815.

[62] Toi, M., Bando, H., Ramachandran, C., Melnick, S. J., Imai, A., Fife, R. S., Carr, R. E., Oikawa, T., & Lansky, E. P. (2003). Preliminary studies on the anti-angiogenic potential of pomegranate fractions in vitro and in vivo. Angiogenesis, 6(2), 121-128.
[63] Karin, M. (2009). NF-κB as a critical link between inflammation and cancer. Cold Spring Harbor perspectives in biology, 1(5), a000141.
[64] Scimeca, M., Urbano, N., Bonfiglio, R., Duggento, A., Toschi, N., Schillaci, O., & Bonanno, E. (2019). Novel insights into breast cancer progression and metastasis: A multidisciplinary opportunity to transition from biology to clinical oncology. Biochimica et Biophysica Acta (BBA)-Reviews on Cancer, 1872(1), 138-148.
[65] Carmeliet, P., & Jain, R. K. (2000). Angiogenesis in cancer and other diseases. Nature, 407(6801), 249-257.
[66] González, M. G., Janssen, A. P., IJzerman, A. P., Heitman, L. H., & van Westen, G. J. (2022). Oncological drug discovery: AI meets structure-based computational research. Drug discovery today, 27(6), 1661-1670.
[67] Bostancı, B., & Akalın, E. (2023). An overview of the therapeutic potentials and safety profiles of Berberis species in Türkiye. Turkish Journal of Biodiversity, 6(2), 159-166.
[68] Imanshahidi, M., & Hosseinzadeh, H. (2008). Pharmacological and therapeutic effects of Berberis vulgaris and its active constituent, berberine. Phytotherapy research, 22(8), 999-1012.
[69] DeBlasi, J. M., & DeNicola, G. M. (2020). Dissecting the crosstalk between NRF2 signaling and metabolic processes in cancer. Cancers, 12(10), 3023.
[70] Salehi, B., Armstrong, L., Rescigno, A., Yeskaliyeva, B., Seitimova, G., Beyatli, A., Sharmeen, J., Mahomoodally, M. F., Sharopov, F., & Durazzo, A. (2019). Lamium plants—A comprehensive review on health benefits and biological activities. Molecules, 24(10), 1913.
[71] Polat, D. Ç., İlgün, S., Karatoprak, G. Ş., Akkol, E. K., & Capasso, R. (2022). Phytochemical profiles, antioxidant, cytotoxic, and anti-inflammatory activities of traditional medicinal plants: Centaurea pichleri subsp. pichleri, Conyza canadensis, and Jasminum fruticans. Molecules, 27(23), 8249.
[72] Raphael, B. J., Hruban, R. H., Aguirre, A. J., Moffitt, R. A., Yeh, J. J., Stewart, C., Robertson, A. G., Cherniack, A. D., Gupta, M., & Getz, G. (2017). Integrated genomic characterization of pancreatic ductal adenocarcinoma. Cancer cell, 32(2), 185-203. e113.
[73] Sanchez-Vega, F., Mina, M., Armenia, J., Chatila, W. K., Luna, A., La, K. C., Dimitriadoy, S., Liu, D. L., Kantheti, H. S., & Saghafinia, S. (2018). Oncogenic signaling pathways in the cancer genome atlas. Cell, 173(2), 321-337. e310.
[74] Cox, A. D., & Der, C. J. (2025). "Undruggable KRAS": druggable after all. Genes & development, 39(1-2), 132-162.
[75] Parikh, K., Banna, G., Liu, S. V., Friedlaender, A., Desai, A., Subbiah, V., & Addeo, A. (2022). Drugging KRAS: current perspectives and state-of-art review. Journal of hematology & oncology, 15(1), 152.
[76] Wade, M., Li, Y.-C., & Wahl, G. M. (2013). MDM2, MDMX and p53 in oncogenesis and cancer therapy. Nature Reviews Cancer, 13(2), 83-96.
[77] O'Connor, M. J. (2015). Targeting the DNA damage response in cancer. Molecular cell, 60(4), 547-560.
[78] Lord, C. J., & Ashworth, A. (2017). PARP inhibitors: Synthetic lethality in the clinic. Science, 355(6330), 1152-1158.
[79] Kim, R. D., Sarker, D., Meyer, T., Yau, T., Macarulla, T., Park, J.-W., Choo, S. P., Hollebecque, A., Sung, M. W., & Lim, H.-Y. (2019). First-in-human phase I study of fisogatinib (BLU-554) validates aberrant FGF19 signaling as a driver event in hepatocellular carcinoma. Cancer discovery, 9(12), 1696-1707.
[80] Österberg, F., Morris, G. M., Sanner, M. F., Olson, A. J., & Goodsell, D. S. (2002). Automated docking to multiple target structures: incorporation of protein mobility and structural water heterogeneity in AutoDock. Proteins: Structure, Function, and Bioinformatics, 46(1), 34-40.
[81] Rarey, M., Kramer, B., Lengauer, T., & Klebe, G. (1996). A fast flexible docking method using an incremental construction algorithm. Journal of molecular biology, 261(3), 470-489.
[82] Morris, G. M., Goodsell, D. S., Halliday, R. S., Huey, R., Hart, W. E., Belew, R. K., & Olson, A. J. (1998). Automated docking using a Lamarckian genetic algorithm and an empirical binding free energy function. Journal of computational chemistry, 19(14), 1639-1662.
[83] Trott, O., & Olson, A. J. (2010). AutoDock Vina: improving the speed and accuracy of docking with a new scoring function, efficient optimization, and multithreading. Journal of computational chemistry, 31(2), 455-461.
[84] Pettersen, E. F., Goddard, T. D., Huang, C. C., Meng, E. C., Couch, G. S., Croll, T. I., Morris, J. H., & Ferrin, T. E. (2021). UCSF ChimeraX: Structure visualization for researchers, educators, and developers. Protein Science, 30(1), 70-82.
[85] Morris, G. M., Huey, R., Lindstrom, W., Sanner, M. F., Belew, R. K., Goodsell, D. S., & Olson, A. J. (2009). AutoDock4 and AutoDockTools4: Automated docking with selective receptor flexibility. Journal of computational chemistry, 30(16), 2785-2791.
[86] Hanwell, M. D., Curtis, D. E., Lonie, D. C., Vandermeersch, T., Zurek, E., & Hutchison, G. R. (2012). Avogadro: an advanced semantic chemical editor, visualization, and analysis platform. Journal of cheminformatics, 4(1), 17.
[87] Kitchen, D. B., Decornez, H., Furr, J. R., & Bajorath, J. (2004). Docking and scoring in virtual screening for drug discovery: methods and applications. Nature reviews Drug discovery, 3(11), 935-949.
[88] Jones, G., Willett, P., Glen, R. C., Leach, A. R., & Taylor, R. (1997). Development and validation of a genetic algorithm for flexible docking. Journal of molecular biology, 267(3), 727-748.
[89] Warren, G. L., Andrews, C. W., Capelli, A.-M., Clarke, B., LaLonde, J., Lambert, M. H., Lindvall, M., Nevins, N., Semus, S. F., & Senger, S. (2006). A critical assessment of docking programs and scoring functions. Journal of medicinal chemistry, 49(20), 5912-5931.

[90] Jejurikar, B. L., & Rohane, S. H. (2021). Drug designing in discovery studio.
[91] Seeliger, D., & de Groot, B. L. (2010). Ligand docking and binding site analysis with PyMOL and Autodock/Vina. Journal of computer-aided molecular design, 24(5), 417-422.
[92] Burley, S. K., Berman, H. M., Christie, C., Duarte, J. M., Feng, Z., Westbrook, J., Young, J., & Zardecki, C. (2018). RCSB Protein Data Bank: Sustaining a living digital data resource that enables breakthroughs in scientific research and biomedical education. Protein Science, 27(1), 316-330.
[93] Berman, H. M., Westbrook, J., Feng, Z., Gilliland, G., Bhat, T. N., Weissig, H., Shindyalov, I. N., & Bourne, P. E. (2000). The protein data bank. Nucleic acids research, 28(1), 235-242.
[94] Hauschild, A.-C., Pastrello, C., Ekaputeri, G. K. A., Bethune-Waddell, D., Abovsky, M., Ahmed, Z., Kotlyar, M., Lu, R., & Jurisica, I. (2023). MirDIP 5.2: tissue context annotation and novel microRNA curation. Nucleic acids research, 51(D1), D217-D225.
[95] Anderson, A. C. (2003). The process of structure-based drug design. Chemistry & biology, 10(9), 787-797.
[96] Mishima, K., Kaneko, H., & Funatsu, K. (2014). Development of a new de novo design algorithm for exploring chemical space. Molecular Informatics, 33(11-12), 779-789.
[97] Lionta, E., Spyrou, G., K Vassilatis, D., & Cournia, Z. (2014). Structure-based virtual screening for drug discovery: principles, applications and recent advances. Current topics in medicinal chemistry, 14(16), 1923-1938.
[98] Patricelli, M. P., Janes, M. R., Li, L.-S., Hansen, R., Peters, U., Kessler, L. V., Chen, Y., Kucharski, J. M., Feng, J., & Ely, T. (2016). Selective inhibition of oncogenic KRAS output with small molecules targeting the inactive state. Cancer discovery, 6(3), 316-329.
[99] Vassilev, L. T., Vu, B. T., Graves, B., Carvajal, D., Podlaski, F., Filipovic, Z., Kong, N., Kammlott, U., Lukacs, C., & Klein, C. (2004). In vivo activation of the p53 pathway by small-molecule antagonists of MDM2. Science, 303(5659), 844-848.
[100] Holzer, P., Masuya, K., Furet, P., Kallen, J., Valat-Stachyra, T., Ferretti, S., Berghausen, J., Bouisset-Leonard, M., Buschmann, N., & Pissot-Soldermann, C. (2015). Discovery of a dihydroisoquinolinone derivative (NVP-CGM097): a highly potent and selective MDM2 inhibitor undergoing phase 1 clinical trials in p53wt tumors. In: ACS Publications.
[101] Kettner, N. M., Voicu, H., Finegold, M. J., Coarfa, C., Sreekumar, A., Putluri, N., Katchy, C. A., Lee, C., Moore, D. D., & Fu, L. (2016). Circadian homeostasis of liver metabolism suppresses hepatocarcinogenesis. Cancer cell, 30(6), 909-924.
[102] Zhu, J.-Y., Cuellar, R. A., Berndt, N., Lee, H. E., Olesen, S. H., Martin, M. P., Jensen, J. T., Georg, G. I., & Schönbrunn, E. (2017). Structural basis of wee kinases functionality and inactivation by diverse small molecule inhibitors. Journal of medicinal chemistry, 60(18), 7863-7875.
[103] Joshi, J. J., Coffey, H., Corcoran, E., Tsai, J., Huang, C.-L., Ichikawa, K., Prajapati, S., Hao, M.-H., Bailey, S., & Wu, J. (2017). H3B-6527 is a potent and selective inhibitor of FGFR4 in FGF19-driven hepatocellular carcinoma. Cancer research, 77(24), 6999-7013.
[104] Hagel, M., Miduturu, C., Sheets, M., Rubin, N., Weng, W., Stransky, N., Bifulco, N., Kim, J. L., Hodous, B., & Brooijmans, N. (2015). First selective small molecule inhibitor of FGFR4 for the treatment of hepatocellular carcinomas with an activated FGFR4 signaling pathway. Cancer discovery, 5(4), 424-437.
[105] Lin, X., Yosaatmadja, Y., Kalyukina, M., Middleditch, M. J., Zhang, Z., Lu, X., Ding, K., Patterson, A. V., Smaill, J. B., & Squire, C. J. (2019). Rotational freedom, steric hindrance, and protein dynamics explain BLU554 selectivity for the hinge cysteine of FGFR4. ACS medicinal chemistry letters, 10(8), 1180-1186.
[106] Ryan, K., Bolaños, B., Smith, M., Palde, P. B., Cuenca, P. D., VanArsdale, T. L., Niessen, S., Zhang, L., Behenna, D., & Ornelas, M. A. (2021). Dissecting the molecular determinants of clinical PARP1 inhibitor selectivity for tankyrase1. Journal of biological chemistry, 296.
[107] Skoulidis, F., Li, B. T., Dy, G. K., Price, T. J., Falchook, G. S., Wolf, J., Italiano, A., Schuler, M., Borghaei, H., & Barlesi, F. (2021). Sotorasib for lung cancers with KRAS p. G12C mutation. New England Journal of Medicine, 384(25), 2371-2381.
[108] Adhikary, T., & Basak, P. (2024). In-silico approach to investigate the phytochemicals of terminalia arjuna as multitarget inhibitors of proteins involved with lung cancer. Letters in Drug Design & Discovery, 21(2), 329-338.
[109] Mahmoud, A., Elkhalifa, D., Alali, F., Al Moustafa, A.-E., & Khalil, A. (2020). Novel polymethoxylated chalcones as potential compounds against KRAS-mutant colorectal cancers. Current pharmaceutical design, 26(14), 1622-1633.
[110] Lei, H., Guo, M., Li, X., Jia, F., Li, C., Yang, Y., Cao, M., Jiang, N., Ma, E., & Zhai, X. (2020). Discovery of novel indole-based allosteric highly potent ATX inhibitors with great in vivo efficacy in a mouse lung fibrosis model. Journal of medicinal chemistry, 63(13), 7326-7346.
[111] Prinsa, Saha, S., Bulbul, M. Z. H., Ozeki, Y., Alamri, M. A., & Kawsar, S. M. (2024). Flavonoids as potential KRAS inhibitors: DFT, molecular docking, molecular dynamics simulation and ADMET analyses. Journal of asian natural Products research, 26(8), 955-992.
[112] Rajasegaran, T., How, C. W., Saud, A., Ali, A., & Lim, J. C. W. (2023). Targeting inflammation in non-small cell lung cancer through drug repurposing. Pharmaceuticals, 16(3), 451.
[113] Siddique, H. R., Liao, D. J., Mishra, S. K., Schuster, T., Wang, L., Matter, B., Campbell, P. M., Villalta, P., Nanda, S., & Deng, Y. (2012). Epicatechin-rich cocoa polyphenol inhibits Kras-activated pancreatic ductal carcinoma cell growth in vitro and in a mouse model. International Journal of Cancer, 131(7), 1720-1731.
[114] Wang, Y., Liu, Y., Du, X., Ma, H., & Yao, J. (2020). The anti-cancer mechanisms of berberine: A review. Cancer management and research, 695-702.

[115]Wang, K.-B., Liu, Y., Li, J., Xiao, C., Wang, Y., Gu, W., Li, Y., Xia, Y.-Z., Yan, T., & Yang, M.-H. (2022). Structural insight into the bulge-containing KRAS oncogene promoter G-quadruplex bound to berberine and coptisine. Nature Communications, 13(1), 6016.

[116]Lohberger, B., Glänzer, D., Kaltenegger, H., Eck, N., Leithner, A., Bauer, R., Kretschmer, N., & Steinecker-Frohnwieser, B. (2022). Shikonin derivatives cause apoptosis and cell cycle arrest in human chondrosarcoma cells via death receptors and MAPK regulation. BMC cancer, 22(1), 758.

[117]Hao, G., Zhai, J., Jiang, H., Zhang, Y., Wu, M., Qiu, Y., Fan, C., Yu, L., Bai, S., & Sun, L. (2020). Acetylshikonin induces apoptosis of human leukemia cell line K562 by inducing S phase cell cycle arrest, modulating ROS accumulation, depleting Bcr-Abl and blocking NF-κB signaling. Biomedicine & Pharmacotherapy, 122, 109677.

[118]Han, R., Yang, H., Ling, C., & Lu, L. (2022). Tiliroside suppresses triple-negative breast cancer as a multifunctional CAXII inhibitor. Cancer Cell International, 22(1), 368.

[119]Azme, E., Hasan, M. M., Ali, M. L., Alam, R., Hoque, N., Noushin, F., Kabir, M. F., Islam, A., Nipun, T. S., & Hossen, S. M. (2025). Computational identification of potential natural terpenoid inhibitors of MDM2 for breast cancer therapy: molecular docking, molecular dynamics simulation, and ADMET analysis. Frontiers in Chemistry, 13, 1527008.

[120]Basha, N. J., Akshay, K., Mohan, R., Javeed, M., & Sharma, O. M. (2025). Synthesis, molecular docking, drug likeness, in silico toxicity and DFT studies of small molecules as p53-MDM2 interaction and COX-2 dual inhibitors. Journal of Molecular Structure, 1322, 140393.

[121]Oraibi, A. I., Dawood, A. H., Debbabi, N., Almukram, A. M. A., Almaary, K. S., Dabiellil, F., Chekir-Ghedira, L., & Kilani-Jaziri, S. (2025). Resveratrol-derived MDM2 inhibitors: Synthesis, characterization, and biological evaluation against MDM2 and HCT-116 cells. Open Chemistry, 23(1), 20250142.

[122]Shoaib, T. H., Abdelmoniem, N., Mukhtar, R. M., Alqhtani, A. T., Alalawi, A. L., Alawaji, R., Althubyani, M. S., Mohamed, S. G., Mohamed, G. A., & Ibrahim, S. R. (2023). Molecular docking and molecular dynamics studies reveal the anticancer potential of medicinal-plant-derived lignans as MDM2-P53 interaction inhibitors. Molecules, 28(18), 6665.

[123]da Mota, V. H. S., de Melo, F. F., de Brito, B. B., da Silva, F. A. F., & Teixeira, K. N. (2022). Molecular docking of DS-3032B, a mouse double minute 2 enzyme antagonist with potential for oncology treatment development. World Journal of Clinical Oncology, 13(6), 496.

[124]Gounder, M. M., Bauer, T. M., Schwartz, G. K., Weise, A. M., LoRusso, P., Kumar, P., Tao, B., Hong, Y., Patel, P., & Lu, Y. (2023). A first-in-human phase I study of milademetan, an MDM2 inhibitor, in patients with advanced liposarcoma, solid tumors, or lymphomas. Journal of clinical oncology, 41(9), 1714-1724.

[125]Shiferaw, D. G., & Kalluraya, B. (2024). Synthesis, characterization, biological evaluation, and molecular docking studies of new 1, 3, 4-oxadiazole-thioether derivative as antioxidants and cytotoxic agents. Heliyon, 10(7).

[126]Takebe, N., Naqash, A. R., O'Sullivan Coyne, G., Kummar, S., Do, K., Bruns, A., Juwara, L., Zlott, J., Rubinstein, L., & Piekarz, R. (2021). Safety, antitumor activity, and biomarker analysis in a phase I trial of the once-daily Wee1 inhibitor adavosertib (AZD1775) in patients with advanced solid tumors. Clinical Cancer Research, 27(14), 3834-3844.

[127]Lheureux, S., Cristea, M. C., Bruce, J. P., Garg, S., Cabanero, M., Mantia-Smaldone, G., Olawaiye, A. B., Ellard, S. L., Weberpals, J. I., & Hendrickson, A. E. W. (2021). Adavosertib plus gemcitabine for platinum-resistant or platinum-refractory recurrent ovarian cancer: a double-blind, randomised, placebo-controlled, phase 2 trial. The Lancet, 397(10271), 281-292.

[128]Leijen, S., van Geel, R. M., Sonke, G. S., de Jong, D., Rosenberg, E. H., Marchetti, S., Pluim, D., van Werkhoven, E., Rose, S., & Lee, M. A. (2016). Phase II study of WEE1 inhibitor AZD1775 plus carboplatin in patients with TP53-mutated ovarian cancer refractory or resistant to first-line therapy within 3 months. Journal of clinical oncology, 34(36), 4354-4361.

[129]Pandey, P., Lakhanpal, S., Mahmood, D., Kang, H. N., Kim, B., Kang, S., Choi, J., Moon, S., Pandey, S., & Ballal, S. (2025). Bergenin, a bioactive flavonoid: advancements in the prospects of anticancer mechanism, pharmacokinetics and nanoformulations. Frontiers in pharmacology, 15, 1481587.

[130]Yamamoto, G., Tanaka, K., Kamata, R., Saito, H., Yamamori-Morita, T., Nakao, T., Liu, J., Mori, S., Yagishita, S., & Hamada, A. (2025). WEE1 confers resistance to KRASG12C inhibitors in non-small cell lung cancer. Cancer letters, 611, 217414.

[131]Yildirim, M., Cimentepe, M., Dogan, K., Necip, A., & Amangeldinova, M. (2025). Next-generation antibacterial cryogels: Berberine-infused smart membranes with molecular docking-guided targeting of MRSA and MDR E. coli. Biophysical Chemistry, 107481.

[132]Wang, Y., Liu, Q., Liu, Z., Li, B., Sun, Z., Zhou, H., Zhang, X., Gong, Y., & Shao, C. (2012). Berberine, a genotoxic alkaloid, induces ATM-Chk1 mediated G2 arrest in prostate cancer cells. Mutation Research/Fundamental and Molecular Mechanisms of Mutagenesis, 734(1-2), 20-29.

[133]Lin, C.-C., Lin, S.-Y., Chung, J.-G., Lin, J.-P., Chen, G.-W., & Kao, S.-T. (2006). Down-regulation of cyclin B1 and up-regulation of Wee1 by berberine promotes entry of leukemia cells into the G2/M-phase of the cell cycle. Anticancer Research, 26(2A), 1097-1104.

[134]Hu, X., Wu, X., Huang, Y., Tong, Q., Takeda, S., & Qing, Y. (2014). Berberine induces double-strand DNA breaks in Rev3 deficient cells. Molecular medicine reports, 9(5), 1883-1888.

[135]Xu, J., Cui, J., Jiang, H., Zeng, Y., & Cong, X. (2023). Phase 1 dose escalation study of FGFR4 inhibitor in combination with pembrolizumab in advanced solid tumors patients. Cancer Medicine, 12(7), 7762-7771.

[136]Fan, L., Xie, H., Wang, W., Peng, G., Fu, Z., & Ye, Q. (2025). Structure-based identification of potent fibroblast growth factor receptor 4 (FGFR4) inhibitors as potential therapeutics for hepatocellular carcinoma. PeerJ, 13, e19183.

[137]Schwarz, M., Kurkunov, M., Wittlinger, F., Rudalska, R., Wang, G., Schwalm, M. P., Rasch, A., Wagner, B., Laufer, S. A., & Knapp, S. (2024). Development of Highly Potent and Selective Covalent FGFR4 Inhibitors Based on SNAr Electrophiles. Journal of medicinal chemistry, 67(8), 6549-6569.

[138]Zandarashvili, L., Langelier, M.-F., Velagapudi, U. K., Hancock, M. A., Steffen, J. D., Billur, R., Hannan, Z. M., Wicks, A. J., Krastev, D. B., & Pettitt, S. J. (2020). Structural basis for allosteric PARP-1 retention on DNA breaks. Science, 368(6486), eaax6367.

Kastamonu University
Journal of Engineering and Sciences
e-ISSN 2667-8209
http://dergipark.gov.tr/kastamonujes

Application of GC-MS for Simultaneous Identification of Malathion and 4F-MDMB-BUTICA in Forensic Analysis

Ebru Gökmeşe[a, *], Melike Küyük[b], Faruk Gökmeşe[a]

[a] Department of Chemistry, Faculty of Engineering and Natural Sciences, Hitit University, Çorum, Türkiye
[b] Ministry of Interior Gendarmerie and Coast Guard Academy, Ankara, Türkiye
***Corresponding Author:** ebrugokmese@hitit.edu.tr

Received: **September 13, 2025** ◆ Accepted: **December 16, 2025** ◆ Published Online: **December 25, 2025**

Abstract: Synthetic cannabinoids are chemicals developed to mimic the effects of natural marijuana (THC), and they are much more powerful and dangerous than THC. These types of substances are sprayed into herbal mixtures known as "bonzai" and put into the illegal drug market. Malathion is an organophosphorus (OP) insecticide used for the destruction and control of pests in agriculture. Even with low toxicity to humans, exposure to malathion has adverse effects on the respiratory tract and nervous system. In this study, a GC-MS method was developed for the simultaneous detection of pesticide residues used with synthetic cannabinoids with sedative effects in samples. Malathion, an organophosphate insecticide, and 4-Fluoro-MDMB-BUTICA, a new generation synthetic cannabinoid, were qualitatively analyzed on plant samples. As a result of the data obtained, Malathion pesticide, which has a sedative effect and is absorbed into herbs, will be detected and analyzed. In this study, qualitative analysis of pesticides was performed using the experimental method optimized with the Gas Chromatography-Mass Spectrometry (GC-MS) device.

Keywords: Malathion, Cannabinoid, Forensic Analysis, GC-MS

Adli Analizde Malathion ve 4F-MDMB-BUTICA'nın Eşzamanlı Tanımlanması için GC-MS Uygulaması

Öz: Sentetik kannabinoidler, doğal esrarın (THC) etkilerini taklit etmek üzere geliştirilmiş kimyasallar olup, THC'den çok daha güçlü ve tehlikelidirler. Bu tip maddeler "bonzai" gibi isimler ile bilinen bitkisel karışımlara püskürtülerek yasa dışı uyuşturucu pazarına sürülür. Malathion, tarımda zararlıların yok edilmesi ve kontrolü için kullanılan organofosforlu (OP) bir insektisittir. İnsanlar için düşük toksisitede bile malathiona maruz kalmanın solunum yolları ve sinir sistemi üzerinde olumsuz etkileri vardır. Bu çalışmada, sedatif etkiye sahip sentetik kannabinoidler ile birlikte kullanılan tarım ilacı kalıntılarının numunelerde eş zamanlı tespit edilmesine yönelik bir GC-MS metodu geliştirilmiştir. Organofosfatlı insektisitlerden Malathion ve yeni nesil sentetik kannabinoidlerden 4-Fluoro-MDMB-BUTICA, bitkisel numuneler üzerinde kalitatif olarak analiz edilmiştir. Elde edilen veriler neticesinde sedatif etkide bitkisel otların içerisine emdirilen Malathion tarım ilacı tespit edilerek analizine olanak sağlanacaktır. Bu çalışmada tarım ilaçlarının kalitatif analizi, Gaz Kromatografi-Kütle Spektrometresi (GC-MS) cihazı ile optimize edilen deney metodu kullanılarak yapılmıştır.

Anahtar Kelimeler: Malathion, kanabinoid, Adli Analiz, GC-MS

1. Introduction

The consumption of conventionally produced food contributes to environmental degradation. Industrial agricultural practices, characterized by the intensive use of machinery, pesticides, herbicides, fungicides, and fertilizers, generate substantial ecological pressures [1, 2]. While pesticides contribute to food security, they have simultaneously led to severe ecological, health, and socio-economic problems [3, 4]. Although the use of pesticides increases agricultural output, their improper and excessive application poses significant risks to both human and environmental health. The consumption of foods containing high levels of pesticide residues may cause acute or chronic poisoning in humans and other organisms within the environment [5].

The improper or excessive use of pesticides harms non-target organisms, leads to biodiversity loss, and has adverse effects on ecosystems [6]. Furthermore, the contamination of soil and water with pesticide residues poses a significant threat to ecosystem health [7]. Organophosphate-based synthetic pesticides (OPs) have been widely used for pest control since the mid-1940s. These highly toxic compounds are recognized as potential hazards to human health [8, 9].

Malathion (MAL) (S-(1,2-dicarbethoxyethyl) O, O-dimethyldithiophosphate) (Figure 1) has been utilized in agriculture, industry, and veterinary medicine since 1980. The toxicity of MAL primarily arises from its metabolites. Various factors such as product purity, route of exposure, nutritional status, genetic background, and sex influence its toxicological effects [10]. Malathion-based formulations are used to control a wide range of insects in the environment. Product formulations include emulsifiable concentrates, various soluble powders, and solutions.

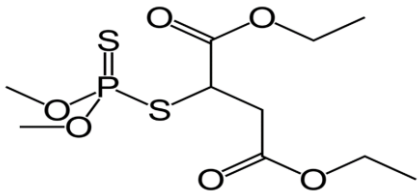

Figure 1. Chemical structure of Malathio

The chemical name of Malathion is Diethyl 2-[(dimethoxyphosphorothioyl)sulfanyl]butanedioate. It is used in the control of pests affecting vegetables, legumes, oilseeds, fruits, alfalfa insects, cotton leafworms, green stink bugs, bean larvae, and potato moths, among others [11].

In addition to its efficacy against harmful insects, Malathion exhibits toxicity toward numerous non-target species, including beneficial arthropods, amphibians, certain freshwater fish, and invertebrates, even at concentrations as low as 0.06 ppb [12]. As an organophosphorus insecticide, Malathion and its residues have been detected in aquatic environments. The type and characteristics of water used during pesticide application directly influence the pesticide's effectiveness and environmental persistence [13]. A poisoning incident reported in Italy, which focused solely on worker honeybees, revealed the presence of Malathion in 105 bee samples [14, 15].

Synthetic cannabinoids are generally encountered in solid or oily forms. They typically appear as pure, fine crystalline powders, varying in color from white to gray, brown, or yellow. Most synthetic cannabinoid compounds are lipophilic and show good solubility in solvents such as methyl alcohol, ethyl alcohol, acetonitrile, ethyl acetate and acetone [16, 17]. After being dissolved in acetone, ethanol, or methanol, the solution is sprayed onto plant material; the solvent is then evaporated. The crude drug mixture is subsequently dried again before being packaged and distributed.

Synthetic cannabinoids are chemical compounds developed to mimic the effects of natural cannabis (THC), yet they are considerably more potent and hazardous than THC. It has been emphasized that synthetic cannabinoids can induce multisystem toxicity, are rapidly spreading among young individuals, and may lead to fatal outcomes [18]. Compared with traditional narcotics, their easy accessibility and low cost have contributed to widespread consumption, particularly among low-income populations and adolescents. Numerous cases of severe intoxication and several fatalities have been attributed to the lack of early dosing information, the unpredictable and adverse effects of newly emerging substances, and the absence of specific diagnostic and therapeutic measures in emergency care. The detection of synthetic cannabinoids in biological fluids remains a critical issue in toxicology and forensic medicine applications [19].

4-Fluoro-MDMB-BUTICA

4-Fluoro-MDMB-BUTICA (Methyl (S)-2-{[1-(4-fluorobutyl)-1H-indazole-3-carbonyl]amino}-3,3-dimethylbutanoate) is one of the newly identified fifth-generation synthetic cannabinoid derivatives detected in recent years. Substances of this type are sprayed onto herbal mixtures marketed under names such as “spice” or “bonzai,” and subsequently distributed within the illicit drug market. These synthetic cannabinoids are classified as new psychoactive substances (NPS), and due to their unpredictable dosage, purity, and pharmacological effects, they pose a significant health risk to users.

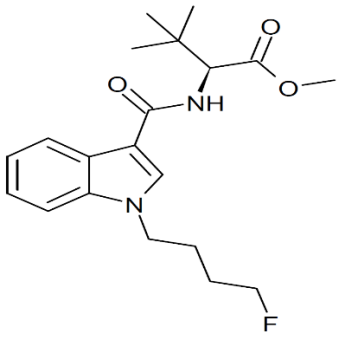

Figure 2. Chemical structure of 4-Fluoro Mdmb Butica

4-Fluoro-MDMB-BUTICA was first identified in herbal plant material seized in the United States in May 2020. As of July 2020, it had begun to appear in toxicological cases and was subsequently linked to at least 26 forensic cases in the United States. In Hungary, 11 fatal cases reported between May and August 2020 were associated with 4-Fluoro-MDMB-BUTICA [20]. This compound is considered one of the most dangerous newly emerging illicit synthetic cannabinoids of 2020. The use of reliable analytical methods to confirm the intake of 4-Fluoro-MDMB-BUTICA is a critical issue in forensic practice. In some cases, despite severe symptoms of intoxication, concentrations of the synthetic cannabinoid in urine and blood were found to be extremely low [21]. Analysis of the primary metabolites of synthetic cannabinoids is suitable for routine testing, as their rapid metabolism leads to a relatively rapid decline in the concentration of the parent compound in urine and blood [22]. Synthetic 4-Fluoro-MDMB-BUTICA has been characterized, and its 1H NMR, 13C NMR, and IR spectral properties have been reported [23]. Reference standards of 4-Fluoro-MDMB-BUTICA are available from commercial suppliers to support the implementation of routine analytical methods for forensic and clinical investigations. Chromatographic, spectroscopic, and mass spectrometric techniques have been employed for the identification and quantification of 4-Fluoro-MDMB-BUTICA in seized materials and biological sample matrices [24].

Since most plants used for drug purposes are contaminated with pesticides, it is common to encounter insecticide residues in materials impregnated with synthetic cannabinoids. Therefore, simultaneous analysis of Malathion and 4-Fluoro-MDMB-BUTICA in the same matrix enables the joint evaluation of two different toxic agents in forensic samples, strengthening both diagnostic accuracy and toxicological interpretation.

2. Material and Method

The methodological perspective of this study is grounded in the development of a reliable and reproducible GC-MS method for the simultaneous qualitative identification of sedative synthetic cannabinoids and pesticide residues in plant-based samples. The research adopts a systematic analytical approach that includes optimization of the sample preparation procedure, selection of an appropriate solvent mixture, adjustment of the GC column temperature program, and standardization of the ionization conditions.

Within this framework, retention times, mass spectral matching, and characteristic fragmentation patterns of the organophosphate insecticide Malathion and the new-generation synthetic cannabinoid 4-Fluoro-MDMB-BUTICA serve as primary verification criteria. The methodological structure is further supported by calibration steps of the GC-MS system, optimization of injection parameters, implementation of a cleaning protocol between analyses, and reproducibility assessments. This approach enables the reliable analytical identification of pesticides and synthetic drug compounds commonly encountered in forensic toxicology and criminal investigations involving complex plant matrices.

Chemicals and Reagents

Methanol (gradient grade), ethanol (≥99.9%), ethyl acetate (Merck, gradient grade), chloroform (≥99.8%), and acetone (gradient grade) were obtained from Merck. An Agilent Technologies 19091S-433 GC-MS system was used for all analyses.

Sample Preparation

Herbal samples, which were light green in color and in solid form, were weighed in the range of 0.1–0.5 g. Each sample was taken into glass tubes; It was extracted in a volume of 5 mL with a solvent mixture consisting of ethyl alcohol, methyl alcohol, chloroform and ethyl acetate. The samples were kept in an ultrasonic bath for 5 minutes to ensure that the target compounds passed into solution. The extracts obtained after sonication were filtered and transferred to containers suitable for GC-MS analysis. To evaluate the reproducibility of the method, the same preparation procedure was applied again and a second set of samples was analyzed under the same conditions.

GC-MS Instrumentation and Chromatographic Conditions

Analyses were performed using an Agilent 8890 GC coupled with a mass selective detector. A HP-5MS (5% phenyl-methyl siloxane) capillary column was used. The injector operated in splitless mode at 250 °C. Helium served as the carrier gas at a constant flow rate of 1.0 mL/min. The oven temperature program was as follows:

- initial temperature 80 °C (hold 1 min),
- ramp at 20 °C/min to 325 °C,
- final hold at 325 °C for 5 min.

The MS interface temperature was set to 280 °C and electron impact (EI) ionization at 70 eV was used. The scan range was m/z 40–550. Injection volume was 1 µL.

Method Development and Qualitative Validation

A qualitative GC-MS method was developed initially for Malathion and subsequently adapted for simultaneous detection of 4-Fluoro-MDMB-BUTICA. During optimization, injector temperature, column temperature program, solvent efficiency, and septum/liner replacement intervals were evaluated to improve chromatographic resolution and signal quality.

Between each run, a cleaning step was applied using a mixture of ethyl alcohol, methyl alcohol, ethyl acetate, and chloroform to prevent carryover. A reference solution with known composition was analyzed in triplicate to assess qualitative repeatability.

The optimized method yielded clear separation of both analytes. Based on SWGDRUG library matching, 4-Fluoro-MDMB-BUTICA eluted at 7.734 min, whereas Malathion eluted at 6.061 min. Retention times showed no significant variability between replicate analyses, confirming the method's qualitative consistency.

3. Results

Performance Analysis

The significant role of agricultural products in the export economies of many countries necessitates verifying that these products are free from chemical residues. Due to this obligation, quality control and quality assurance parameters emerged as indicators of analytical accuracy and reliability in the field of pesticide residue analysis in the late 1990s. The IAEA "Food and Environmental Protection Department – Agrochemicals Unit" pioneered this training and workshop project. In this study, a method was first developed to perform the qualitative analysis of the insecticidal active ingredient malathion using a GC-MS system. To demonstrate that the active substances of agricultural pesticides impregnated into plants can be detected—particularly due to the frequent synthesis of new sedative-active plant materials today—a GC-MS method was developed. During the development of this method, the parameters influencing the analysis were identified.

The analysis result of the green plant fragment prepared and analyzed in the laboratory is shown in Figure 3. The chromatogram corresponding to 4-Fluoro-MDMB-BUTICA and Malathion can be seen in this figure. Figure 4 presents the mass spectrum of 4-Fluoro-MDMB-BUTICA, and Figure 5 shows the mass spectrum of Malathion.

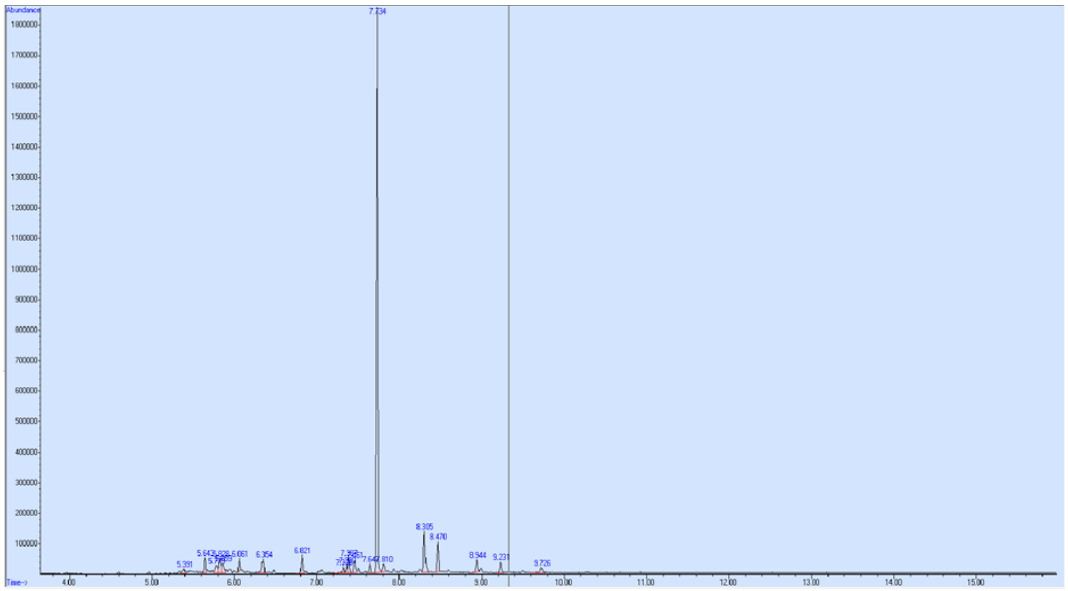

Figure 3. Chromatogram of the plant material (showing 4-Fluoro-MDMB-BUTICA and Malathion, respectively)

In the chromatogram shown in Figure 3, a strong peak is observed around ~7.3–7.8 min, constituting a significant portion of the signal. This peak most likely corresponds to 4F-MDMB-BUTICA. Malathion, which possesses an organophosphorus structure and generally elutes later, is estimated to appear at approximately ~8–10 min.

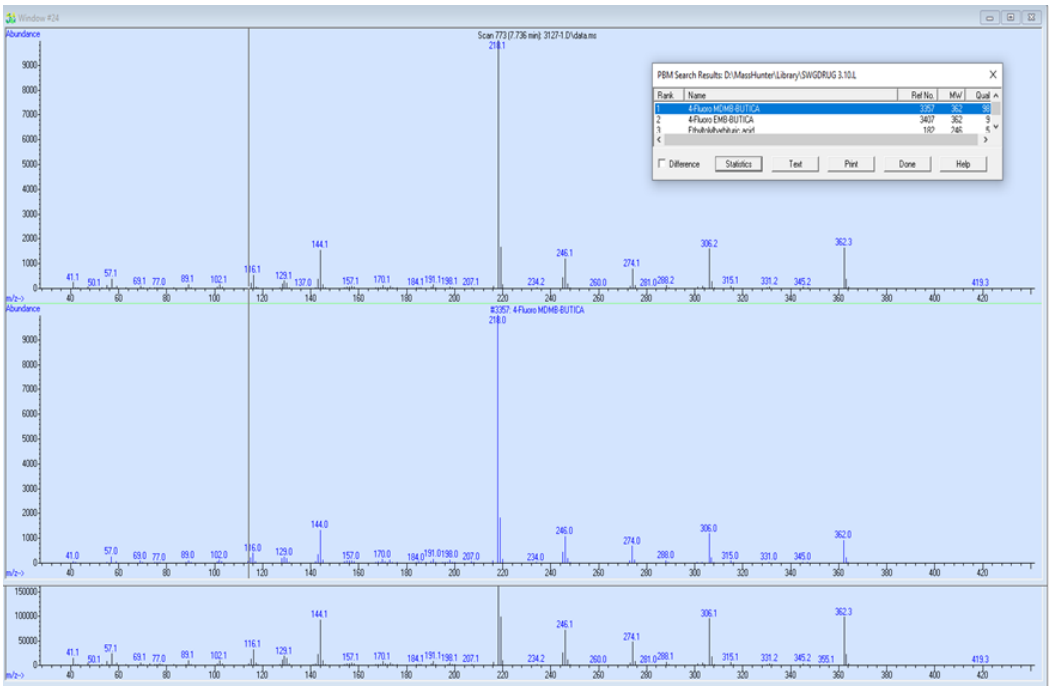

Figure 4. Mass spectrum of 4-Fluoro-MDMB-BUTICA

According to the spectral matching results obtained from the GC-MS instrument, 4F-MDMB-BUTICA appears as the top hit (Figure 4). The sample spectrum, the library-derived spectrum, and the difference spectrum are presented together.

Intense peak values are observed within the 100–400 m/z range. In particular, the m/z 214 and 340 fragments are among the characteristic ions of this compound. The spectral lines show excellent overlap.

The library match of this spectrum exhibits high similarity to 4F-MDMB-BUTICA. Therefore, it can be conclusively stated that the central peak observed at approximately 7.3–7.8 minutes in the sample corresponds to 4F-MDMB-BUTICA.

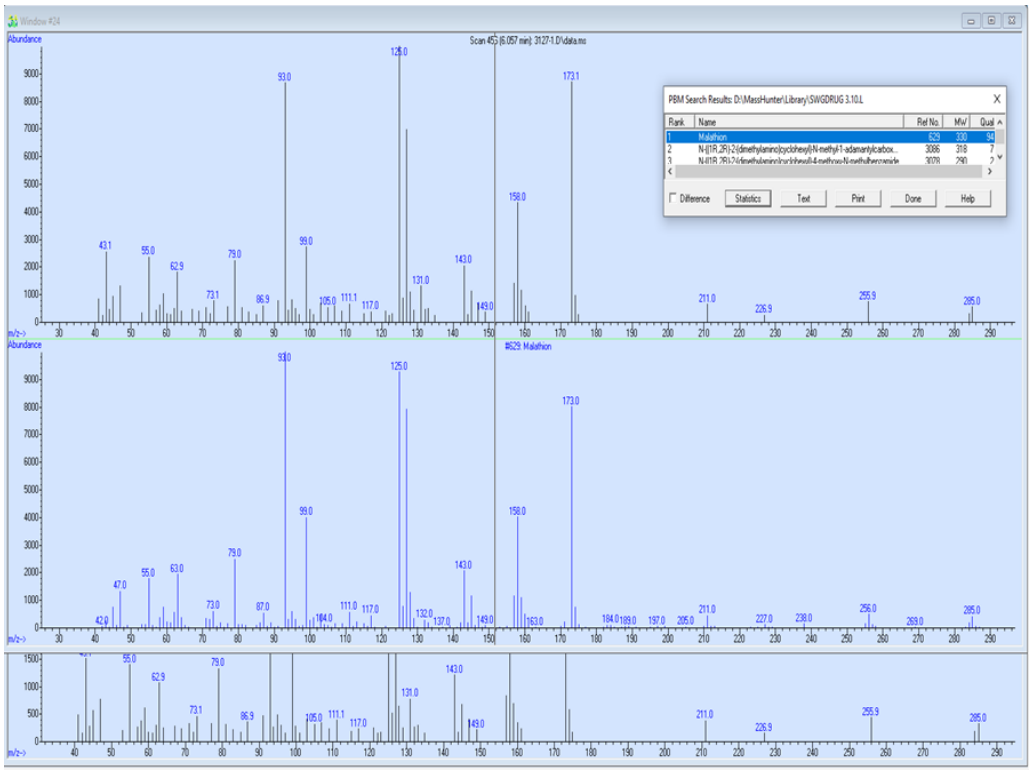

Figure 5. Mass spectrum of Malathion

Examining the spectral match of Malathion reveals the following major ions: m/z 99, 125, 127, 158, 173, 186, 201, 227, and 238. These ions include sulfur-containing and diester-derived fragments, fragments originating from the diethyl-succinate portion of the molecule, and larger organophosphorus fragments. Nearly all of these ions are present in the sample spectrum, and their relative intensities almost perfectly overlap with the library spectrum. The consistency of all characteristic ions confirms the definitive identification of Malathion.

Using GC-MS analysis, the two compounds were distinguished with high match scores. The central peak at a retention time of 7.34 minutes showed an intense library match with 4F-MDMB-BUTICA (Match > 850). The second peak at approximately 8.42 minutes was matched with Malathion (Match ≈ 845).

The analysis results are summarized in Table 1. Retention times for both compounds remained constant in repeated measurements, and the fact that the results did not change in the re-prepared samples shows the qualitative reliability of the method.

Table 1. Summary of GC-MS findings for Malathion and 4F-MDMB-BUTICA

Parameter	Malathion	4F-MDMB-BUTICA	Description
Retention time (RT)	6.061 min	7.734 min	Consistent in all repeated analyses
Mass spectral match	High	High	Verified using SWGDRUG library
Ionization mode	EI, 70 eV	EI, 70 eV	Stable ionization for both analytes
Replicate analysis (n = 3)	Consistent	Consistent	RT and spectra showed no significant variation
Re-prepared sample	Unchanged result	Unchanged result	Confirms reliability and repeatability of the method
Carry-over after cleaning	Not observed	Not observed	Washing protocol effectively prevented carry-over
Chromatographic separation	Good	Good	No peak interference observed
Matrix effect	Low	Low	Sample matrix suitable for GC-MS analysis
Method purpose	Qualitative	Qualitative	No quantitative validation performed

4. Discussion

The presence of pesticides in addition to harmful sedative substances poses serious health risks and has led to cases resulting in severe illness and even death. The analysis of pesticides plays a crucial role in the field of Forensic Sciences. In cases such as suicide, property damage, suspicious death, and poisoning involving the use of agricultural chemicals, the analysis of these substances and the interpretation of the results are of critical importance for elucidating such incidents. 4-Fluoro-MDMB-BUTICA is a hallucinogenic synthetic compound that induces perceptual alterations, cognitive impairment, and disorientation in terms of direction, distance, and time. The body rapidly absorbs aliphatic organophosphates such as Malathion and can be detected in urine. In cases of intoxication, patients must receive treatment within 48 hours. Although Malathion is rapidly hydrolyzed in human tissues, its absorption or ingestion leads to the metabolic formation of the toxic metabolite malaoxon.

Evidence submitted to forensic laboratories for pesticide-related investigations may include food samples, liquid samples, plant-derived materials, animal-based food products, beverages, and wastewater samples.

Drug use and trafficking constitute one of the greatest threats to public health and safety both in our country and globally. In recent years, this threat has expanded with new dangers associated with synthetic cannabinoids. Although extensive medical and forensic experience exists regarding well-known narcotics such as heroin, cocaine, and cannabis, authorities urgently require enhanced detection capabilities and rapid intervention strategies for synthetic cannabinoids.

This study accomplished the chromatographic identification of Malathion, an insecticide found in plant materials infused with synthetic cannabinoids. Approximately 2.5 million tons of pesticides are used worldwide each year. The World Health Organization reports that roughly 3 million people suffer from pesticide poisoning annually and that 220,000 of these cases result in death. Pesticide use in our country accounts for about 1% of global consumption. Organophosphates are the most frequent cause of poisoning in rural regions of our country. These compounds pose significant challenges in the health and agricultural production sectors.

Organophosphates have been widely used as a significant class of insecticides since the 1940s. They are favored due to their selective toxicity towards insects and limited residue formation, which contributes to their global prevalence. Organophosphates irreversibly inhibit the enzyme acetylcholinesterase in the central and autonomic nervous systems, as well as in red blood cells, leading to tissue accumulation of acetylcholine. The resulting neurotoxic effects lead to acute or chronic poisoning. This indicates that precautionary measures should be taken regarding the teratogenic potential of Malathion, even at low doses, despite its reputation as a relatively safer and less toxic pesticide compared to others commonly used in our country and worldwide.

In terms of forensic evaluation, the presence of both Malathion and 4F-MDMB-BUTICA in the same sample requires reconsidering possible exposure routes. In the literature, it has been reported that in some forensic cases, unexpected toxic symptoms after consumption of synthetic cannabinoids were aggravated due to accompanying pesticide residues [25]. Detecting these substances together; suggests that the user was exposed to both compounds simultaneously from one source, thus toxicological findings may result from a complex combined effect. In clarifying the events, the source of exposure, toxicity profile and possible interactions can be evaluated more accurately. For this reason, the developed method provides an important contribution to forensic toxicology applications as a complement to both screening and verification processes.

5. Conclusion

Through this study, the necessary quality procedures were completed, and a new analytical method was developed. The method can be used for the analysis of evidence submitted in cases of poisoning, suspicious death, suicide, property damage, and similar incidents involving Malathion as an active insecticidal compound within sedative plant-based materials. Additionally, this original work provides evidence supporting the reliability of results produced to date by the GC-MS systems of the Chemical Analysis Laboratory of the Gendarmerie Criminal Department, Central Laboratory Command.

Competing Interest / Conflict of Interest

The authors declare that they have no competing interests.

Author Contribution

Conceptization: EG, MK, FG; methodology and laboratory analyzes: EG, MK, FG; writing draft: EG, MK, FG; proof reading and editing: Other: All authors have read and agreed to the published version of manuscript.

Acknowledgements

We would like to thank the Gendarmerie Criminal Directorate, Central Laboratory Directorate, for their support in carrying out the experimental studies.

6. References

[1] Muñoz, P.; Antón, A.; Núñez, M., Paranjpe, A., Ariño, J., Castells, X., Montero, J., Rieradevall, J. (2008). Comparing the Environmental Impacts of Greenhouse Versus Open-Field Tomato Production in The Mediterranean Region. Acta Horticulturae, 801: 1591–1596.

[2] Ehrlich, P.R. (2011). A Personal View: Environmental Education—Its Content and Delivery. Journal of Environmental Studies and Sciences. 1: 6–13.

[3] Aktar, M. W., Sengupta, D., Chowdhury, A. (2009). Impact of Pesticides use in Agriculture: Their Benefits and Hazards. Interdisciplinary Toxicology. 2(1): 1–12.

[4] Carvalho, F. P. (2017). Pesticides, Environment, and Food Safety. Food and Energy Security. 6 (2): 48–60.

[5] FAO. (2022). The State of the World's Land and Water Resources for Food and Agriculture. Rome: Food and Agriculture Organization of the United Nations.

[6] Sanchez-Bayo, F., Wyckhuys, K. A. G. (2019). Worldwide Decline of the Entomofauna: A Review of its Drivers. Biological Conservation. 232: 8–27.

[7] Silva, V., Mol, H. G. J., Zomer, P., Tienstra, M., Ritsema, C. J., Geissen, V. (2019). Pesticide Residues in European Agricultural Soils – A Hidden Reality Unfolded. Science of the Total Environment. 653: 1532–1545.

[8] Ozsoy A.Z., Nursal A.F., Karsli M.F., et al. (2016). Protective Effect of intravenous Lipid Emulsion Treatment on Malathion-induced Ovarian Toxicity in Female Rats. European Review for Medical and Pharmacological Sciences. 20: 2425–2434.

[9] Uysal M., Karaman S., (2018). Invivoeffects ofintravenous Lipid Emulsion on Lung Tissue in an Experimental Model of Acute Malathion intoxication. Toxicol Ind Health. 34:110–118.

[10] Varol S., Başarslan S.K., Fırat U., et al. (2015). Detection of Borderline Dosage of Malathion intoxication in a rat's brain. European Review for Medical and Pharmacological Sciences. 19: 2318–2323.

[11] Kassiri, H., Rabbani, D., Mohebi, F., Dehghani, R., Takhtfiroozeh, S. (2021). A Review on the Removal Methods of Organophosphate Insecticide. Journal of Entomological Research. 45 (1) : 145-152.

[12] Schroeder-Spain, K., Fisher, L.L. and Smee, D.L. (2018). Uncoordinated: Effects of Sublethal Malathion and Carbaryl Exposures on Juvenile and Adult Blue Crabs (Callinectes sapidus). Journal of Experimental Marine Biology and Ecology. 504: 1-9.

[13] Bokulıć Petrıć, A., Stipičević, S., Mešić, A. (2023). Stability of Malathion, Diazinon and Chlorpyrifos in Different Water Types –a review. Journal of Central European Agriculture. 24 (4): 873-887.

[14] Porrini, C., Sabatini, A. G., Girotti, S., Fini, F., Monaco, L., Celli, G., Bortolotti, L., Ghini, S. (2003). The Death of Honey Bees and Environmental Pollution by Pesticides: The Honey Bees as Biological Indicators. Bulletin of Insectology. 56 (1): 147-152.

[15] Guo, D., Liu, W., Yao, T., et al, (2021). Combined Endocrine Disruptive Toxicity of Malathion and Cypermethrin to Gene Transcription and Hormones of the HPG Axis of Male Zebrafish (Daniorerio). Chemosphere. 267: 128864.

[16] Gurdal F., Asirdizer M., Aker R.G., Korkut S., Gocer Y., Kucukibrahimoglu E.E. et al. (2013). Review of Detection Frequency and Type of Synthetic Cannabinoids in Herbal Compounds Analyzed by Istanbul Narcotic Department of the Council of Forensic Medicine, Turkey. Journal of Forensic and Legal Medicine. 20: 667-672.

[17] Liechti, M. (2015). Novel Psychoactive Substances (designer drugs): Overview and Pharmacology of Modulators of Monoamine Signaling. Swiss Medical Weekly. 14 (145): 14043.

[18] Alzubi, A., Almahasneh, F., Khasawneh, R., Abu-El Rub, E., Baker, W.B., Zaoubi, R.M. (2024). The Synthetic Cannabinoids Menace: A Review of Health Risks and Toxicity. European Journal of Medical Research. 29: 49.

[19] Diao X., Huestis M.A. (2017). Approaches, Challenges, and Advances in Metabolism of New Synthetic Cannabinoids and Identification of Optimal Urinary Marker Metabolites. Clinical Pharmacology and Therapeutics. 101: 239–253.

[20] Krotulski, A.J., Papsun, D.M., Walton, S.E., Logan, B.K. (2023). Positivity of New Synthetic Cannabinoid 4F-MDMB-BICA Increasing in U.S. as Prevalence of 5-MDMB-PICA Wanes. CFSRE, Redefining Excellence in Forensic Science. NCJ Number 307389.

[21] Diao X., Huestis M.A. (2019). New Synthetic Cannabinoids Metabolism and Strategies to Best Identify Optimal Marker Metabolites. Frontiers in Chemistry. 7: 109.

[22] Kovács K., Kereszty É., Berkecz R., Tiszlavicz L., Sija É., Körmöczi T., et al. (2019). Fatal Intoxication of a Regular Drug User Following N-ethyl-hexedrone and ADB-FUBINACA Consumption. Journal of Forensic and Legal Medicine. 65: 92–100.

[23] Cannaert, A., Sparkes, E., Pike, E., Luo, J. L., Fang, A., Kevin, R. C., Ellison, R., Gerona, R., BANISTER, S. D., Stove, C. P. (2020). Synthesis and in Vitro Cannabinoid Receptor 1 Activity of Recently Detected Synthetic Cannabinoids 4F-MDMB-BICA, 5F-MPP-PICA, MMB-4enPICA, CUMYL-CBMICA, ADB-BINACA, APP-BINACA, 4F-MDMB-BINACA, MDMB-4en-PINACA, A-CHMINACA, 5F-AB-P7AICA, 5F-MDMB-P7AICA, and 5F-AP7AICA. ACS Chemical Neuroscience. 11: 4434-4446.

[24] European Monitoring Centre for Drugs and Drug Addiction, (2021). Risk Assessment Report on a New Psychoactive Substance: methyl 2-{[1-(4- fluorobutyl)-1H-indole-3-carbonyl]amino}-3,3-dime- thylbutanoate (4F-MDMB-BICA) in Accordance with Article 5c of Regulation (EC) No 1920/2006.

[25] Dryburgh, L. M., Bolan, N. S., Rout, P. R., Manevski, K., Halim, A., & Sarkar, B. (2021). Cannabis contaminants: Sources, distribution, human toxicity and regulatory considerations. Environmental Pollution, 287, 117562.

doi:10.55385/kastamonujes.1828190 KUJES 11(2):104-113, 2025

Kastamonu University
Journal of Engineering and Sciences
e-ISSN 2667-8209
http://dergipark.gov.tr/kastamonujes

Effect of *Limnospira platensis* and *Cladophora glomerata* Inoculation on Some Biological Properties of Lentil Rhizosphere

Elif Doğan[a], A. Cenap Cevheri[b], Çiğdem Küçük[b,*], Göksal Sezen[b]

[a]Institute of Natural Sciences, Harran University, Şanlıurfa, Türkiye
[b]Department of Biology, Faculty of Arts and Sciences, Harran University, Şanlıurfa, Türkiye
***Corresponding Author:** ckucuk@harran.edu.tr

Received: **November 21, 2025** ◆ Accepted: **December 19, 2025** ◆ Published Online: **December 25, 2025**

Abstract: This study investigated the positive effect of *Limnospira platensis* and *Cladophora glomerata* on plant growth in lentils and on soil respiration and glucosidase enzyme activity. The application of different doses of *L. platensis and C. glomerata* significantly promoted seedling growth and certain microbiological properties of the soil in both species in a dose-dependent manner. In the study, planned according to a factorial experimental design with randomised plots, *L. platensis* microalgae and *C. glomerata* macroalgae were applied separately and in mixtures at different doses (control (0%), 0.2%, 0.4%, 0.6%, 0.8% and 1%) to the seedling root zone. Twelve weeks after sowing, both algal applications increased the green shoot weight, plant height, root length, and chlorophyll content of the seedlings compared to the control. Furthermore, the application of *L. platensis* and *C. glomerata* had a positive effect on soil respiration and β-glucosidase enzyme activity, which are important indicators of soil health. Compared to the separate application of *L. platensis* and *C. glomerata*, the combined application of high doses was found to be more effective on the characteristics studied. Our findings show that the separate and combined application of *L. platensis* and *C. glomerata* to soils improves both plant and soil health and may be an alternative to chemical fertilisers used in agriculture in preventing environmental pollution.

Keywords: Macroalgae, Microalgae, Application dose, Seedling growth, B-Glucosidase enzyme activity, Soil respiration

Limnospira platensis ve *Cladophora glomerata* Inokulasyonunun Mercimek Rizosferindeki Bazı Biyolojik Özelliklere Etkisi

Öz: Bu çalışmada *Limnospira platensis* ve *Cladophora glomerata*'nın mercimekte bitki büyümesi ve toprağın solunum ve glukosidaz enzim aktivitesi üzerindeki olumlu etkisi incelenmiştir. *L. platensis* ve *C. glomerata*'nın farklı dozlarının uygulanması, her iki türde de doza bağlı bir şekilde fide büyümesini ve toprağın bazı mikrobiyolojik özelliklerini büyük ölçüde teşvik etmiştir. Tesadüf parselleri faktöriyel deneme desenine göre planlanan çalışmada farklı dozlarda (kontrol (%0), %0.2, %0.4, %0.6, %0.8 ve %1) mikroalg olan *L. platensis* ve makro alg *C. glomerata*'nın ayrı ayrı ve karışımları fide kök bölgesine uygulanmıştır. Ekimden 12 hafta sonra hasat edilen fidelerde her iki alg uygulaması; fidelerin yeşil aksam ağırlıkları, bitki boyu, kök uzunluğu, klorofil içeriğini kontrole göre artırmıştır. Ayrıca *L. platensis* ve *C. glomerata* uygulanması, toprak sağlığının belirlenmesinde önemli olan toprak solunumu ve β-glukosidaz enzim aktivitesinde de olumlu bir etki göstermiştir. İncelenen özellikler üzerine *L. platensis* ve *C. glomerata*'nın ayrı ayrı uygulanmasına göre yüksek dozların birlikte uygulanması daha etkili bulunmuştur. Bulgularımız, topraklara uygulanan *L. platensis* ve *C. glomerata*'nın ayrı ayrı ve birlikte uygulanmasının hem bitki hem de toprak sağlığını artırdığını göstermekle birlikte, tarımda kullanılan kimyasal gübrelere karşı çevre kirliğinin önlenmesinde alternatif olabilir.

Anahtar Kelimeler: Makroalg, Mikroalg, Uygulama dozu, Fide gelişimi, B-Glukosidaz enzim aktivitesi, Toprak solunumu

1. Introduction

The rapid growth of the world population has led to increased demand for food, which has been met by the excessive use of chemical fertilizers to boost agricultural production. However, alongside increased crop production, the excessive and indiscriminate use of chemical fertilizers has led to serious environmental problems such as greenhouse gas emissions, soil and water quality degradation, water eutrophication, and loss of biodiversity [1, 2]. The continuous application of chemical fertilizers also poses a risk to the health of living organisms through the food chain. Furthermore, the negative effects of urbanization, erosion, and climate change, coupled with the decline in productive agricultural land, have complicated the situation as farmers use step by step increasingly more chemical fertilizers to obtain more plant products from less land [1, 3,4].

In recent years, researchers have recommended the use of biofertilizers and biostimulants, which offer various advantages over traditional fertilizers in reducing the negative effects of chemical fertilizers [5, 6, 2]. Biological fertilizers support plant growth and development by allowing easier and faster absorption of nutrients such as nitrogen, phosphorus, potassium, and minerals in the soil as a result of plant colonization by organisms such as bacteria, fungi, and micro-macroalgae [7, 8]. Additionally, even when applied in very small amounts, biostimulants have been found to be resources that promote plant nutrition without harming the environment, increase nutrient use efficiency, enhance stress tolerance, and increase yield or quality [7, 9].

Many algae-based formulations are attracting attention as promising plant nutrient sources in agriculture due to their effects on improving soil fertility and supporting plant growth [10, 2]. Microalgae extracts have been found to contain many micro and macro nutrients, particularly N, P and K, and algae extracts have been recognized as organic and slow-release fertilizers [11]. Studies have revealed that algae contain substances that promote plant growth, such as auxin, cytokinin, betaine, amino acids, vitamins, and antifungal compounds [12, 7, 13] observed that aqueous extracts of *Acutodesmus dimorphus* had a positive effect on tomato plant growth. The application of *Chlorella vulgaris* has been found to result in higher biomass accumulation in lettuce and better absorption of nutrients required by plants from the soil [13].

Microalgae with biostimulant effects that are most commonly used in research include *Chlorella vulgaris, Scenedesmus quadricauda, Dunaliella salina, L. platensis* and *Calothrix elenkinii* [14]. It has been reported that the most researched among them are *L. platensis* species [15, 16]. *L. platensis*, a filamentous photosynthetic blue-green (Cyanobacteria) microalgae that is easier to cultivate than other algae, has gained popularity worldwide as a food source due to its high protein content and nutritional value [8]. Recently, *L. platensis* has also been proposed as an alternative to chemical fertilizers, as it can be used as a rich source of macro- and micronutrients for plants [17, 15].

Cladophora glomerata (L.) Kütz. is a green alga belonging to the Cladophoraceae family (Chlorophyta, Ulvophyceae) and is one of the most common algae found in freshwater [18]. Qualitative and quantitative analyses of this algal extract have reported that it is rich in phenolic acids and flavonoids, which are known antioxidants, as well as macro and microelements. [19, 20, 21, 22].

Cladophora glomerata is a green macroalgae applied as a plant growth biostimulant. Limited research has been conducted on the use of this alga in agricultural development. Extracts prepared from *C. glomerata* have shown a positive effect on the development of carrots [23], radishes [24], and soybeans [25, 26, 24]. Extracts prepared from algae such as *Saccorhiza polyschides, C. glomerata*, etc., used as biostimulants, have reduced the plant's need for chemical fertilizers while improving plant growth and quality characteristics, as well as resistance to abiotic and biotic stress, due to the bioactive compounds they contain [27, 28].

The macroalgae *C. glomerata* can be used in solid form as a fertilizer and soil conditioner or in liquid form as a biostimulant for plant growth, as reported by Michalak and Messyasz [18]. It has been found that a mixture of macroalgae (*C. glomerata*) and mycorrhiza increases the development of corn plants and increases the alkaline phosphatase, urease, dehydrogenase, and β-glucosidase enzyme activities of soils [29]. High doses of extracts obtained from the green macroalgae *C. glomerata* were found to be effective on the growth of pea seedlings [28]. The aim of this study is to determine and evaluate whether different doses of the microalgae *L. platensis* and the macroalgae *C. glomerata*, separately and together, affect the growth of lentil seedlings and certain microbiological activities in the soil.

2. Material and Method

The macroalgae *Cladophora glomerata* and microalgae *Limnospira platensis* used in the study were obtained from the Department of Hydrobiology, Faculty of Biology, Harran University. Dried, ground samples of *C. glomerata* and *L. platensis* (100 g each) were mixed separately in 1000 ml of distilled water and used at the desired doses [30, 29]. Soil taken from a depth of 0-30 cm from a fallow field was used in the experiment. The pH of the soil used in the experiment was 7.6; organic matter (%) 1.27; lime (%) 2.35; nitrogen content was 0.09%, and it had a clayey texture.

2.1. Application of *C. glomerata* and *L. Platensis* to Soil

Pots (3 kg) were filled with soil that had been passed through a 2 mm sieve and sterilized by autoclaving for three consecutive days. Ten days after the germination of *C. glomerata* and *L. platensis* plants, different doses of both (0% (control), 0.2%, 0.4%,

0.6%, 0.8%, and 1%) were applied separately and in mixtures (the suspensions of both algae prepared at different doses were mixed in equal amounts to prepare the mixtures) were applied to 50 ml of soil in the plant root zone. Ten lentil seeds were sown in each pot and thinned to 5 plants after germination. The applications were repeated three times at 10-day intervals until harvest. Control pots without macro- and microalgae were only watered with tap water. Plants were watered once a week with tap water according to the soil's field capacity and the plants' water requirements and harvested 12 weeks after sowing. The experiment was set up in a greenhouse in a randomized block design with three replications.

2.2. Basic Plant Parameters

At harvest time, the plant height of the lentil seedlings was measured using a ruler, and the green parts and roots were cut at the root collar and weighed. The roots were washed with tap water to remove soil, excess water was absorbed with filter paper, root length was measured, and fresh weight was weighed and recorded. The green parts of the plants were placed in separate paper bags and kept at 70°C for 48 hours to determine their dry weight, and the dry weight of the samples was weighed [31].

2.3. Calculation of Photosynthetic Pigments

The method proposed by Arnon [32] was used to determine the amount of chlorophyll a and b in fresh leaf samples. A 1 g sample taken from the leaves was homogenized with 80% (v/v) acetone, and the chlorophyll content was measured at 645 and 663 nm wavelengths using a spectrophotometer (Shimadzu, Japan).

2.4. Rhizosphere β-glucosidase Enzyme Activity

β-glucosidase enzyme activity in soil adhering to roots and collected from around roots was analyzed according to Eivazi & Tabatabai [33] and Mukherjee et al. [34]. Toluene, buffer solution, and enzyme substrate were added to the soil sample in sequence and incubated at 37°C for 60 minutes. After incubation, $CaCl_2$ and Tris solution were added to the content and centrifuged. The absorbance of the supernatant was measured at a wavelength of 410 nm using a spectrophotometer (Shimadzu, Japan).

2.5. Basal Soil Respiration

Respiration in rhizosphere soil samples was determined using the Isermayer method. Samples for each treatment were taken from the root region at harvest time and incubated at 25 °C for 24 hours in a beaker containing an alkaline solution. At the end of the incubation period, the liquid solution was titrated with 1 M HCl using phenolphthalein indicator, and measurements were performed according to Anderson [35].

2.6. Statistical Analysis

The data were subjected to two-way analysis of variance using the JMP 11 software package (Statistical Graphics Corporation, 1991). The Tukey HSD multiple comparison test was used to analyze whether there were differences between the groups.

3. Results

In this study, adding *L. platensis* and *C. glomerata* to the soil (rhizosphere region) increased plant height. Increasing doses of *L. platensis* increased plant height, with the lowest plant height observed in the control group where no application was made, and the highest plant height determined at a 1% application dose of *L. platensis* (31.6% increase). Similarly, increasing doses of *C. glomerata* also increased plant height compared to the control, with the highest increase compared to the control being 37.1% at a 1% application dose of *C. glomerata* (Table 1). The combined application of *C. glomerata* and *L. platensis* yielded better results compared to other applications, with the highest plant height obtained at the application doses of 0.8% *L. platensis* + 1% *C. glomerata* (Lp-0.8+Cl-1).

Although the applications caused an increase in plant height compared to the control, none of these increases were found to be statistically significant when compared to the control application. The applications also showed differences in green shoot dry weight. When increasing doses of *L. platensis* and *C. glomerata* were applied together, an increase in plant dry weight was determined, and this increase was found to be statistically significant ($p<0.05$). The integrated (Lp+Cl) applications of high doses of macro- and microalgae used in the experiment yielded better results when compared to the results obtained with individual applications (Lp or Cl) (Table 1). The applications also caused an increase in green shoot dry weight, and this increase was statistically significant compared to the control. In particular, the increase in green shoot dry weight determined in the Lp-0.8+Cl-1 and Lp-1+Cl-1 applications was statistically significant ($p<0.05$) compared to the control where no application was made. While the dry weight of green parts was 1.2 g/plant in the control, it was determined to be 5.2 g/plant in the Lp-1+Ch-1 application and 5.3 g/plant in the Lp-0.8+Cl-1 application. Increasing doses of microalgae and macroalgae were also found to be effective on root length.

Table 1. Effects of *C. glomerata* and *L. platensis* applications on lentil seedling plant height, root length and green parts weight**.**

	C. glomerata (%)					
L.platensis (%)						
Plant height (cm)	0	0.2	0.4	0.6	0.8	1
0	19.9 s*	23.3 op	21.8 qr	25.0 mn	26.4 h-l	26.9 g-j
0.2	24.6 no	25.3 k-n	26.8 g-j	27.1 f-j	25.2 lmn	27.3 e-ı
0.4	21.0 rs	22.8 pq	23.1 p	24.4 no	27.3 d-h	28.1 c-g
0.6	23.3 op	25.2 lmn	25.9 j-m	26.6 h-k	27.7 d-h	28.3 c-f
0.8	24.1 nop	26.5 h-l	27.0 f-j	27.0 f-j	29.0 c	31.0 a
1	26.2 ı-m	27.3 e-l	28.5 cde	28.7 cd	29.4 bc	30.4 ab
LSD (p<0.05): 1.31						
Green part dry weight (g/plant))						
0	1.2 q	1.2 q	1.3 pq	1.3 pq	1.4 pq	1.5 p
0.2	2.0 mno	1.8o	1.8 no	2.0 lmn	2.1 lm	2.2 kl
0.4	2.2 lm	2.4 k	3.6 hıj	3.9 c	3.9 d	3.9 efg
0.6	3.42 ıj	3.4 ıj	3.4 j	3.6 hı	4.1 fg	4.6 def
0.8	3.5 ıj	3.5 ıj	3.5 ıj	3.9 ef	4.2 de	5.3 a
1	3.55 ıj	3.5 ıj	3.6 hı	3.8 gh	4.9 b	5.2 a
LSD (p<0.05): 0.21						
Root length (cm)						
0	12.0 r	13.1 qr	13.2 qr	14.1 opq	15.6 k-n	16.7ıjk
0.2	12.9 qr	13.7 pq	13.7 pq	17.1 hıj	21.3 f	20.0 g
0.4	14.2 opq	14.4 nop	14.8 m-p	17.2 hıj	23.3 e	22.0 ef
0.6	14.5 nop	15.3 k-n	16.2 jkl	18.1 h	23.3 e	27.0 c
0.8	15.2 l-o	17.2 hıj	18.3 h	20.0 g	25.7 d	28.3 ab
1	15.5 klm	17.6 hı	21.2 fg	27.1 bc	28 bc	29.3 a
LSD (p<0.05): 0.12						

*Different letters in the same column indicate statistically significant differences (p<0.05) between the means within each application.

The highest root length was determined in the Lp-1+Cl-1 and Lp-0.8+Cl-1 applications, respectively (Table 1), causing an increase compared to the control, and these increases were statistically significant (p<0.05). Chlorophyll a and b levels in all plants treated with *L. platensis* and *C. glomerata* increased with increasing application doses. The lowest chlorophyll contents were determined in the control, while the highest chlorophyll a was detected in the Lp-1+Cl-1 application and the highest chlorophyll b was detected in the Lp-1+Cl-1 and Lp-0.8+Cl-1 applications (Figure 1). The increases in chlorophyll content obtained when compared to the control with increasing dose applications were statistically significant (p<0.05). The applications also affected β-glucosidase enzyme activity, with the highest activity determined in the Lp-1+Ch-1 application, followed by Lp-0.8+Cl-1, Lp-1+Ch-0.8, and Lp-1+Ch-0.6 (Figure 2).

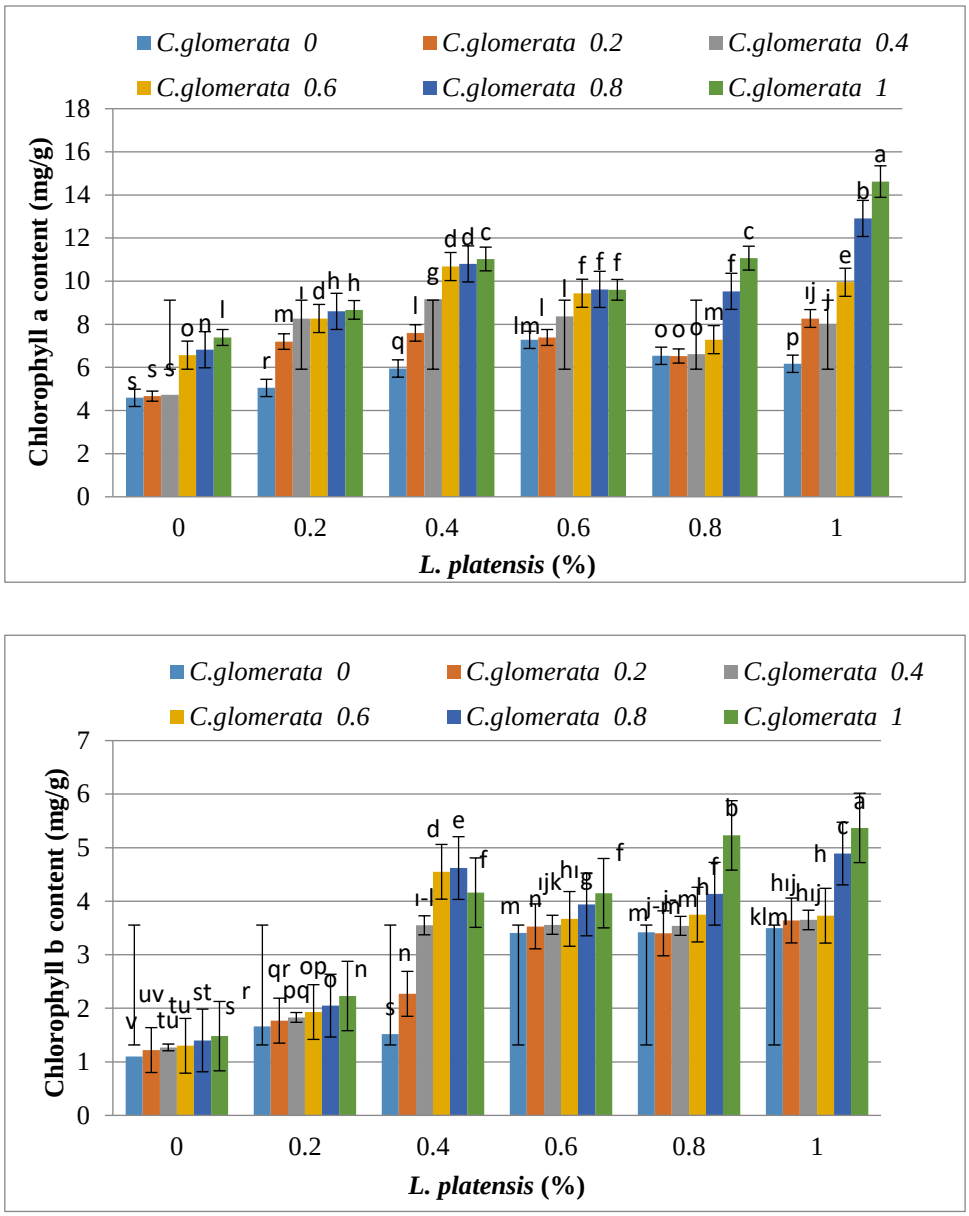

Figure 1. *C. glomerata* and *L. platensis* applications on chlorophyll a and b content in lentil seedling leaves. Different letters indicate significant differences ($p<0.05$) between means within each treatment. Error bars indicate standard error (n=3).

The lowest activity was observed in the control where no treatment was applied. Increasing doses of both *L. platensis* and *C. glomerata*, when applied separately, significantly increased soil respiration compared to the control ($p<0.05$). The 1% application dose of *L. platensis* increased respiration by 110.4% compared to the control, while the 1% application dose of *C. glomerata* increased it by 89.7% (Figure 2). The application of mixtures increased soil respiration, with the highest increase observed in the Lp-1+Ch-1 application. This was followed by the Lp-1+Cl-0.8, Lp-1+Ch-0.6, and Lp-0.8+Ch-0.6 applications, respectively. When the increasing doses of the applications were compared with the control, a statistically significant increase in soil respiration was observed ($p<0.05$).

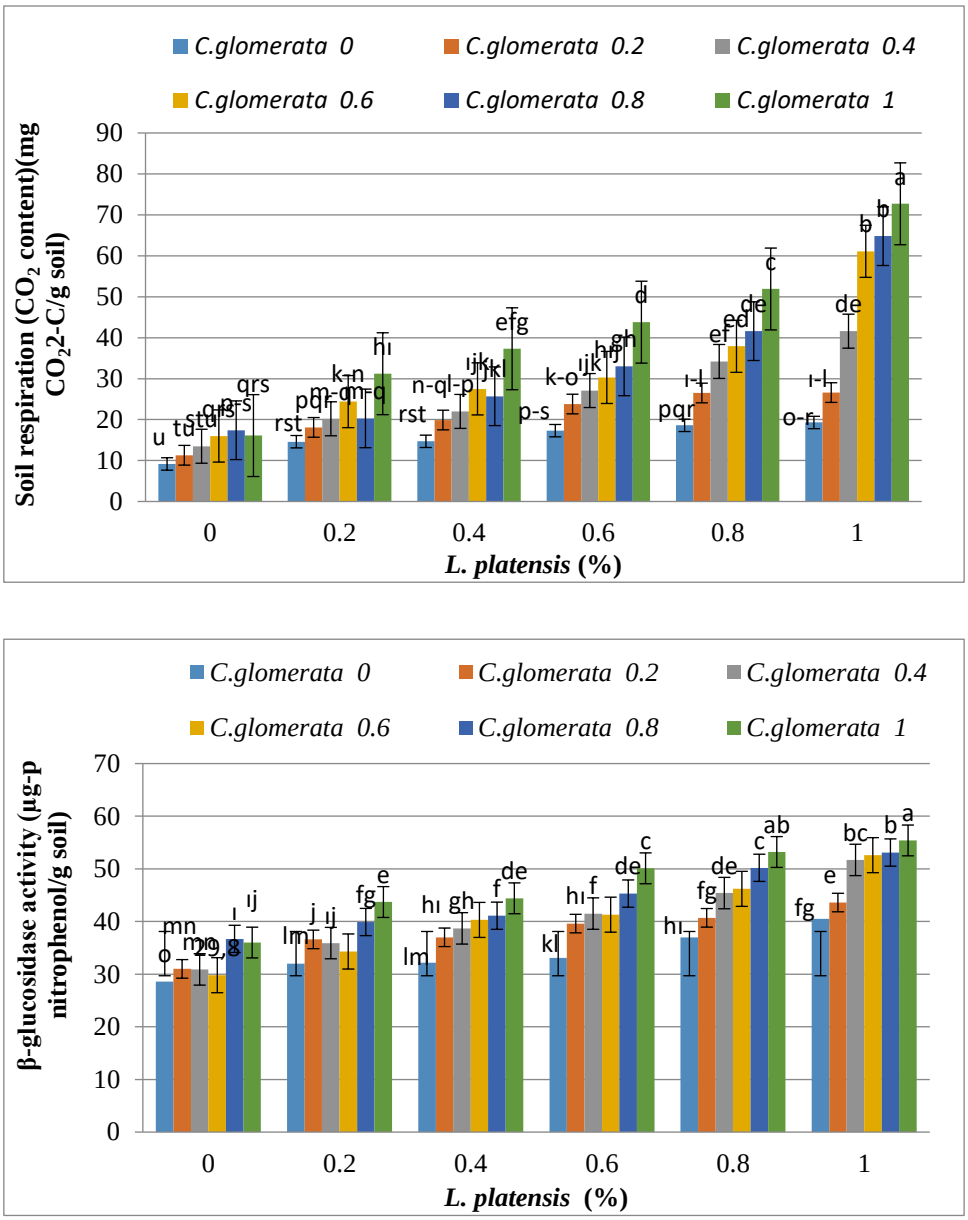

Figure 2. Effects of *C. glomerata* and *L. platensis* applications on respiration and β-glucosidase enzyme activity of lentil rhizosphere. Different letters indicate significant differences ($p<0.05$) between the means in each treatment. Error bars indicate standard error (n=3).

4. Discussion

The use of biostimulants in agriculture, especially those derived from algae extracts, is becoming widespread worldwide. Agricultural biostimulants contain different types of bioactive compounds such as microorganisms, plant growth regulators, enzymes, and macro- and microalgae extracts [16]. Biostimulants are known to improve plant resistance to abiotic and biotic stresses and increase yield by affecting plant physiology. These products can alter root growth and structure [36]. In our study, as shown in Table 1, root length was positively affected by algal applications. Two different algal applications at different doses increased root length compared to the control. Root length in the Lp-1+Cl-1 application increased by 144.1% compared to the control. The difference determined between the applications stems from the fact that algal application doses affect root structure, resulting in different effects on root development [37]. Since high doses of algae contain more bioactive compounds, stimulation of roots by these active compounds, the assimilation of carbon dioxide by algae applied to the soil, thereby increasing the soil's organic carbon content, and the fixation of atmospheric nitrogen by cyanobacterial heterocyst cells to meet the plant's nitrogen requirements also affect root length [38]. The increase in root length observed has been noted in various crops, regardless of whether the extracts were applied to the leaves or soil. This effect has also been detected in cucumbers, tomatoes, barley, raspberries, and beans [39. 40, 41]. Different studies have also investigated the increase in plant growth with the use of microalgae [42, 43, 44].

Algae have properties that not only enhance plant growth, performance, and quality but also improve nutrient uptake and efficiency [9, 17]. The study determined that the separate and combined application of *C. glomerata* and *L. platensis* increased various plant growth parameters such as plant height, green shoot dry weight, and root length. The results are supported by previous reports indicating that different algal applications and doses can increase plant green matter weight, plant height, and root length compared to the control application [25, 46, 14]. Since algae contain bioactive compounds, they can improve plant development [47, 1, 48] and increasing the activity of enzymes involved in the release of nutrients required by plants [49].

Therefore, we believe that increasing doses of *L. platensis* and *C. glomerata* applied to the soil increase the green shoot weight, plant height, and root length of lentil seedlings. El-Aziz Kasim et al. [50] reported that inoculation with seaweed extracts increased the photosynthetic pigment content in the leaves of radish plants. On the other hand, Mahmoud et al. [46] showed that the application of macroalgae extracts led to an increase in the chlorophyll a, chlorophyll b, chlorophyll a + b, and carotenoid content of the leaves.

In this study, the increase in chlorophyll a and b content with increasing doses of *L. platensis* and *C. glomerata* and the combined application of high doses is also supported by the researchers' findings. The rhizosphere, the interface between plant roots and soil, contains the microbiome that is important for enhancing plant growth and health [51]. This is because rhizosphere microbiota can protect plants against harmful pathogens [52] and assist in plant nutrition [53]. Microbiota can increase the production of plant growth hormones, stimulate the plant immune system, improve nutrient uptake, and enhance soil fertility [51]. Therefore, the use of macro- and microalgae extracts as a natural and chemical-free nutrient source can significantly improve plant growth and performance while also supporting the health of the rhizosphere and microbiota. Algal application accelerated plant growth and increased microbial biomass by supporting the development of root systems that release more exudates into the soil. Therefore, both *L. platensis* and *C. glomerata* applications increased microbial activity in the rhizosphere, and compared to the control, the increases in soil respiration due to the applications were statistically significant ($p<0.05$). The improvement in soil structure may be due to the presence of polysaccharides such as alginates and fucoidan found in algal extracts [34].

Studies show that increased microbial activity resulting from an increase in the microorganism population in the rhizosphere leads to improved nutrient uptake by plants and enhanced plant growth [51]. It has been observed that combined application methods, including the use of natural plant growth stimulants such as algal extracts along with other materials, increase crop yield and rhizosphere enzymatic activity [3]. This is attributed to changes in the physical and chemical properties of the soil, allowing the plant to utilize nutrients that are otherwise difficult for plant roots to access [44].

Microalgae have the ability to fertilize soil through the production of polysaccharides, which serve as a carbon source [43]. Organic fertilization through the application of macro- and microalgal biomass can affect the biomass, activity, and structure of microbial communities in soils by altering their physical and chemical properties [48]. Many researchers have reported that cyanobacteria produce extracellular polymeric substances that serve as a carbon source for rhizosphere bacteria, thereby altering the soil microbiota [54, 55].

The improvement in soil structure stems from the presence of polysaccharides such as alginates and fucoidans found in algal extracts, which can bind to metallic ions in the soil, leading to better water retention and aggregation [56]. It can also facilitate the development of a robust root system responsible for nutrient uptake. The addition of *C. glomerata* and *L. platensis* to the soil also affected the β-glucosidase enzyme activity in the rhizosphere ($p<0.05$). This may be due to the fact that *C. glomerata* and *L. platensis* added to the soil act as carbon and energy sources for organisms in the soil, causing an increase in the population and activity of microorganisms, which in turn stimulates enzyme activity in the soil. Organic materials added to the soil increase microbial activity in the soil. Following the death and decomposition of these organisms in the environment, the soil's carbon, nitrogen, and various nutrient content increases, leading to an increase in enzymes, proteins, and organic acids during metabolic activities [7]. The increase in glucosidase enzyme activity with the combined application of increasing doses of *L. platensis* and *C. glomerata* can be attributed to the positive role of organic matter decomposition, which has resulted in an increase in the number of organisms in the soil due to the increased use of nutrients necessary for growth, thereby increasing enzymatic activity [43]. The increased microbial diversity resulting from the addition of organic materials to the soil supports the decomposition of organic carbon [43]. This is consistent with the increased activity of β-glucosidase when both *L. platensis* and *C. glomerata* were applied separately and together compared to the control (Figure 2). When the applications were compared, the rhizosphere β-glucosidase enzyme activity was found to be statistically significant ($p<0.05$) in the Lp-1+Cl-1 application. β-glucosidase activity, generally considered the most sensitive indicator of soil quality and reported to increase in soils with both organic and chemical fertilizers, was also found to be affected by the applications in this study.

Increased soil enzyme activities can be associated with high carbon accumulation because soil microbial biomass and heterotrophic respiration have been reported to increase with plant density Marks et al. [57] and Barone et al. [7] found that soil respiration increased with algal applications and that the development of a stable community of eukaryotic and prokaryotic microorganisms on the soil surface accelerated. In our study, the high rhizospheric respiration observed particularly in the Lp-1+ Cl-1 application supports the researcher's findings. The combined use of natural growth promoters such as *L. platensis* and *C. glomerata* may provide benefits for sustainable agriculture and plant production.

5. Conclusions

The study examined how adding *C. glomerata* and *L. platensis* to the soil promoted the growth of lentil seedlings and increased rhizosphere respiration and glucosidase enzyme activity compared to the control. However, applying *C. glomerata* and *L. platensis* together was found to be more effective than using them separately. In particular, applications at increasing doses were found to be statistically significant. Contents prepared by utilizing the biomass production of *C. glomerata* and *L. platensis* will emerge as an economically viable and environmentally sustainable alternative. The use of *C. glomerata* and *L. platensis* can promote the phytostimulation activities of plants, act as stimulating factors such as phytohormones as growth enhancers, and at the same time reduce the use of chemical fertilizers by positively affecting soil health. Consequently, the application of *C. glomerata* and *L. platensis*, depending on the application rates, can contribute to sustainable agriculture by significantly altering the rhizosphere structure, thereby promoting both soil quality and plant development.

Competing Interest / Conflict of Interest

The authors declare that they have no competing interests.

Author Contribution

Conceptization: ED, CC, ÇK, GS; methodology and laboratory analyzes: ED, CC, ÇK, GS; writing draft: ED, ÇK, CC; proof reading and editing: Other: All authors have read and agreed to the published version of manuscript.

Acknowledgements

This study was financially supported by Harran University, Scientific Research Projects Unit (HÜBAP) with project number 21266.

6. References

[1] Chiaiese, P., Corrado, G., Colla, G., Kyriacou, M.C., & Rouphael, Y. (2018). Renewable sources of plant biostimulation: Microalgae as a sustainable means to improve crop performance. Frontiers Plant Sciences, 9, 1782.

[2] Gonçalves, J., Freitas, J., Fernandes, I., & Silva, P. (2023). Microalgae as Biofertilizers: A Sustainable way to improve soil fertility and plant growth. Sustainability, 15(16), 12413.

[3] Povero, G., Mejia, J.F., di Tommaso, D., Piaggesi, A., & Warrior, P.A. (2016). Systematic approach to discover and characterize natural plant biostimulants. Frontiers Plant Sciences, 7, 435.

[4] Prisa, D., & Spagnuolo, D. (2023). Plant Production with Microalgal Biostimulants. Horticulturae, 9, 829.

[5] Mzibra, A., Aasfar, A., Benhima, R., Khouloud, M., Boulif, R., & Kadmiri, I. (2020). Biostimulants derived from moroccan seaweeds: Seed germination metabolomics and growth promotion of tomato plant. Journal of Plant Growth Regulation, 40, 353–370.

[6] Kumar, S., Diksha, S., Sindhu, S.S., & Kumar, R. (2022). Biofertilizers: An ecofriendly technology for nutrient recycling and environmental sustainability. Current Research in Microbial Sciences, 3, 100094.

[7] Barone, V., Baglieri, A., & Stevanato, P. (2018). Root morphological and molecular responses induced by microalgae extracts in sugar beet (*Beta vulgaris* L.). Journal of Applied Phycology, 30, 1061–1071.

[8] Prisa, D., & Prisa, D. (2019). Possible use of *Spirulina* and klamath algae as biostimulants in Portulacagrandiflora (Moss Rose). World Journal of Advanced Research and Reviews, 3, 1–6.

[9] Kopta, T., Pavlíkova, M., Sękara, A., Pokluda, R., & Marsalek, B. (2018). Effect of bacterial-algal biostimulant on the yield and internal quality of Lettuce (*Lactuca sativa* L.) produced for spring and summer crop. Notulae Botanicae Horti Agrobotanici Cluj-Napoca, 46, 615–621.

[10] Vigani, M., Parisi, C., Rodríguez-Cerezo, E., Barbosa, M.J., Sijtsma, L., & Enzing, C. (2015). Food and feed products from micro-algae: market opportunities and challenges for the EU. Trends in Food Science & Technology, 42,81–92.

[11] Coppens, J., Lindeboom, R., Muys, M., Coessens, W., Alloul, A., Meerbergen, K., Lievens, B., Clauwaert, P., Boon N., & Vlaeminck, S.E. (2016). Nitrification and microalgae cultivation for two-stage biological nutrient valorization from source separated urine. Bioresoure Technology, 211, 41–50.

[12] Garcia-Gonzalez, J., & Sommerfeld, M. (2016). Biofertilizer and biostimulant properties of the microalga *Acutodesmus dimorphus*. Journal of Applied Phycology, 28, 1051–1061.

[13] Faheed, F.A., & Abd-El Fattah, Z. (2008). Effect of *Chlorella vulgaris* as bio-fertilizer on growth parameters and metabolic aspects of lettuce plant. Journal of Agriculture & Social Sciences, 4, 165–169.

[14] Colla, G., & Rouphael, Y. (2020). Microalgae: new source of plant biostimulants. Agronomy, 10,1240.

[15] Arahou, F., Hassikou, R., & Arahou, M. (2021). Influence of culture conditions on *Arthrospira platensis* growth and valorization of biomass as input for sustainable agriculture. Aquaculture International, 29, 2009–2020.

[16] Fais, G., Manca, A., Bolognesi, F., Borselli, M., Concas, A., & Giannaccare, G. (2022). Wide range applications of *Spirulina*: from earth to space missions. Marine Drugs, 20, 299.

[17] Ertani, A., Nardi, S., & Francioso, O. (2019). Effects of two protein hydrolysates obtained from chickpea (*Cicer arietinum* l.) and *Spirulina platensis* on *Zea mays* (L.) plants. Frontiers Plant Sciences, 10, 954.

[18] Michalak, I., & Messyasz, B. (2021). Concise review of *Cladophora* spp.: macroalgae of commercial interest. Journal of Applied Phycology, 33, 133–166.

[19] Borowitzka, M. A., Critchley, A. T., Kraan, S., Peters, A., Sjøtun, K., & Notoya, M. (2013). Developments in applied phycology. Algae for biofuels and energy, 5, 133-152. Borowitzka, M. A. Developments in Applied Phycology 8.

[20] Korzeniowska, K., Łęska, B., & Wieczorek, P. P. (2020). Isolation and determination of phenolic compounds from freshwater *Cladophora glomerata*. Algal Research, 48, 101912.

[21] Ceylan, B., & Sezen, G. (2024). Determination of biological activity of some macro/micro algae. Kastamonu University Journal of Engineering and Sciences, 10(1), 1-6.

[22] Çayci, M., Ceylan, B., & Sezen, G. (2024). Determination of Heavy Metal Contents in Macro/Micro Algae Samples by ICP-OES. Menba Kastamonu Üniversitesi Su Ürünleri Fakültesi Dergisi, 10(3), 30-35.

[23] Michalak, I., Annika, B., Sylwia, B., Sylwia, L., Jerzy, D., Michal, L., & Henry, B. (2020). *Cladophora glomerata* extract and static magnetic field influences the germination of seeds and multielemental composition of carrot. Ecological Chemistry and Engineering, 27, 629–641.

[24] Dziergowska, K., Lewandowska, S., Mech, R., Pol, M., Detyna, J., & Michalak, I. (2021). Soybean Germination Response to Algae Extract and a Static Magnetic Field Treatment. Applied Sciences, 11(18), 8597.

[25] Lewandowska, S., Michalak, I., Niemczyk, K., Detyna, J., Bujak, H., & Arik, P. (2019). Influence of the static magnetic field and algal extract on the germination of soybean seeds. Open Chemistry, 17, 516–525.

[26] Michalak, I., Lewandowska, S., Niemczy, K., Detyna, J., Bujak, H., & Arik, P. (2019). Germination of soybean seeds exposed to the static/alternating magnetic field and algal extract. Engineering in Life Sciences, 9, 986–999.

[27] Soares, C., Svarc-Gajic, J., Oliva-Teles, M. T., Pinto, E., Nastic, N., & Delerue-Matos, C. (2020). Mineral composition of subcritical water extracts of *Saccorhiza polyschides*, a brown seaweed used as fertilizer in the North of Portugal. Journal of Marine Science and Engineering, 8(4), 244.

[28] Lewandowska, S., Dziergowska, K., & Galek, R. (2023). *Cladophora glomerata* extracts produced by Ultrasound-Assisted Extraction support early growth and development of lupin (*Lupinus angustifolius* L.). Scientific Reports, 13, 17867.

[29] Küçük, Ç., Uslu, P., & Sezen, G. (2024). *C. glomerata* ve Arbüsküler Mikorizal Fungus (AMF) Spor Aşılamasının Mısır Bitkisinin (*Zea mays* L.) Gelişim Parametreleri ve Bazı rizosfer toprak enzimlerine etkisi. Süleyman Demirel Üniversitesi Fen Bilimleri Enstitüsü Dergisi, 28(2), 189-196.

[30] Kumar, G., & Sahoo, D. (2011). Effect of seaweed liquid extract on growth and yield of *Triticum aestivum* var. Pusa Gold. Journal of Applied Phycology, 23, 251–255.

[31] Yıldız, M., & Özgen, M. (2004). The effect of media sucrose concentration on total phenolics content and adventitous shoot regeneration from sugarbeet (*Beta vulgaris* L.) leaf and petiole explants. Plant Cell, Tissue and Organ Culture, 77, 111-115.

[32] Arnon, D.T. (1967). Copper Enzymes in isolated chloroplast polyphenol oxidase in *Beta vulgaris*. Plant Physiology, 24, 1-15.

[33] Eivazi, F. & Tabatabai, M.A. (1988) Glucosidases and Galactosidases in Soils. Soil Biology and Biochemistry, 20, 601-606.

[34] Mukherjee, A., Gaurav, A.K., Patel, A.K., Singh, S., Chouhan, G.K., & Lepcha, A. (2021). Unlocking the potential plant growth-promoting properties of chickpea (*Cicer arietinum* l.) seed endophytes bio-inoculants for improving soil health and crop production. Land Degradation & Development, 32 (15), 4362–4374.

[35] Anderson, J.P.E. (1982). Soil respiration. In: methods of soil analysis, part 2, chemical and microbiological properties (Ed. A.L. Page). ASA-SSSA, Madison, Winsconsin. pp. 831-871.

[36] Lucini, L., Rouphael, Y., Cardarelli, M., Canaguier, R., Kumar, P., & Colla, G. (2015). The effect of a plant-derived biostimulant on metabolic profiling and crop performance of lettuce grown under saline conditions. Scientific Horticture, 182, 124–133.

[37] Bulgari, R., Cocetta, G., Trivellini, A., Vernieri, P., & Ferrante, A. (2015). Biostimulants and crop responses: a review. Biological Agriculture & Horticulture, 31, 1–17.

[38] Lee, S.M., & Ryu, C.M. (2021). Algae as new kids in the beneficial plant microbiome. Frontier in Plant Science, 12, 599742.

[39] Steveni, C.M., Norrington-Davies, J., & Hankins, S.D. (1992). Efect of seaweed concentrate on hydroponically grown spring barley. Journal of Applied Phycology, 4, 173–180.

[40] Stirk, W.A., & Van Staden, J. (1997). Comparison of cytokinin and auxinlike activity in some commercially used seaweed extracts. Journal of Applied Phycology, 8,503–508.

[41] Spinelli, F., Fiori, G., Noferini, M., Sprocatti, M., & Costa, G. (2010). A novel type of seaweed extract as a natural alternative to the use of iron chelates in strawberry production. Scientia Horticulturae, 125, 263–269.

[42] Mukherjee, C., Chowdhury, R., Sutradhar, T., Begam, M., Ghosh, S.M., & Ray, K. (2016). Parboiled rice efuent: a wastewater niche for microalgae and cyanobacteria with growth coupled to comprehensive remediation and phosphorus biofertilization. Algal Research, 19, 225–236.

[43] Kholssi, R., Marks, E.A.N., Montero, O., Mate, A.P., Debdoubi, A., Rad, C. (2018). The growth of flamentous microalgae is increased on biochar solid supports. Biocatalysis and Agricultural Biotechnology, 13, 182–185. https://doi.org/10.1016/j.bcab.2017.12.011

[44] Schreiber, C., Schiedung, H., & Harrison, L. (2018). Evaluating potential of green alga *Chlorella vulgaris* to accumulate phosphorus and to fertilize nutrient-poor soil substrates for crop plants. Journal of Applied Phycology, 30, 2827–2836.

[45] Isinkaralar, K. (2022). Some atmospheric trace metals deposition in selected trees as a possible biomonitor. Romanian Biotechnological Letters, 27(1), 3227-3236.

[46] Mahmoud, S.H., Salama, D.M., El-Tanahy, A.M.M., & Abd El-Samad, E.H. (2019). Utilization of seaweed (*Sargassum vulgare*) extract to enhance growth, yield and nutritional quality of red radish plants. Annals Agricultural Sciences, 64, 167–175.

[47] Van Oosten, M.J., Pepe, O., & De Pascale, S. (2017). The role of biostimulants and bioeffectors as alleviators of abiotic stress in crop plants. Chemistry Biologyical Technologies in Agriculture, 4, 5.

[48] Renuka, N., Guldhe, A., Prasanna, R., Singh, P., Bux, F. (2018). Microalgae as multi-functional options in modern agriculture: current trends, prospects and challenges. Biotechnology Advances, 36, 1255-1273.

[49] De Caire, G.Z., De Cano, M.S., Palma, R.M., De Mule, C.Z. (2000). Changes in soil enzyme activities following additions of cyanobacterial biomass and exopolysaccharide. Soil Biology & Biochemistry, 32,1985-1987.

[50] El-Aziz Kasim, W.A., Saad-Allah, K.M., & Hamouda, M. (2016). Seed priming with extracts of two seaweeds alleviates the physiological and molecular impacts of salinity stress on radish (*Raphanus sativus*). International Journal of Agriculture & Biology, 18, 653–660.

[51] Vives-Peris, V., de Ollas, C., Gomez-Cadenas, C., Pérez-Clemente, R.M. (2020). Root exudates: from plant to rhizosphere and beyond. Plant Cell Reports, 39 (1), 3-17.

[52] Rolfe, S.A., Griffiths, J. & Ton, J. (2019) Crying out for help with root exudates: adaptive mechanisms by which stressed plants assemble health promoting soil microbiomes. Current opinion in microbiology, 49, 73–82.

[53] Bulgarelli, D., Schlaeppi, K., Spaepen, S., Van Themaat, E.V.L. & SchulzeLefert, P. (2013) Structure and functions of the bacterial microbiota of plants. Annual Review of Plant Biology, 64, 807–838.

[54] Manjunath, M., Kanchan, A., Ranjan, K., Venkatachalam, S., Prasanna, R., Ramakrishnan, B., & Singh, B. (2016). Beneficial cyanobacteria and eubacteria synergistically enhance bioavailability of soil nutrients and yield of okra. Heliyon, 2(2).

[55] Xiao, R., & Zheng, Y. (2016). Overview of microalgal extracellular polymeric substances (EPS) and their applications. Biotechnology advances, 34(7), 1225-1244.

[56] Khan W, Rayirath UP, Subramanian S, Jithesh MN, Rayorath P, Hodges DM, Critchley AT, Craigie JS, Norrie J, Prithiviraj B (2009) Seaweed extracts as biostimulants of plant growth and development. J Plant Growth Regul 28:386–399.

[57] Marks, E.A.N., Minon, J., Pascual, A., Montero, O., Navas, L.M., & Rad, C. (2017). Application of a microalgal slurry to soil stimulates heterotrophic activity and promotes bacterial growth. Science of the Total Environment, 606,610–617.